ChemPubSoc Europe

DOI: 10.1002/cbic.201402087

Synthetic Polyamine BPA-C8 Inhibits TGF-β1-Mediated Conversion of Human Dermal Fibroblast to Myofibroblasts and Establishment of Galectin-1-Rich Extracellular Matrix in Vitro

Alžběta Mifková,[a, b] Ondřej Kodet,[a, c] Pavol Szabo,[a] Jan Kučera,[a, c] Barbora Dvořánková,[a] Sabine André,[d] Girish Koripelly,[e] Hans-Joachim Gabius,[d] Jean-Marie Lehn,*[e] and Karel Smetana, Jr.*[a]

Cancer-associated fibroblasts (CAFs) play a role in the progression of malignant tumors. They are formed by conversion of fibroblasts to smooth muscle α-actin-positive (SMA-positive) myofibroblasts. Polyamines are known to change the arrangement of the actin cytoskeleton by binding to the anionic actin. We tested the effect of the synthetic polyamine BPA-C8 on the transition of human dermal fibroblasts to myofibroblasts induced either by TGF-β1 alone or by TGF-β1 together with adhesion/growth-regulatory galectin-1. Pre-existing CAFs, myofibroblasts from pancreatitis, and rat smooth muscle cells were also exposed to BPA-C8. BPA-C8 impaired myofibroblast formation from activated fibroblasts, but it had no effect on cells already expressing SMA. BPA-C8 also reduced the occurrence of an extracellular matrix around the activated fibroblasts. The reported data thus extend current insights into polyamine activity, adding interference with tumor progression to the tumor-promoting processes warranting study.

Introduction

The level of complexity within human tumors can be likened to an ecosystem.[1] As has been established in culture systems, cancer cells can thrive in vivo in microenvironments suited to support cell proliferation, locally invasive properties, and propensity for distant metastasis.[2] Moreover, such a so-called niche maintains functionality of cancer stem cells.[3] On the cellular level, a variety of cell types, especially inflammatory cells and cancer-associated fibroblasts (CAFs), are counted among the major constituents that shape the growth-favoring surroundings of tumor cells through the action of a series of secreted factors, such as cytokines, chemokines or growth factors, together with the extracellular matrix.[4] CAFs are myofibroblast-like cells characterized by presence of smooth muscle α-actin (SMA).[5] Rather similar cells are also present in healing wounds, where they are involved in wound contraction, and in fibrotic tissues or organs.[6, 7]

Literature data indicate that CAFs can arise from local fibroblasts, pericytes, endothelial cells, and macrophages, and also probably by epithelial to mesenchymal transition from cancer cells.[4, 8, 9]

Transforming growth factor-β1 (TGF-β1) has been identified as a molecular switch for the generation of myofibroblasts as CAFs from normal fibroblasts in vitro.[10] Another molecular mediator, the endogenous adhesion/growth-regulatory lectin galectin-1 (Gal-1), with activity stronger than those of galectins-3, -4, and -7,[11, 12] is able to enhance the effect of TGF-β1 on fibroblasts.[13] CAFs are strong activators of growth and migration for many types of cancer cells.[5] We have previously demonstrated that CAFs isolated from human basal carcinomas of the skin and squamous cell (head and neck) carcinomas have a significantly different gene expression profile from normal fibroblasts, including upregulated transcription of genes coding for protumoral factors such as interleukin-6.[14–16] CAFs are able to modify the in vitro characteristics of normal epithelial cells to make them similar to cancer cells and to influence the phenotype of breast cancer cells of an established line.[17–19]

As one of many biochemical parameters, the production of polyamines is significantly increased in malignant tumors of

[a] Dr. A. Mifková, Dr. O. Kodet, Dr. P. Szabo, Dr. J. Kučera, Dr. B. Dvořánková, Prof. Dr. K. Smetana, Jr.
Institute of Anatomy, Charles University, 1st Faculty of Medicine
U Nemocnice 3, 128 00 Prague (Czech Republic)
E-mail: karel.smetana@lf1.cuni.cz

[b] Dr. A. Mifková
Department of Otorhinolaryngology and Head and Neck Surgery
Charles University, 1st Faculty of Medicine
V Úvalu 5, 150 00 Prague (Czech Republic)

[c] Dr. O. Kodet, Dr. J. Kučera
Department of Dermatovenereology, Charles University
1st Faculty of Medicine
U Nemocnice 2, 128 08 Prague (Czech Republic)

[d] Dr. S. André, Prof. Dr. H.-J. Gabius
Institute of Physiological Chemistry, Ludwig-Maximilians-University Munich
Faculty of Veterinary Medicine
Veterinärstrasse 13, 80539 Munich (Germany)

[e] Dr. G. Koripelly, Prof. Dr. J.-M. Lehn
Institut de Sciences et d'Ingénierie Supramoléculaires (ISIS)
University of Strasbourg
8 allée Gaspard Monge, 67000 Strasbourg (France)
E-mail: lehn@unistra.fr

 © 2014 Wiley-VCH Verlag GmbH & Co. KGaA, Weinheim

different nature. 3T3 fibroblasts, transfected with cDNA for ornithine decarboxylase, thereby increasing the production of polyamines, acquired properties of transformed cells. Correspondingly, deactivation of this enzyme reduced the malignant potential of cancer cells.[20,21] On the molecular level, polycations, including polyamines of different nature and structure, become engaged in F-actin cytoskeleton formation, namely by bundling F-actin fibers.[22,23] These substances then even shift the actin status to building F-actin lamellipodia in 3T3 fibroblasts.[24] The toxic plant-derived polyamine pavetamine has a destructive effect on the actin cytoskeletons of cardiomyocytes, leading to heart failure in ruminants.[25] Conversely, inhibition of natural polyamine synthesis by blocking arginase improved wound healing, accompanied by a high incidence of myofibroblasts in granulation tissue in mice.[26]

Given this context and the described process of transformation into a salient tumor-promoting factor in the microenvironment, the question of the impact of polyamines on formation of myofibroblasts is addressed here. We tested the effect of the synthetic polyamine BPA-C8 on the level of generation of

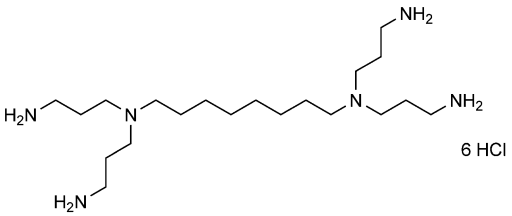

BPA-C8 hexahydrochloride

myofibroblasts from normal human dermal fibroblasts (HFs) either with TGF-β1 alone or with the combination of TGF-β1 and Gal-1. The results obtained were compared with data from experiments performed with CAFs isolated from a squamous cell (head and neck) carcinoma, myofibroblasts from chronic pancreatitis, and smooth muscle cells from rat aorta, all exposed to BPA-C8, thereby also providing information on BPA-C8's effects on cell viability.

Results and Discussion

Number of cells and Ki67 positivity in cultured HFs

BPA-C8 reduced the number of HFs when it was applied to fibroblast cultures at a concentration of 100 μM (Figures 1A and 2A). At 20 μM, no notable effect was seen. TGF-β1 alone or combined with Gal-1 had a strong stimulatory effect on fibroblast growth. In this experimental setting, both tested concentrations of the polyamine—that is, 20 μM and 100 μM—significantly reduced the number of HFs stimulated by TGF-β1 with or without Gal-1. On comparing these data with levels of the proliferation marker Ki67, the proportion of cells with positive nuclei was fairly constant under all experimental conditions (Figures 1B and 2B).

Influence of BPA-C8 on conversion of HFs to myofibroblasts

To set the baseline, all primary HF cultures were immuno-cytochemically monitored for SMA presence; no more than five SMA-positive cells were found on the coverslips (Figure 1B). Supplementing the culture medium with TGF-β1 resulted in the expected formation of myofibroblasts from the HFs. This process was further enhanced by adding Gal-1. The experimental conditions were thus set for the assays, and both concentrations of BPA-C8—that is, 20 μM and 100 μM—completely precluded the occurrence of SMA-positive cells.

Influence of BPA-C8 on the establishment of extracellular matrix fibers rich in Gal-1 and tenascin

As a biochemical aspect of TGF-β1 activity, we next tested the effect of the polyamine on production of an extracellular matrix, characterized by presence of tenascin and Gal-1. Immunofluorescence analysis revealed that HFs produced only negligible quantities of extracellular matrix in relation to cells exposed to TGF-β1, both without and with Gal-1. Both Gal-1 and tenascin were detected in this meshwork on probing for a matrix-presented effector and a typical proteoglycan.

The matrix generation was conspicuously sensitive to the presence of BPA-C8 (Figure 1C).

Evaluation of the levels of senescence and the ratios between viable and dead cells

Application of TGF-β1 together with Gal-1 to fibroblast cultures increased the number of senescence-associated β-galactosidase-positive cells in sites with high cell density. When the medium also contained BPA-C8, the extent of positivity was reduced (Figure 3). It is also apparent that more dead cells were detected in this case than in that of the BPA-C8-free cultures.

Influence of BPA-C8 on smooth muscle cells from the aorta of the rat, CAFs isolated from squamous cell carcinoma, and myofibroblasts from chronic pancreatitis

Smooth muscle cells (genuinely positive for SMA), CAFs, and myofibroblasts were not sensitive to exposure to BPA-C8. Clearly, no effect on the expression of SMA was observed in these cell types after culture in the presence of the polyamine at the two concentrations (20 and 50 μM) tested (Figure 4). Establishment of an extracellular matrix rich in fibronectin was also not sensitive to polyamine treatment (Figure 4B, C).

The key finding of this study is the observation that the polyamine BPA-C8, when added to the culture medium of TGF-β1-exposed human dermal fibroblasts, disrupts the program of myofibroblast formation. This effect appears to be accompanied by a reduction of cell viability, with indications of dose dependency. A decrease in cell number was observed in control fibroblasts exposed to 100 μM of the polyamine, whereas even as little as 20 μM led to this effect in TGF-β1-treated cells. This activity of BPA-C8 does not appear to be related to suppression of proliferative activity, because the presence of the

© 2014 Wiley-VCH Verlag GmbH & Co. KGaA, Weinheim

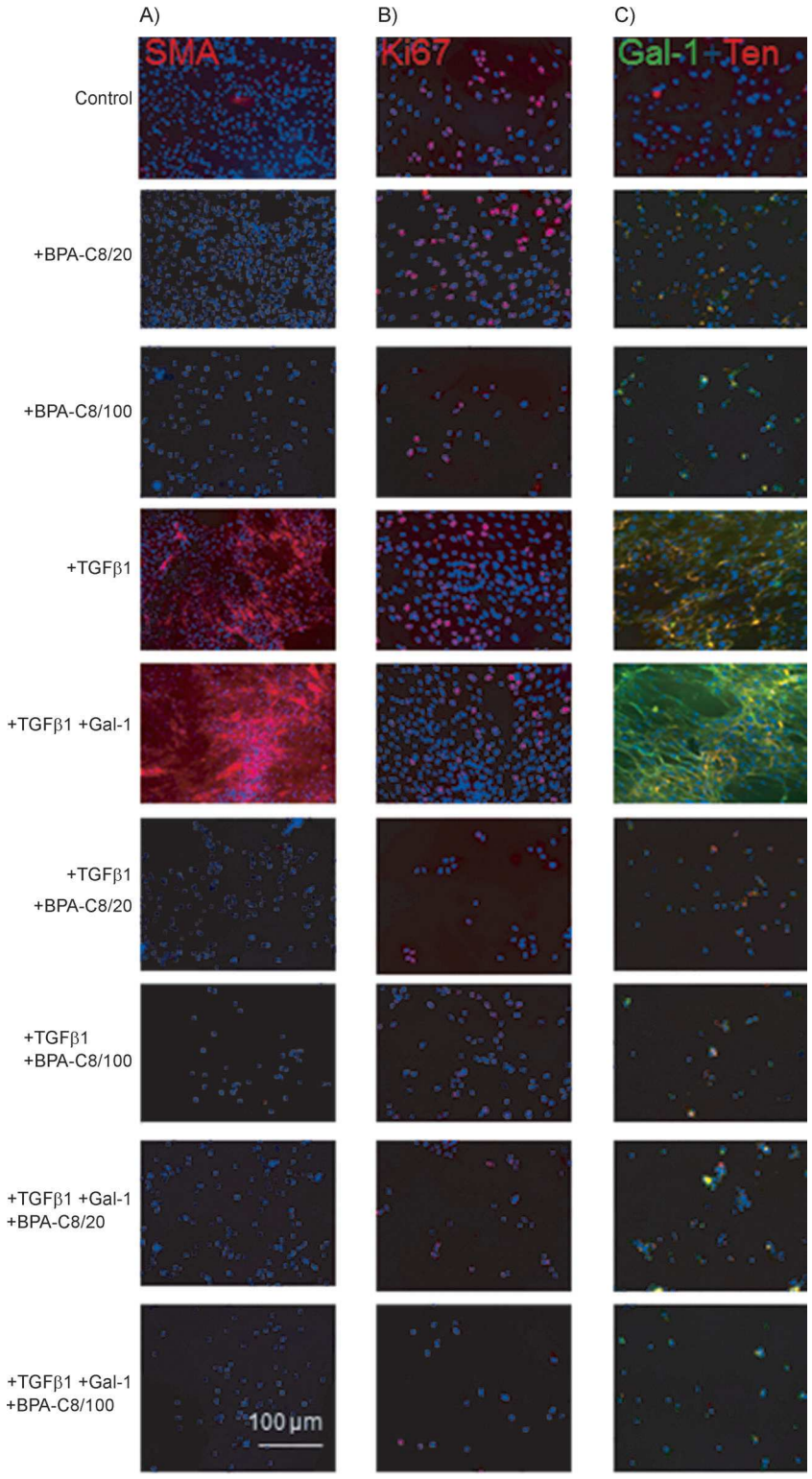

Figure 1. Immunocytochemical detection of A) α-smooth muscle actin (SMA, red signal), B) the proliferation marker Ki67 (red signal) and C) galectin-1 (Gal-1, green signal) and tenascin (Ten, red signal) in normal human fibroblasts (control) and in fibroblasts exposed both to BPA-C8 at concentrations of 20 μM (BPA-C8/20) and 100 μM (BPA-C8/100) and to TGF-β1, either alone or in combination with Gal-1. Nuclei were counterstained with DAPI (blue signal). Illustrations document that TGF-β1, both alone and together with Gal-1, stimulated conversion of fibroblasts into myofibroblasts (A). This process was blocked by both concentrations of BPA-C8 (A). The level of proliferation was markedly decreased by the high concentration of BPA-C8 (100 μM) under all experimental conditions, and also by the 20 μM concentration when used in combination with TGF-β1 (B). Production of tenascin and Gal-1 was increased by TGF-β1, a process impaired by BPA-C8 (C).

compound is not able to affect the occurrence of Ki67-positive (proliferating) cells significantly. With regard to cellular targets, the actin monomer is an anionic protein, and its polymerization is prone to be disturbed by polycations.[27] Introducing a synthetic polyamine into this system can therefore inhibit the formation of SMA-based fibers, a process that can be fatal for the cell. In addition, targeting actin (and other polyanions) might account for further biochemical consequences, a reduction in the extent of generation of extracellular matrix. The production of this molecular meshwork (with strong positivity for Gal-1 and tenascin, forming a scaffold suited to the presentation of mediators such as lectins) by CAFs appears to be relevant for tumor progression.[28,29] With regard to at Gal-1, the best-studied member of this lectin family,[12,30] contact of T-cells to (thymic) stromal cells, a source of the lectin, or Matrigel loaded with Gal-1 triggers the apoptotic elimination of the defense cells.[31] The induction of T-cell apoptosis, in a caspase-3-dependent manner, by Gal-1 from tumor-associated stroma obtained from a patient with cutaneous T-cell lymphoma required p56lck/ZAP70 tyrosine kinases.[32] Similarly, Gal-1 presentation in skin can at least contribute to the accumulation of $CD4^+$ $CD7^-$ T-cells (resistant to Gal-1-dependent apoptosis induction through CD7 ligation) during progression of the Sézary syndrome,[33] Gal-1 presence showed a negative correlation to $CD45^+$ lymphocytes in laryngeal squamous cell carcinomas,[34] and stromal (not tumor) presence of a galectin was an unfavorable prognostic marker in breast cancer.[35]

Exploiting new insights from tumor biology to devise innovative means to set limits to tumor progression is the driving force

© 2014 Wiley-VCH Verlag GmbH & Co. KGaA, Weinheim

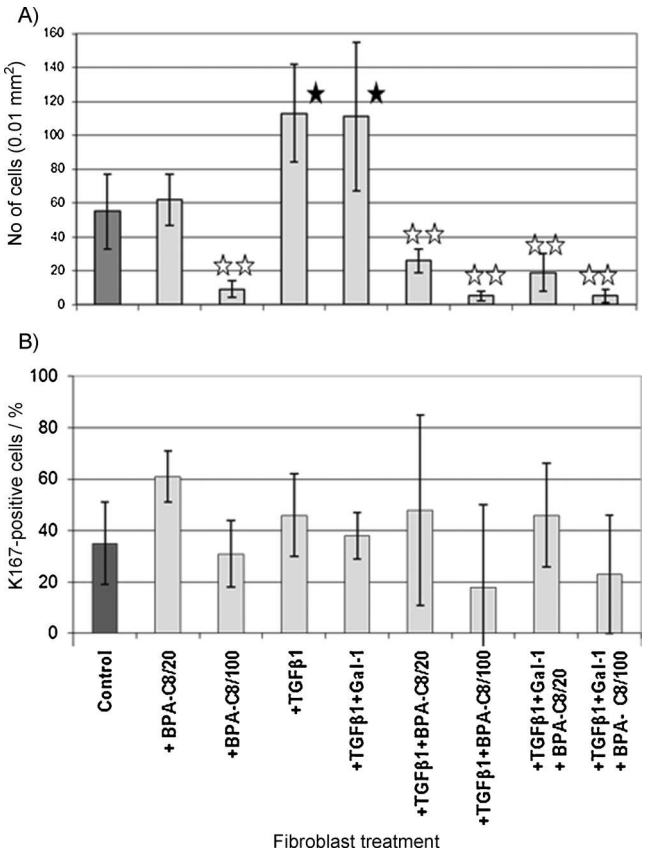

Figure 2. A) TGF-β1 (alone or in combination with Gal-1) increased the cell number, whereas BPA-C8/100 significantly reduced this parameter. The stimulatory effect of TGF-β1 was neutralized by BPA-C8 at both tested concentrations. B) Percentages of marker-positive (Ki67) cells under all tested conditions. Experimental measurements significantly higher than those for the control (gray column) with $p < 0.05$ are each marked with a black asterisk, and those significantly lower than those for the control with $p < 0.01$ by two open asterisks. All data were processed by use of Student's paired t-test after examination of 50 view fields in technical triplicate. For abbreviations, see the legend to Figure 1.

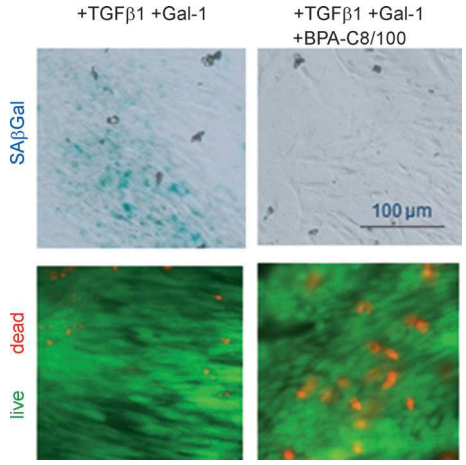

Figure 3. Cytochemical detection of senescence-associated β-galactosidase (SAβGal, blue signal) revealed higher levels in cultures of stimulated cells than in cells additionally exposed to 100 µM of BPA-C8 (top). The ratio of dead cells (red/orange signal) to viable cells (green) was shifted by BPA-C8 in the direction of dead cells (bottom).

behind therapeutic advances.[36] Although a mainstream approach of the pharmaceutical industry is focused predominantly on attacking cancer cells, the risk of invasion and spread, with contributions from the microenvironment, should also be taken into consideration.[37] Along these lines, targeting CAFs or their interaction with cancer cells involving the surrounding matrix with presented effectors can open a promising route. Our control observation that BPA-C8 did not affect the SMA status of smooth muscle cells allays immediate concerns for a negative impact on vessels. It appears warranted to envision further applicability tests on hypertrophic/keloid scars.

Conclusions

A challenge for synthetic chemistry is to develop new reagents to interfere with the effect of CAFs on tumor progression, an increasingly documented factor in this process. The polyamine BPA-C8 has a strong inhibitory effect on the transformation of fibroblasts into myofibroblasts. It also inhibits production of extracellular matrix. On the other hand, it has only negligible effect on SMA-positive cells, such as smooth muscle cells or pre-existing myofibroblasts from chronically inflamed tissue.

Experimental Section

Preparation of BPA-C8 polyamine: The branched polyamine BPA-C8 was prepared by treatment of acrylonitrile with octane-1,8-diamine to afford the corresponding tetranitrile. Reduction of this with Raney nickel afforded BPA-C8 as a light yellow oil. It was converted into, and stored as, its hexahydrochloride salt, as described in detail previously.[24]

Preparation of Gal-1: Human Gal-1 was obtained by recombinant production and purified by affinity chromatography on lactosylated Sepharose 4B as crucial step, routinely followed by the removal of any lipopolysaccharide contamination.[38] Product analysis was performed 1) for purity, by one- and two-dimensional gel electrophoresis, gel filtration, and mass spectrometric fingerprinting, as well as 2) for activity, through hemagglutination, cell surface binding, and induction of anoikis.[39–42]

Preparation of cells

Primary culture of normal human fibroblasts (HFs): HFs were freshly prepared by taking advantage of free migration from small fragments of the dermis from the skin of a breast specimen obtained from the Department of Aesthetic Surgery of the 3rd Faculty of Medicine (Charles University, Prague, Czech Republic) with informed consent of the donor and the local ethical committee according to the Declaration of Helsinki. They were cultured in Dulbecco's modified Eagle's medium (DMEM, Biochrom, Berlin, Germany) supplemented with fetal bovine serum (FBS, Biochrom, Berlin, Germany, 10%) at 37 °C and under CO_2 (5%).

Primary culture of squamous cell CAFs and fibroblasts from chronic pancreatitis: CAFs were prepared from a specimen of a human laryngeal squamous cell carcinoma obtained from the Department of Otorhinolaryngology and Head and Neck Surgery of the 1st Faculty of Medicine (Charles University). A fibroblast population rich in myofibroblasts was prepared from human chronic pancreatitis of a tissue specimen received from the 1st Department of Surgery of the 1st Faculty of Medicine (Charles University) according to the

© 2014 Wiley-VCH Verlag GmbH & Co. KGaA, Weinheim

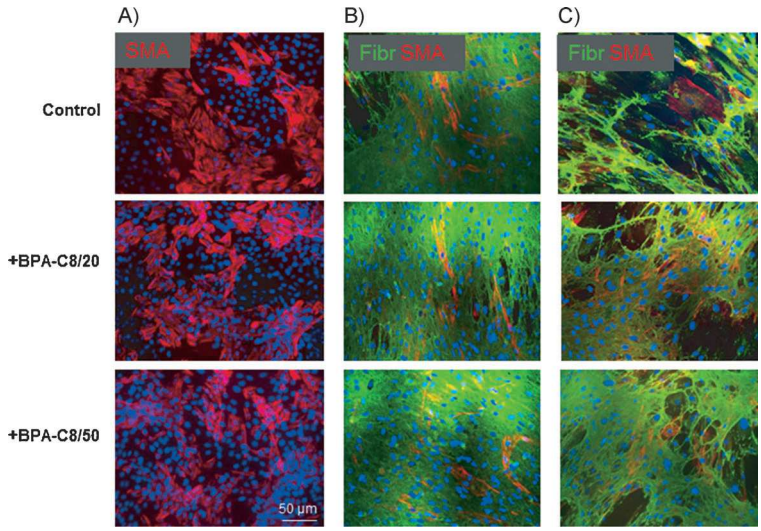

Figure 4. Immunocytochemical detection of SMA (red/orange signals) A) in rat smooth muscle cells, B) in CAFs from a squamous cell carcinoma, and C) in myofibroblasts from chronic pancreatitis, as well as of fibronectin (green signals) in cultures of CAFs (B) and myofibroblasts (C), control without the test substance and tests in the presence of 20 μM and 50 μM of BPA-C8, respectively. Nuclei were counterstained with DAPI.

ethical standard given above. Both types of cells were prepared by previously published protocols.[12,14]

Primary culture of smooth muscle cells from rat aorta: Smooth muscle cells of a degree of about 80% purity were freshly prepared and provided by Dr. Lucie Bačáková (Institute of Physiology, Academy of Sciences of the Czech Republic, Prague, Czech Republic) as described,[43] and then cultured under the same conditions as used for the other cell preparations used in this study.

Culture of stimulated fibroblasts with BPA-C8 polyamine: Fibroblasts were inoculated at a density of 800 cells cm^{-2} on glass coverslips placed in 6-well dishes (TPP, Trasadingen, Switzerland) and further cultured in DMEM, variously with no additions, after addition of TGF-β1 (10 ng mL^{-1}, Sigma–Aldrich), and after addition of TGF-β1 (10 ng mL^{-1}) and Gal-1 (300 ng mL^{-1}) as described.[11] BPA-C8 was tested at final concentrations of 20 μM and 100 μM as before in assays on lamellipodial growth.[24] Cultures without addition of BPA-C8 were used as control. Cells were cultured at 37 °C under CO_2 (5%) for one week; medium was changed every 48 h.

Culture of CAFs, myofibroblasts from chronic pancreatitis, and smooth muscle cells with PBA-C8 polyamine: All three types of cells were inoculated at a density of 2500 cells cm^{-2} in DMEM on glass coverslips placed in 6-well dishes. After 24 h, the medium was changed, and DMEM containing BPA-C8 (20 or 50 μM) was added. Cells kept in DMEM were cultured in parallel as control. All cells were maintained at 37 °C under CO_2 (5%) for one week; medium was changed every 48 h. Coverslips were washed with phosphate-buffered saline (Biochrom), dried, and stored at −20 °C for cytochemical processing.

Immunocytochemistry: Cells were briefly fixed with paraformaldehyde (4%, *w/v*) at pH 7.2 and washed in phosphate-buffered saline solution. The specimens were routinely processed for detection of α-smooth muscle actin (DAKO, Glostrup, Denmark), the proliferation marker Ki67 (DAKO), and tenascin (Sigma–Aldrich) with specific mouse monoclonal antibody preparations diluted as recommended by the supplier. Fibronectin presence was visualized with a specific rabbit polyclonal antibody (DAKO). Gal-1 was localized with a home-made polyclonal antibody (rigorously tested for presence of crossreactive fractions against other human galectins, which were then removed chromatographically), applied at 20 μg mL^{-1}.[28,44] Swine-anti rabbit immunoglobulin G labeled with fluorescein isothiocyanate (FITC, DAKO) and tetramethylrhodamine isothiocyanate (TRITC)-labeled goat anti-mouse immunoglobulin G (Sigma–Aldrich) were used as second-step reagents. Nuclear DNA was visualized with 4′,6-diamidino-2-phenylindole (DAPI, Sigma–Aldrich). Controls for specificity were performed by omission of the specific antibodies from processing and by their replacement with irrelevant isotypic antibodies or preimmune serum. Specimens were mounted to Vectashield (Vector Laboratories, Burlingame, CA) and then inspected with an Eclipse 90i fluorescence microscope (Nikon) equipped with filter blocks for FITC, TRITC, and DAPI and a Cool-1300Q CCD camera (Vosskühler, Osnabrück, Germany); microphotographs were analyzed with a LUCIA 5.1 computer-assisted image analysis system (Laboratory Imaging, Prague, Czech Republic).

Evaluation of levels of senescence and cell death: To determine levels of senescence and death in the culture cells, commercial staining kits (CS0030-1KT and 04511, Sigma–Aldrich) were used.

Acknowledgements

This study was supported by the Grant Agency of the Ministry of Health of the Czech Republic (No. 13488-4), by Charles University (projects PRVOUK-27-1, UNCE 204013), by a Specific University Research grant from the European Regional Development Fund BIOCEV (No. CZ.1.05/1.1.00/02.0109), and by the EC FP7 program (grant agreement no. 317297(GLYCOPHARM)). G.K. thanks the CNRS and the University of Strasbourg for postdoctoral financial support. The authors are grateful to Dr. Lucie Bačáková of the Institute of Physiology of the Academy of Sciences of the Czech Republic for her generous gift of smooth muscle cells, as well as to Marie Jindráková and Radana Kavková for their excellent technical assistance.

Keywords: actin · cancer · galectin · polycations · tenascin

[1] I. Kareva, *Transl. Oncol.* **2011**, *4*, 266 – 270.
[2] M. Allen, J. L. Jones, *J. Pathol.* **2011**, *223*, 162 – 176.
[3] T. Borovski, F. De Sousa, E. Melo, L. Vermeulen, J. P. Medema, *Cancer Res.* **2011**, *71*, 634 – 639.
[4] J. Plzák, L. Lacina, M. Chovanec, B. Dvořánková, P. Szabo, Z. Čada, K. Smetana Jr., *Anticancer Res.* **2010**, *30*, 455 – 462.
[5] K. Smetana Jr., B. Dvořánková, P. Szabo, H. Strnad, M. Kolář in *Dermal Fibroblasts: Histological Perspectives, Characterization and Role in Disease* (Ed.: X. Bai), Nova Sciences Publishers, New York, **2013**, pp. 83 – 94.
[6] B. Hinz, *J. Invest. Dermatol.* **2007**, *127*, 526 – 537.
[7] V. S. LeBleu, G. Taduri, J. O'Connell, Y. Teng, V. G. Cooke, C. Woda, H. Sugimoto, R. Kalluri, *Nat. Med.* **2013**, *19*, 1047 – 1053.
[8] O. De Wever, P. Demetter, M. Mareel, M. Bracke, *Int. J. Cancer* **2008**, *123*, 2229 – 2238.
[9] I. Haviv, K. Polyak, W. Qiu, M. Hu, I. Campbell, *Cell Cycle* **2009**, *8*, 589 – 595.
[10] J. Brenmoehl, S. N. Miller, C. Hofmann, D. Vogl, W. Falk, W. Schölmerich, G. Rogler, *World J. Gastroenterol.* **2009**, *15*, 1431 – 1442.
[11] H. Kaltner, H.-J. Gabius, *Histol. Histopathol.* **2012**, *27*, 397 – 416.

© 2014 Wiley-VCH Verlag GmbH & Co. KGaA, Weinheim

[12] K. Smetana Jr., S. André, H. Kaltner, J. Kopitz, H.-J. Gabius, *Expert Opin. Ther. Targets* **2013**, *17*, 379 – 392.
[13] B. Dvořánková, P. Szabo, L. Lacina, P. Gal, J. Uhrova, T. Zima, H. Kaltner, S. André, H.-J. Gabius, E. Syková, K. Smetana Jr., *Cells Tissues Organs* **2011**, *194*, 469 – 480.
[14] H. Strnad, L. Lacina, M. Kolář, Z. Čada, Č. Vlček, B. Dvořánková, J. Betka, J. Plzák, M. Chovanec, J. Šáchová, J. Valach, M. Urbanová, K. Smetana Jr., *Histochem. Cell Biol.* **2010**, *133*, 201 – 211.
[15] P. Szabó, M. Kolář, B. Dvořánková, L. Lacina, J. Štork, Č. Vlček, H. Strnad, M. Tvrdek, K. Smetana Jr., *Biol. Cell* **2011**, *103*, 233 – 248.
[16] M. Kolář, P. Szabo, B. Dvořánková, L. Lacina, H.-J. Gabius, H. Strnad, J. Šáchová, C. Vlček, J. Plzák, M. Chovanec, Z. Čada, J. Betka, Z. Fík, J. Pačes, H. Kovářová, J. Motlík, K. Jarkovská, K. Smetana Jr., *Biol. Cell* **2012**, *104*, 738 – 751.
[17] L. Lacina, K. Smetana Jr., B. Dvořánková, R. Pytlík, L. Kideryová, L. Kučerová, Z. Plzáková, J. Štork, H.-J. Gabius, S. André, *Br. J. Dermatol.* **2007**, *156*, 819 – 829.
[18] L. Lacina, B. Dvořánkova, K. Smetana Jr., M. Chovanec, J. Plzák, R. Tachezy, L. Kideryová, L. Kučerová, Z. Čada, J. Bouček, R. Kodet, S. André, H.-J. Gabius, *Int. J. Radiat. Biol.* **2007**, *83*, 837 – 848.
[19] D. Dvořánková, P. Szabo, L. Lacina, O. Kodet, E. Matoušková, K. Smetana Jr., *Histochem. Cell Biol.* **2012**, *137*, 679 – 685.
[20] S. Kubota, H. Kiyosawa, Y. Nomura, T. Yamada, S. Seyama, *J. Natl. Cancer Inst.* **1997**, *89*, 567 – 571.
[21] S. Iwata, Y. Sato, M. Asada, M. Takagi, A. Tsujimoto, T. Inaba, T. Yamada, S. Sakamoto, J.-i. Yata, T. Shimogori, K. Igarashi, S. Mizutani, *Oncogene* **1999**, *18*, 165 – 172.
[22] C. Oriol-Audit, M. W. Hosseini, J.-M. Lehn, *Eur. J. Biochem.* **1985**, *151*, 557 – 559.
[23] A. Muhlrad, E. E. Grintsevich, E. Reisler, *Biophys. Chem.* **2011**, *155*, 45 – 51.
[24] I. Nedeva, G. Koripelly, D. Caballero, L. Chièze, B. Guichard, B. Romain, E. Pencreach, J.-M. Lehn, M.-F. Carlier, D. Riveline, *Nat. Commun.* **2013**, *4*, 2165.
[25] C. E. Ellis, D. Naicker, K. M. Basson, C. J. Botha, R. A. Meintjes, R. A. Schultz, *Toxicon* **2010**, *55*, 1071 – 1079.
[26] S. L. Kavalukas, A. R. Uzgare, T. J. Bivalacqua, A. Barbul, *Surgery* **2012**, *151*, 287 – 295.
[27] K. Shikinaka, A. Kakugo, Y. Osada, J. P. Gong, *Langmuir* **2009**, *25*, 1554 – 1557.
[28] J. Valach, Z. Fík, H. Strnad, M. Chovanec, J. Plzák, Z. Čada, P. Szabo, J. Šáchová, M. Hroudová, M. Urbanová, M. Šteffl, J. Pačes, J. Mazánek, Č. Vlček, J. Betka, H. Kaltner, S. André, H.-J. Gabius, R. Kodet, K. Smetana Jr., P. Gál, M. Kolář, *Int. J. Cancer* **2012**, *131*, 2499 – 2508.
[29] M. Adams, J. L. Jones, R. A. Walker, J. H. Pringle, S. C. Bell, *Cancer Res.* **2002**, *62*, 3289 – 3297.
[30] H.-J. Gabius, S. André, J. Jiménez-Barbero, A. Romer, D. Solís, *Trends Biochem. Sci.* **2011**, *36*, 298 – 313.
[31] J. He, L. G. Baum, *J. Biol. Chem.* **2004**, *279*, 4705 – 4712.
[32] F. Kovács-Sólyom, A. Blaskó, R. Fajka-Boja, R. L. Katona, L. Végh, J. Novák, G. J. Szebeni, L. Krenács, F. Uher, V. Tubak, R. Kiss, E. Monostori, *Immunol. Lett.* **2010**, *127*, 108 – 118.
[33] G. Rappl, H. Abken, J. M. Muche, W. Sterry, W. Tilgen, S. André, H. Kaltner, S. Ugurel, H.-J. Gabius, U. Reinhold, *Leukemia* **2002**, *16*, 840 – 845.
[34] S. Saussez, C. Decaestecker, F. Lorfevre, D. R. Cucu, G. Mortuaire, D. Chevalier, A. Wacreniez, H. Kaltner, S. André, G. Toubeau, I. Camby, H.-J. Gabius, R. Kiss, *Int. J. Oncol.* **2007**, *30*, 1109 – 1117.
[35] A. Moisa, P. Fritz, A. Eck, H. D. Wehner, T. Mürdter, W. Simon, H.-J. Gabius, *Anticancer Res.* **2007**, *27*, 2131 – 2139.
[36] K. Smetana Jr., B. Dvořánková, L. Lacina, *Folia Biol.* **2013**, *59*, 207 – 216.
[37] J. Brábek, M. Fernandes, *Lancet Oncol.* **2012**, *13*, e2 – e3.
[38] K. Sarter, S. André, H. Kaltner, M. Lensch, S. Schulze, V. Urbonaviciute, G. Schett, M. Herrmann, H.-J. Gabius, *Biochem. Biophys. Res. Commun.* **2009**, *379*, 155 – 159.
[39] H.-J. Gabius, R. Engelhardt, S. Rehm, F. Cramer, *JNCI J. Natl. Cancer Inst.* **1984**, *73*, 1349 – 1357.
[40] T. Purkrábková, K. Smetana Jr., B. Dvoránková, Z. Holíková, C. Böck, M. Lensch, S. André, R. Pytlík, F.-T. Liu, J. Klíma, K. Smetana, J. Motlík, H.-J. Gabius, *Biol. Cell* **2003**, *95*, 535 – 545.
[41] S. André, H. Sanchez-Ruderisch, H. Nakagawa, M. Buchholz, J. Kopitz, P. Forberich, W. Kemmner, C. Böck, K. Deguchi, K. M. Detjen, B. Wiedenmann, M. von Knebel Doeberitz, T. M. Gress, S.-I. Nishimura, S. Rosewicz, H.-J. Gabius, *FEBS J.* **2007**, *274*, 3233 – 3256.
[42] M. Amano, H. Eriksson, J. C. Manning, K. M. Detjen, S. André, S.-I. Nishimura, J. Lehtiö, H.-J. Gabius, *FEBS J.* **2012**, *279*, 4062 – 4080.
[43] M. Parizek, N. Kasalkova, L. Bacakova, P. Slepicka, V. Lisa, M. Blazkova, V. Svorcik, *Int. J. Mol. Sci.* **2009**, *10*, 4352 – 4374.
[44] T. Grendel, J. Sokolský, A. Vaščáková, V. Hudák, M. Chovanec, F. Sabol, S. André, H. Kaltner, H.-J. Gabius, M. Frankovičová, P. Lenčeš, J. Betka, K. Smetana Jr., P. Gál, *Folia Biol.* **2012**, *58*, 135 – 143.

Received: March 10, 2014
Published online on ■■ ■■, 0000

© 2014 Wiley-VCH Verlag GmbH & Co. KGaA, Weinheim

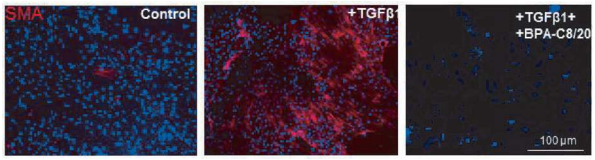

Don't start! (But do go on) TGF-β1 stimulates the conversion of fibroblasts to smooth muscle α-actin (SMA)-positive myofibroblasts. The polyamine BPA-C8 inhibits this conversion, but has no effect on cells that already express SMA. It also reduces the occurrence of an extracellular matrix around the activated fibroblasts. BPA-C8 could thus interfere with fibroblasts' effect on tumor progression.

A. Mifková, O. Kodet, P. Szabo, J. Kučera, B. Dvořánková, S. André, G. Koripelly, H.-J. Gabius, J.-M. Lehn, K. Smetana, Jr.**

■■ – ■■

Synthetic Polyamine BPA-C8 Inhibits TGF-β1-Mediated Conversion of Human Dermal Fibroblast to Myofibroblasts and Establishment of Galectin-1-Rich Extracellular Matrix in Vitro

© 2014 Wiley-VCH Verlag GmbH & Co. KGaA, Weinheim

Tumor Biol.
DOI 10.1007/s13277-015-3259-8

RESEARCH ARTICLE

Effect of cancer-associated fibroblasts on the migration of glioma cells in vitro

Jana Trylcova · Petr Busek · Karel Smetana Jr. · Eva Balaziova · Barbora Dvorankova · Alzbeta Mifkova · Aleksi Sedo

Received: 10 December 2014 / Accepted: 13 February 2015
© International Society of Oncology and BioMarkers (ISOBM) 2015

Abstract Cancer-associated fibroblasts (CAFs) significantly influence biological properties of many tumors. The role of these mesenchymal cells is also anticipated in human gliomas. To evaluate the putative role of CAFs in glioblastoma, we tested the effect of CAF conditioned media on the proliferation and chemotaxis of glioma cells. The proliferation of glioma cells was stimulated to similar extent by both the normal fibroblasts (NFs) and CAF-conditioned media. Nevertheless, CAF-conditioned media enhanced the chemotactic migration of glioma cells significantly more potently than the media from normal fibroblasts. In order to determine whether CAF-like cells are present in human glioblastomas, immunofluorescence staining was performed on tissue samples from 20 patients using markers typical for CAFs. This analysis revealed regular presence of mesenchymal cells expressing characteristic CAF markers α-smooth muscle actin and TE-7 in human glioblastomas. These observations indicate the potential role of CAF-like cells in glioblastoma biology.

Keywords Cancer-associated fibroblasts · Glioma · Mesenchymal cells · Tumor microenvironment

J. Trylcova · P. Busek · E. Balaziova · A. Sedo (✉)
Institute of Biochemistry and Experimental Oncology, First Faculty of Medicine, Charles University in Prague, U Nemocnice 5, 128 53 Prague 2, Czech Republic
e-mail: aleksi@cesnet.cz
URL: http://www.lf1.cuni.cz/lbnb

K. Smetana Jr. · B. Dvorankova · A. Mifkova
Institute of Anatomy, First Faculty of Medicine, Charles University in Prague, U Nemocnice 3, 128 53 Prague 2, Czech Republic

Introduction

Cancer microenvironment determines the biological properties of malignant tumors including their aggressive local growth and metastatic spread [1]. Cancer-associated fibroblasts (CAFs) are mesenchymal cells that represent a critical component of the tumor microenvironment and are characterized among others by the expression of alpha smooth muscle actin (α-SMA) or the fibroblast markers vimentin or TE-7 [2, 3]. The experimental data demonstrate multiple potential sources of their origin including local fibroblasts, pericytes, macrophages, endothelial cells, and mesenchymal stem cells as reviewed by Smetana and coworkers [4]. There is also evidence suggesting the transformation of cancer cells into CAFs by the process of epithelial–mesenchymal transition [5, 6]. Comparison of the CAF and normal human fibroblast transcriptomes revealed differential expression of almost 600 genes, including the increased expression of genes encoding growth factors, cytokines, and chemokines [7, 8]. The production of bioactive extracellular matrix molecules such as fibronectin, tenascin, and the endogenous lectin galectin-1 by CAFs represents an additional important aspect influencing the tumor microenvironment [9–11]. Interestingly, some biological activities of CAFs seem to be independent on the tumor type of their origin [12].

The local protumorigenic micromilieu in the primary brain tumors, including the most malignant form glioblastoma multiforme (GBM), depends on the presence of several cell types, in particular non-neoplastic astrocytes and endothelial and inflammatory cells such as microglia and macrophages typically infiltrating the tumor bed [13, 14]. Recently, Clavreul et al. [15, 16] isolated a new stromal cell population from the peritumoral tissue in patients with GBM and demonstrated that it shares several phenotypic and functional properties with CAFs. In light of these results, the presence of CAFs or "CAF-like cells" in gliomas seems to be highly probable, but the data are still limited. In addition, the possible

Published online: 25 February 2015

effect(s) of this stromal cell population on the functional properties of glioblastoma cells remain to be determined.

In our study, fibroblasts isolated from malignant melanoma are utilized as a model of CAFs derived from a neuroectodermal tumor, and their influence on the proliferation and migration of glioblastoma cells is investigated. Furthermore, the presence of cells expressing characteristic CAF markers is evaluated in human glioblastoma tissue samples.

Materials and methods

Preparation of primary fibroblast cultures from a melanoma patient and from a healthy donor

CAFs were prepared from the skin metastasis of primary nodular melanoma (Breslow index 2.25 and Clark index III) of a 56-year-old male patient who was treated at the Department of Dermatovenerology, First Faculty of Medicine, Charles University in Prague. The sample of the metastasis was cut into small pieces, which were treated with 0.25 % trypsin (Biochrom, Germany) for 30 min at 37 °C. The tissue explants were transferred to the CellBind 6-well plate (Corning, the Netherlands) and maintained in Dulbecco's modified Eagle's medium (DMEM) with antibiotics and 10 % fetal bovine serum (FBS; all Biochrom, Germany) and cultured at 37 °C and 5 % CO_2. Within 1 week, fibroblasts and keratinocytes started to migrate from the explants.

Normal dermal fibroblasts (NFs) were isolated from a skin sample of a healthy female donor who had undergone esthetic breast surgery at the Department of Plastic Surgery, Third Faculty of Medicine, Charles University in Prague. The tissue was digested overnight in 0.3 % trypsin at 4 °C, the epidermis was peeled off, and the remaining dermal tissue was processed in the same way as described above.

The cells migrating from the explants were periodically harvested by trypsinization (0.25 % trypsin and 0.02 % EDTA, Biochrom) and characterized immunocytochemically. Cultures with more than 90 % of cells negative for the leukocyte (CD45, Sigma-Aldrich Chemie, Czech Republic), the melanocyte (MELAN-A, HMB-45 both Invitrogen, USA), and epithelial (keratins, Abcam, UK) cell markers and positive for vimentin (Dako, Denmark) were considered fibroblasts. Both types of fibroblasts were expanded and the cells from the 5th (NFs) and the 7th (CAFs) passages were used for the experiments.

Cell culture of glioblastoma cell

The human glioma cell line U87 was obtained from Cell Lines Services (CLS, Germany), U373 and T98G were from the American Type Culture Collection (LGC Standards, UK). Cells were cultured under standard conditions at 37 °C in DMEM supplemented with 10 % FBS (all Sigma-Aldrich Chemie) under a humidified (>90 %) atmosphere of 5 % CO_2/95 % air.

Preparation of conditioned medium

1×10^6 fibroblasts (either CAFs or NFs) or U87 cells were seeded in 100 mm dishes in DMEM+10 % FBS. After 24 h, the medium was changed to serum-free DMEM and cells were allowed to grow for additional 72 h. The media were collected, centrifuged (225*g*, 4 °C, 4 min), sterile filtered (0.22-μm pores, Millex GV, Millipore, Ireland), and immediately used for migration and proliferation assays. In control experiments, identically processed DMEM without the exposure to cells was used.

Transwell migration

6×10^4 U87, U373, or T98G cells in DMEM were applied to the 24-well plate cell culture inserts with 8-μm pores (Becton Dickinson, Germany) and allowed to migrate towards the conditioned medium for 8 h or 24 h. Non-migrated cells were removed using a cotton swab. Migrated cells on the lower part of the membrane were fixed with 5 % glutaraldehyde in phosphate-buffered saline (PBS) for 15 min and stained with methylene blue. Five non-overlapping fields per insert were counted manually on Olympus IX70 at 200× magnification (Olympus Czech group, Czech Republic) [17]. All experiments were assayed in quadruplicates and repeated at least two times.

Growth rate analysis, determination of the Ki67 labeling index

U87 and U373 cells were seeded at 1×10^4 cells/well or glass coverslips in 24-well plates in conditioned media supplemented with 1 % FBS or DMEM supplemented with 1 % FBS as a control. After 96 h, 0.5 mL of the appropriate fresh medium was added to the wells. At the indicated time intervals, cells were harvested by trypsin/EDTA (Sigma-Aldrich Chemie) and counted using a Coulter Counter Z2 (Beckman Coulter, CA, USA). All experiments were assayed in quadruplicates and repeated at least two times. Glass coverslips were air-dried and immunocytochemical detection of Ki67 was performed as described below. The percentage of Ki67-positive nuclei was evaluated manually on a fluorescence microscope in five visual fields for each treatment condition.

Immunohistochemical detection of the mesenchymal markers α-smooth muscle actin and TE-7 in human glioblastomas, Ki67 staining in the cultured glioma cells

Glioblastoma tissues were obtained from 20 consenting patients (median age 59 years; 12 males, 8 females) operated at the Hospital Na Homolce in Prague. Tumors were graded in compliance with the current WHO classification criteria. Tissue samples, clear of macroscopic vessels and necrosis, were frozen on solid CO_2 and then stored at −80 °C. Ten-micrometer-thick frozen sections were fixed with 4 % paraformaldehyde, blocked with 10 % fetal calf serum plus 1 % bovine serum albumin in

Tris-buffered saline (TBS) and incubated overnight at 4 °C with the primary antibodies against alpha smooth muscle actin [1A4] (Abcam, ab7817 1:200) or the marker of fibroblasts TE-7 (Millipore, CBL271, 1:100); the anti-GFAP (Abcam, ab7260, 1:500), anti-von Willebrand factor (Dako, 1:200) and anti-CD31 (Abcam, ab28364, 1:50) antibodies were used to visualize the glial and the endothelial cells, respectively, and anti-Ki67 (Dako, clone MIB-5, 1:50) was used to identify proliferating glioma cells in culture. After washing away the non-bound primary antibodies, the slides or cells on coverslips were incubated for 1 h at room temperature with the corresponding Alexa Fluor 488 or 546 conjugated secondary antibodies (1:500, Life Sciences); ToPro (Life Sciences) or DAPI (Sigma-Aldrich Chemie) were used for nuclear counterstaining. The primary antibodies were replaced by irrelevant antibodies of the same isotype or omitted in the staining controls. Slides were mounted in Aqua Polymount (Polysciences, Germany) and viewed on the Olympus IX 81 confocal microscope equipped with the 488, 543, and 633 nm lasers (FluoView 300, Olympus Czech group) or on the ECLIPSE-90i (Nikon, Czech group) fluorescence microscope equipped with a Cool-1300Q CCD camera (Vosskühler, Germany) and the computer-assisted image analysis system LUCIA 5.1 (Laboratory Imaging, Czech Republic).

Statistical analysis

The Statistica 12 software (StatSoft CR s.r.o., Czech Republic) was used for all statistical analyses. The value of $p<0.05$ was considered statistically significant.

Results

CAF- and NF-conditioned media promote the growth of glioma cells in vitro

To determine whether mesenchymal cells produce local mediators that influence the growth properties of glioma

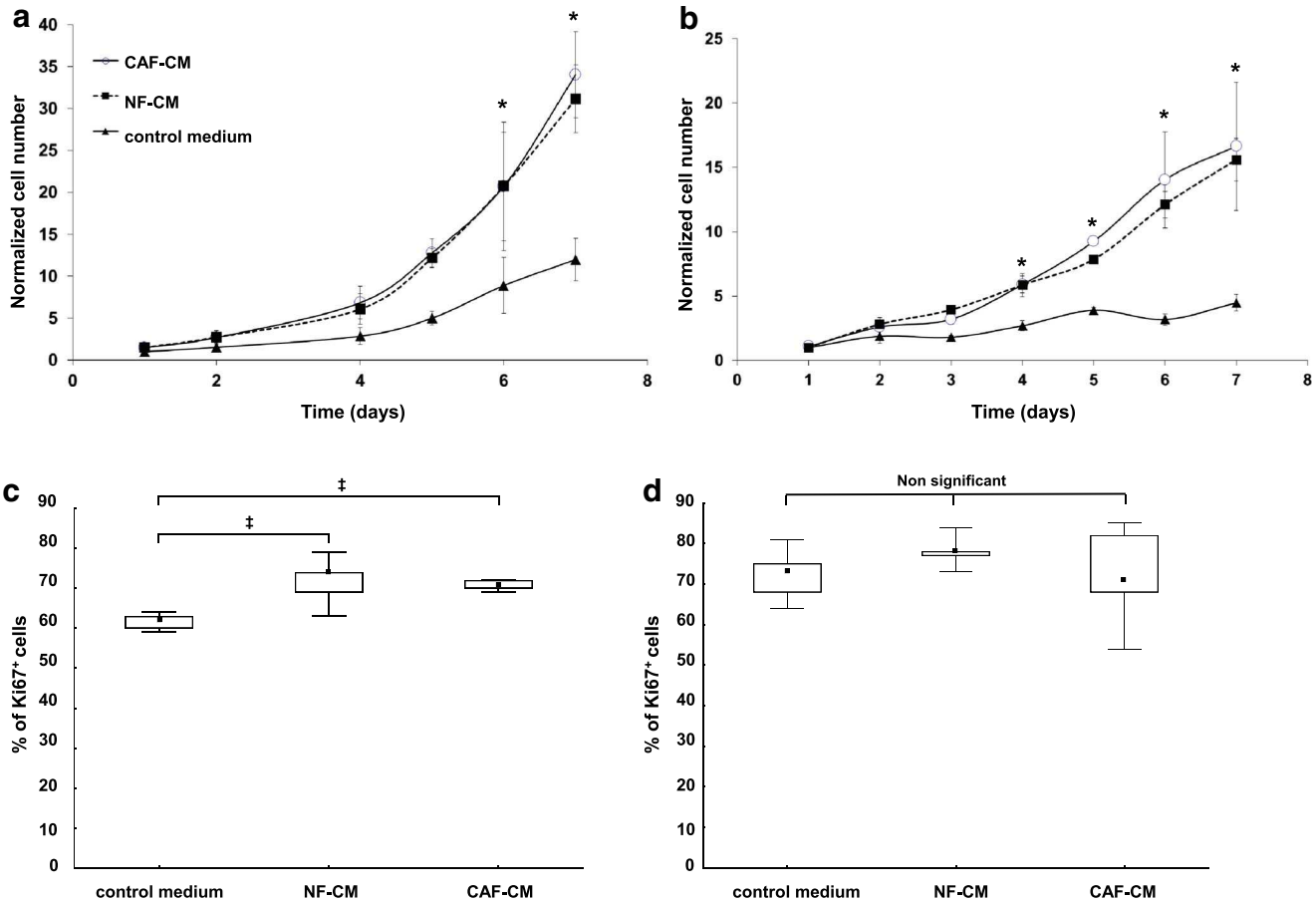

Fig. 1 Growth of **a** U87 and **b** U373 glioma cells cultured in normal fibroblast (NF)- and cancer-associated fibroblast (CAF)-conditioned media supplemented with 1 % FBS. Cell numbers were normalized to the values in control media at day 1; results are depicted as mean±SD from at least two independent experiments performed in quadruplicates. Proportion of Ki67-positive **c** U87 and **d** U373 glioma cells on day 2 of culture in NF- and CAF-conditioned media supplemented with 1 % FBS. *$p<0.01$ (repeated measurement ANOVA, Scheffe post hoc test) and ‡$p<0.05$ (Mann–Whitney U test) for NF- and CAF-conditioned media vs. control

cells, U87 and U373 cells were cultured in CAF- and NF-conditioned medium supplemented with 1 % FBS. We observed increased in vitro cell growth in conditioned media compared to controls in both cell lines (Fig. 1a, b). Compared to controls, the cell numbers in NF- and CAF-conditioned media were 2.6 and 2.8 times higher in U87 and 3.5 and 3.7 times higher in U373 after 1 week. The difference between CAF- and NF-conditioned media was statistically insignificant in both U87 and U373 cells. In U87, the enhanced cell growth in both conditioned media was associated with an increased positivity of the cell proliferation marker Ki67 at day 2 of cell culture (Fig. 1c). The percentage of Ki67-positive U373 cells at day 2 was not significantly influenced by the conditioned media and was above 70 % (Fig. 1d). Using a flow cytometry, we observed very low proportion of the sub-G1 particles (below 5 %) without a clear apoptotic peak in both cell lines suggesting that suppression of apoptosis does not significantly contribute to the growth promoting effect of the conditioned media (data not shown).

Overall, these data indicate that CAFs as well as NFs secrete factor(s) that stimulate the growth of glioma cells in vitro to a similar extent.

CAF-conditioned medium acts as a more potent chemoattractant compared to NF-conditioned medium

In addition to promoting the proliferation of the transformed cells, the stromal cells may also influence their migration. Using a transwell migration assay, we compared the chemotactic effect of the CAF- and NF-conditioned media on U87. Both conditioned media promoted glioma cell migration compared to the control medium (Fig. 2a) with a more pronounced increase in the CAF-conditioned medium (2.2-fold compared to NF-conditioned medium, $p<0.01$). Similar results were obtained in U373 and T98G glioma cells with approximately 40 % more cells migrating in CAF-conditioned medium compared to NF-conditioned medium ($p<0.01$, Fig. 2b). These results indicate that the production of secreted chemotactic mediators by CAFs is qualitatively and/or quantitatively greater compared to NFs.

α-SMA and TE-7 expressing cells are present in human glioblastomas

CAFs are regularly occurring stromal cells in epithelial cancers, but whether an equivalent mesenchymal stromal subpopulation is present in the microenvironment of gliomas is poorly defined

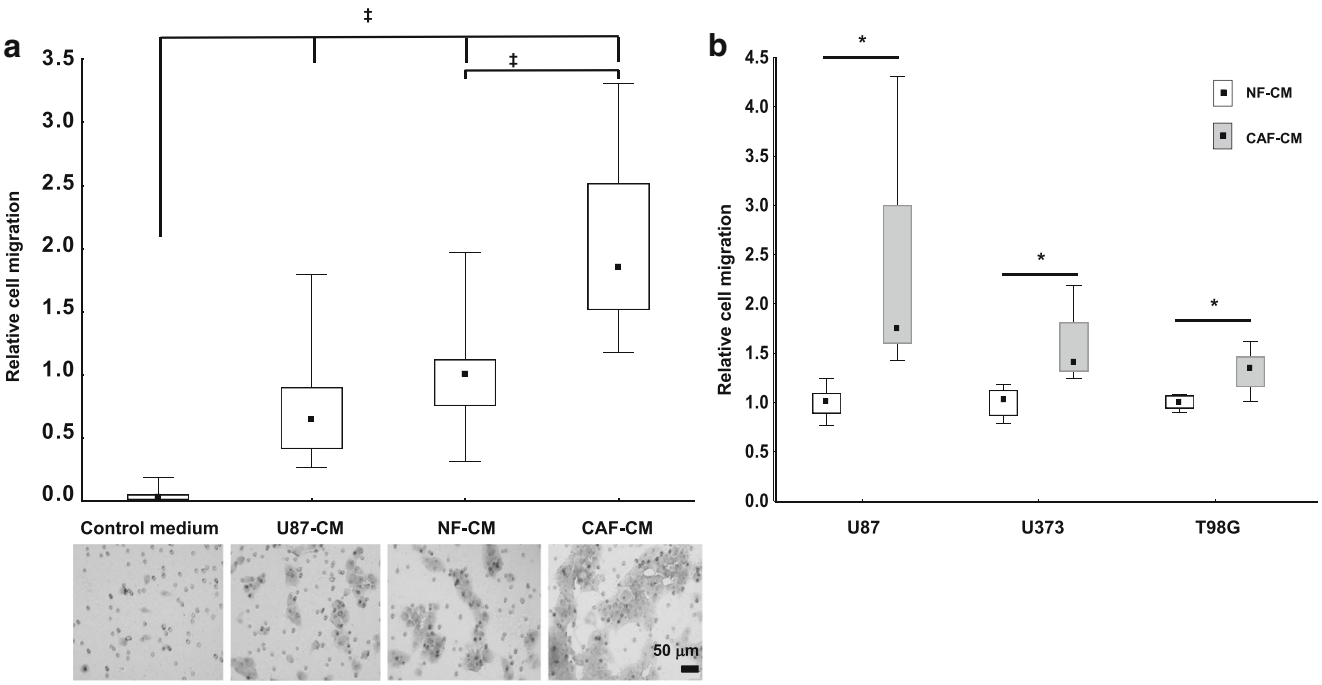

Fig. 2 **a** Chemotaxis of U87 glioma cells towards control non-conditioned serum-free medium and conditioned serum-free media from the cultures of U87 (U87-CM), normal fibroblasts (NF-CM), and cancer-associated fibroblasts (CAF-CM). Cell migration was evaluated after 24 h; representative microphotographs of the transmigrated cells in the specified media are shown below the corresponding boxes. $^{‡}p<0.01$, Kruskal–Wallis test. **b** Chemotaxis of U87, U373, and T98G glioma cells towards the serum-free NF-CM and CAF-CM. Cell migration was evaluated after 8 h, $*p<0.01$, Mann–Whitney *U* test. Cell numbers from at least two independent experiments performed in quadruplicates were normalized to the values of cell migration in normal fibroblast-conditioned media in each individual experiment; *squares*—medians; *boxes*—25–75 % of the values; *bars*—range of non-remote values

[14]. We therefore analyzed the expression of markers typically expressed by CAFs in 20 patients with untreated, newly diagnosed glioblastoma. Using immunohistochemistry, α-SMA was detected in 50 % of the cases and the fibroblast and mesodermal cell marker TE-7 [3, 18] was present in 70 % of the tumors (Fig. 3a). Both markers were expressed in GFAP-negative cells (Fig. 3b) that appeared to be predominantly localized around abnormal blood vessels (Fig. 3c). Thus, host mesenchymal cells exhibiting characteristics of CAFs are present in the tissue of human glioblastomas.

Discussion

The biological processes involved in tumorigenesis, such as cell growth, differentiation, local aggressiveness, and metastatic spread of the transformed cells, are in large part determined by the complex interactions in the tumor microenvironment [19]. Recent findings rank CAFs among the key drivers of the tumor micromilieu [2]. CAFs produce extracellular matrix as well as participate on its proteolytic degradation. In addition, CAFs release a wide variety of local mediators, including growth factors, and thus affect other stromal and tumor cells [4].

Gliomagenesis substantially depends on the tumor microenvironment. For example, the endothelial cells and other components of the neurovascular unit establish a perivascular niche critical for the maintenance of glioma cancer stem-like cells and microglia/macrophages importantly contribute to the invasiveness of glioma cells (reviewed in [20, 21, 14]). In comparison to other solid tumors, it is currently unknown whether and how CAFs or corresponding "CAF-like cells" participate in the glioma formation and further development. The results obtained in our study demonstrate the presence of GFAP-negative cells expressing the CAF markers (α-SMA, TE-7) within the human glioblastoma microenvironment. This is in agreement with the results of Clavreul et al. [15] who isolated a subpopulation of stromal α-SMA expressing cells resembling CAFs from the brain tissue adjacent to glioblastomas. Pericytes frequently express α-SMA and may exhibit functions analogous to fibroblasts such as scar formation in the central nervous system [22]. These cells are thus a potential local source of CAF-like cells in glioblastomas. α-

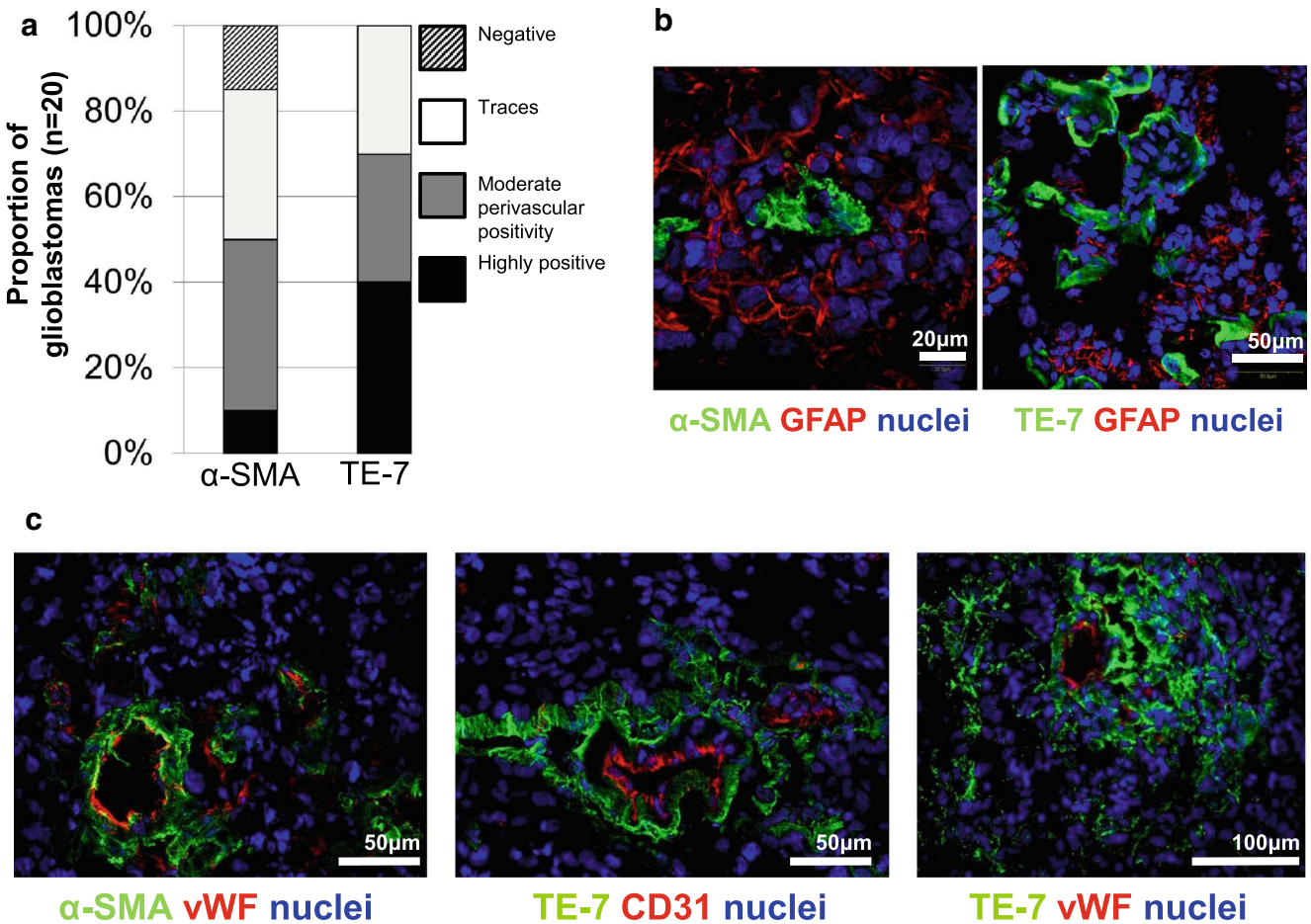

Fig. 3 Detection of the α-smooth muscle actin (α-SMA) and the fibroblast marker TE-7 expressing cells in human glioblastomas by immunohistochemistry. **a** Semiquantitative evaluation of α-SMA and TE-7 expression in 20 human glioblastomas. **b** Double labeling with the marker of astrocytic cells GFAP and **c** the markers of vascular cells CD31 and von Willebrand factor (vWF). Nuclei were counterstained with ToPro-3

SMA-positive pericytes significantly contribute to microvascular proliferates [23] and experimental studies suggest their important role in glioma neovascularization [24]. Another potential source of the CAF-like cells in glioblastomas are the host mesenchymal stem cells that are recruited to gliomas [25] and probably also provide an active support for the tumor neovascularization [26, 16].

In order to analyze the possible paracrine interactions between the mesenchymal cells and glioma cells, CAFs isolated from human melanoma were used in our model. Both glioblastoma and malignant melanoma are of neuroectodermal origin and, moreover, we previously showed that the biological activity of CAFs is not strictly dependent on the tumor type of their origin [12].

Here, we demonstrate that the growth as well as the migration of glioma cells is significantly stimulated by CAF-conditioned media. The growth-promoting effect of the conditioned media is most likely caused by the increased proliferation of the glioma cells as suggested by the higher percentage of the cells expressing Ki67 in U87 cells. The increase of the Ki67-positive fraction was not apparent in U373 cells, possibly due to their overall high (above 70 %) Ki67-labeling index under control conditions. In our experimental setting, the growth enhancement of glioma cells was quantitatively similar in the CAF- and NF-conditioned media. Although normal human fibroblasts may have inhibitory effects on the growth of malignant cells in the initial phases of malignant transformation, this effect seems to be reversed to growth support in more advanced cancers [27]. Fibroblasts produce a variety of biologically active substances including proteins of the extracellular matrix and growth factors that can support the maintenance of stem cells [28] and similar factors may be involved in their growth-promoting effects in glioma cells. It remains to be determined whether the proproliferative effect of CAFs is mediated by the same set of secreted factors as in NFs.

In contrast to their almost equal growth-promoting effect in glioma cells, CAF- and NF-conditioned media quantitatively differed in their capacity to enhance the glioma cell migration with the CAF-conditioned medium being a more potent inducer. Several paracrine factors known to be secreted by the CAFs—or their appropriate combination—might be responsible for this effect. Galectin-1 participates in the transition of fibroblasts to CAFs [10] and was shown to increase glioma cell migration [29, 30]. In addition, CAFs also produce IL-6, TGF-beta, hepatocyte growth factor (HGF), and chemokines such as CXCL-12 [2] that are known to enhance the migration of glioma cells by a variety of mechanism [29]. The detailed investigation of the secreted factor(s) and signaling pathways responsible for the promigratory effects of CAFs in glioma cells will be the subject of future research.

In conclusion, our observations confirm that stromal cells with mesenchymal characteristics are an integral component of the human glioblastoma microenvironment in vivo. Moreover, our data suggest that this mesenchymal stromal component may specifically participate on the control of glioma cell growth and migration by soluble factor(s).

Acknowledgments This work was supported by the following grants: Grant Agency of the Charles University in Prague (GAUK) project 44214, Internal Grant Agency of the Ministry of Health of the Czech Republic (IGA) project 12237-5/2011, University Research Centers (UNCE) project 204013, Charles University Research Development Schemes (PRVOUK) project P27/LF1/1, Czech Science Foundation (GAČR) project P304-12-1333, Specific Academic Research Projects (SVV) project 260032, and by the project "BIOCEV – Biotechnology and Biomedicine Center of the Academy of Sciences and Charles University" (CZ.1.05/1.1.00/02.0109), from the European Regional Development Fund.

Ethical approval An informed consent was obtained from all individual participants included in the study. All procedures performed in studies involving human participants were in accordance with the ethical standards of the institutional and/or national research committee and with the 1964 Helsinki Declaration and its later amendments or comparable ethical standards. This article does not contain any studies with animals performed by any of the authors.

Conflicts of interest None.

References

1. Polyak K, Haviv I, Campbell IG. Co-evolution of tumor cells and their microenvironment. Trends in genetics. TIG. 2009;25(1):30–8. doi:10.1016/j.tig.2008.10.012.
2. Cirri P, Chiarugi P. Cancer associated fibroblasts: the dark side of the coin. Am J Cancer Res. 2011;1(4):482–97.
3. Goodpaster T, Legesse-Miller A, Hameed MR, Aisner SC, Randolph-Habecker J, Coller HA. An immunohistochemical method for identifying fibroblasts in formalin-fixed, paraffin-embedded tissue. J Histochem Cytochem Off J Histochem Soc. 2008;56(4):347–58. doi:10.1369/jhc.7A7287.2007.
4. Smetana K, Dvorankova B, Szabo P, Strnad H, Kolar M. Role of stromal fibroblasts in cancer originated from squamous epithelia. In: Bai X, editor. Dermal fibroblasts: histological perspectives, characterization and role in disease. New York: Nova Sciences Publishers; 2013. p. 83–94.
5. De Wever O, Demetter P, Mareel M, Bracke M. Stromal myofibroblasts are drivers of invasive cancer growth. Int J Cancer J Int du Cancer. 2008;123(10):2229–38. doi:10.1002/ijc.23925.
6. Haviv I, Polyak K, Qiu W, Hu M, Campbell I. Origin of carcinoma associated fibroblasts. Cell Cycle. 2009;8(4):589–95.
7. Strnad H, Lacina L, Kolar M, Cada Z, Vlcek C, Dvorankova B, et al. Head and neck squamous cancer stromal fibroblasts produce growth factors influencing phenotype of normal human keratinocytes. Histochem Cell Biol. 2010;133(2):201–11. doi:10.1007/s00418-009-0661-6.
8. Kolar M, Szabo P, Dvorankova B, Lacina L, Gabius HJ, Strnad H, et al. Upregulation of IL-6, IL-8 and CXCL-1 production in dermal fibroblasts by normal/malignant epithelial cells in vitro: immunohistochemical and transcriptomic analyses. Biol Cell / Under Auspices Europ Cell Biol Org. 2012;104(12):738–51. doi:10.1111/boc.201200018.

9. Dvorankova B, Szabo P, Lacina L, Gal P, Uhrova J, Zima T, et al. Human galectins induce conversion of dermal fibroblasts into myofibroblasts and production of extracellular matrix: potential application in tissue engineering and wound repair. Cells Tissues Organs. 2011;194(6):469–80. doi:10.1159/000324864.
10. Valach J, Fik Z, Strnad H, Chovanec M, Plzak J, Cada Z, et al. Smooth muscle actin-expressing stromal fibroblasts in head and neck squamous cell carcinoma: increased expression of galectin-1 and induction of poor prognosis factors. Int J Cancer J Int du Cancer. 2012;131(11):2499–508. doi:10.1002/ijc.27550.
11. Mifkova A, Kodet O, Szabo P, Kucera J, Dvorankova B, Andre S, et al. Synthetic polyamine BPA-C8 inhibits TGF-beta1-mediated conversion of human dermal fibroblast to myofibroblasts and establishment of galectin-1-rich extracellular matrix in vitro. Chembiochem Europ J Chem Biol. 2014;15(10):1465–70. doi:10.1002/cbic.201402087.
12. Dvorankova B, Szabo P, Lacina L, Kodet O, Matouskova E, Smetana Jr K. Fibroblasts prepared from different types of malignant tumors stimulate expression of luminal marker keratin 8 in the EM-G3 breast cancer cell line. Histochem Cell Biol. 2012;137(5):679–85. doi:10.1007/s00418-012-0918-3.
13. da Fonseca AC, Badie B. Microglia and macrophages in malignant gliomas: recent discoveries and implications for promising therapies. Clinic Dev Immunol. 2013;2013:264124. doi:10.1155/2013/264124.
14. Charles NA, Holland EC, Gilbertson R, Glass R, Kettenmann H. The brain tumor microenvironment. Glia. 2012;60(3):502–14.
15. Clavreul A, Etcheverry A, Chassevent A, Quillien V, Avril T, Jourdan ML, et al. Isolation of a new cell population in the glioblastoma microenvironment. J Neuro-Oncol. 2012;106(3):493–504. doi:10.1007/s11060-011-0701-7.
16. Clavreul A, Guette C, Faguer R, Tetaud C, Boissard A, Lemaire L, et al. Glioblastoma-associated stromal cells (GASCs) from histologically normal surgical margins have a myofibroblast phenotype and angiogenic properties. J Pathol. 2014;233(1):74–88. doi:10.1002/path.4332.
17. Busek P, Stremenova J, Sromova L, Hilser M, Balaziova E, Kosek D, et al. Dipeptidyl peptidase-IV inhibits glioma cell growth independent of its enzymatic activity. Int J Biochem Cell Biol. 2012;44(5):738–47. doi:10.1016/j.biocel.2012.01.011.
18. Haynes BF, Scearce RM, Lobach DF, Hensley LL. Phenotypic characterization and ontogeny of mesodermal-derived and endocrine epithelial components of the human thymic microenvironment. J Experiment Med. 1984;159(4):1149–68.
19. Li H, Fan X, Houghton J. Tumor microenvironment: the role of the tumor stroma in cancer. J Cell Biochem. 2007;101(4):805–15. doi:10.1002/jcb.21159.
20. Filatova A, Acker T, Garvalov BK. The cancer stem cell niche(s): the crosstalk between glioma stem cells and their microenvironment. Biochim Biophys Acta. 2013;1830(2):2496–508. doi:10.1016/j.bbagen.2012.10.008.
21. Persano L, Rampazzo E, Basso G, Viola G. Glioblastoma cancer stem cells: role of the microenvironment and therapeutic targeting. Biochem Pharmacol. 2013;85(5):612–22. doi:10.1016/j.bcp.2012.10.001.
22. Goritz C, Dias DO, Tomilin N, Barbacid M, Shupliakov O, Frisen J. A pericyte origin of spinal cord scar tissue. Science. 2011;333(6039):238–42. doi:10.1126/science.1203165.
23. Wesseling P, Schlingemann RO, Rietveld FJ, Link M, Burger PC, Ruiter DJ. Early and extensive contribution of pericytes/vascular smooth muscle cells to microvascular proliferation in glioblastoma multiforme: an immuno-light and immuno-electron microscopic study. J Neuropathol Exp Neurol. 1995;54(3):304–10.
24. Najbauer J, Huszthy PC, Barish ME, Garcia E, Metz MZ, Myers SM, et al. Cellular host responses to gliomas. PLoS One. 2012;7(4):e35150. doi:10.1371/journal.pone.0035150.
25. Behnan J, Isakson P, Joel M, Cilio C, Langmoen IA, Vik-Mo EO, et al. Recruited brain tumor-derived mesenchymal stem cells contribute to brain tumor progression. Stem Cells. 2014;32(5):1110–23. doi:10.1002/stem.1614.
26. Birnbaum T, Hildebrandt J, Nuebling G, Sostak P, Straube A. Glioblastoma-dependent differentiation and angiogenic potential of human mesenchymal stem cells in vitro. J Neuro-Oncol. 2011;105(1):57–65. doi:10.1007/s11060-011-0561-1.
27. Cornil I, Theodorescu D, Man S, Herlyn M, Jambrosic J, Kerbel RS. Fibroblast cell interactions with human melanoma cells affect tumor cell growth as a function of tumor progression. Proc Natl Acad Sci U S A. 1991;88(14):6028–32.
28. Prowse AB, McQuade LR, Bryant KJ, Marcal H, Gray PP. Identification of potential pluripotency determinants for human embryonic stem cells following proteomic analysis of human and mouse fibroblast conditioned media. J Proteome Res. 2007;6(9):3796–807. doi:10.1021/pr0702262.
29. Sayegh ET, Kaur G, Bloch O, Parsa AT. Systematic review of protein biomarkers of invasive behavior in glioblastoma. Mol Neurobiol. 2014;49(3):1212–44. doi:10.1007/s12035-013-8593-5.
30. Camby I, Belot N, Lefranc F, Sadeghi N, de Launoit Y, Kaltner H, et al. Galectin-1 modulates human glioblastoma cell migration into the brain through modifications to the actin cytoskeleton and levels of expression of small GTPases. J Neuropathol Exp Neurol. 2002;61(7):585–96.

ANTICANCER RESEARCH
International Journal of Cancer Research and Treatment
ISSN: 0250-7005

Genome-wide Expression Profiling (with Focus on the Galectin Network) in Tumor, Transition Zone and Normal Tissue of Head and Neck Cancer: Marked Differences Between Individual Patients and the Site of Specimen Origin

VERONIKA ZIVICOVA[1,2*], PETR BROZ[3*], ZDENEK FIK[1,2], ALZBETA MIFKOVA[1,2], JAN PLZAK[2], ZDENEK CADA[2], HERBERT KALTNER[4], JANA FIALOVA KUCEROVA[3], HANS-JOACHIM GABIUS[4] and KAREL SMETANA JR.[1,5]

[1]Institute of Anatomy, and [2]Department of Otorhinolaryngology, Head and Neck Surgery, First Faculty of Medicine, Charles University, Prague, Czech Republic;
[3]Institute of Applied Biotechnologies, Prague, Czech Republic;
[4]Institute of Physiological Chemistry, Faculty of Veterinary Medicine, Ludwig Maximilian University, Munich, Germany;
[5]BIOCEV, First Faculty of Medicine, Charles University, Vestec, Czech Republic

Reprinted from
ANTICANCER RESEARCH *37*: 2275-2288 (2017)

ANTICANCER RESEARCH

International Journal of Cancer Research and Treatment

HighWire Press® STANFORD UNIVERSITY

ISSN (print): 0250-7005
ISSN (online): 1791-7530

Editorial Board

P. A. ABRAHAMSSON, *Malmö, Sweden*
B. B. AGGARWAL, *Houston, TX, USA*
T. AKIMOTO, *Kashiwa, Chiba, Japan*
P. Z. ANASTASIADIS, *Jacksonville, FL, USA*
A. ARGIRIS, *San Antonio, TX, USA*
J. P. ARMAND, *Toulouse, France*
V. I. AVRAMIS, *Los Angeles, CA, USA*
D.-T. BAU, *Taichung, Taiwan, ROC*
G. BAUER, *Freiburg, Germany*
E. E. BAULIEU, *Le Kremlin-Bicetre, France*
E. J. BENZ, Jr., *Boston, MA, USA*
J. BERGH, *Stockholm, Sweden*
F. T. BOSMAN, *Lausanne, Switzerland*
M. BOUVET, *La Jolla, CA, USA*
J. BOYD, *Miami, FL, USA*
G. BROICH, *Monza, Italy*
Ø. S. BRULAND, *Oslo, Norway*
J. M. BUATTI, *Iowa City, IA, USA*
M. M. BURGER, *Basel, Switzerland*
M. CARBONE, *Honolulu, HI, USA*
C. CARLBERG, *Kuopio, Finland*
J. CARLSSON, *Uppsala, Sweden*
A. F. CHAMBERS, *London, ON, Canada*
P. CHANDRA, *Frankfurt am Main, Germany*
L. CHENG, *Indianapolis, IN, USA*
J.-G. CHUNG, *Taichung, Taiwan, ROC*
R. CLARKE, *Washington, DC, USA*
E. DE CLERCQ, *Leuven, Belgium*
W. DEN OTTER, *Amsterdam, The Netherlands*
E. P. DIAMANDIS, *Toronto, ON, Canada*
G. TH. DIAMANDOPOULOS, *Boston, MA, USA*
D. W. FELSHER, *Stanford, CA, USA*
J. A. FERNANDEZ-POL, *Chesterfield, MO, USA*
I. J. FIDLER, *Houston, TX, USA*
A. P. FIELDS, *Jacksonville, FL, USA*
H. FU, *Atlanta, GA, USA*
B. FUCHS, *Zurich, Switzerland*
D. FUCHS, *Innsbruck, Austria*
G. GABBIANI, *Geneva, Switzerland*
R. GANAPATHI, *Charlotte, NC, USA*
A. F. GAZDAR, *Dallas, TX, USA*
J. H. GESCHWIND, *Baltimore, MD, USA*
A. GIORDANO, *Philadelphia, PA, USA*
G. GITSCH, *Freiburg, Germany*
R. H. GOLDFARB, *Guilford, CT, USA*
L. HELSON, *Quakertown, PA, USA*
R. HENRIKSSON, *Umeå, Sweden*
R. M. HOFFMAN, *San Diego, CA, USA*
S. C. JHANWAR, *New York, NY, USA*
J. V. JOHANNESSEN, *Oslo, Norway*
B. KAINA, *Mainz, Germany*
P. -L. KELLOKUMPU-LEHTINEN, *Tampere, Finland*
D. G. KIEBACK, *Schleswig, Germany*
R. KLAPDOR, *Hamburg, Germany*
S. D. KOTTARIDIS, *Athens, Greece*
G. R. F. KRUEGER, *Köln, Germany*
Pat M. KUMAR, *Manchester, UK*
Shant KUMAR, *Manchester, UK*
O. D. LAERUM, *Bergen, Norway*
F. J. LEJEUNE, *Lausanne, Switzerland*
S. LINDER, *Linköping, Sweden*
L. F. LIU, *Piscataway, NJ, USA*
D. M. LOPEZ, *Miami, FL, USA*
E. LUNDGREN, *Umeå, Sweden*
Y. MAEHARA, *Fukuoka, Japan*
J. MAHER, *London, UK*
J. MARESCAUX, *Strasbourg, France*
J. MARK, *Skövde, Sweden*
S. S. MARTIN, *Baltimore, MD, USA*
S. MITRA, *Houston, TX, USA*
S. MIYAMOTO, *Fukuoka, Japan*
S. MONCADA, *Manchester, UK*
M. MUELLER, *Villingen-Schwenningen, Germany*
F. M. MUGGIA, *New York, NY, USA*
M. NAMIKI, *Kanazawa, Ishikawa, Japan*
R. NARAYANAN, *Boca Raton, FL, USA*
K. NILSSON, *Uppsala, Sweden*
S. PATHAK, *Houston, TX, USA*
J.L. PERSSON, *Malmö, Sweden*
G. J. PILKINGTON, *Portsmouth, UK*
C. D. PLATSOUCAS, *Norfolk, VA, USA*
A. POLLIACK, *Jerusalem, Israel*
M. RIGAUD, *Limoges, France*
U. RINGBORG, *Stockholm, Sweden*
M. ROSELLI, *Rome, Italy*
S.T. ROSEN, *Duarte, CA, USA*
A. SCHAUER, *Göttingen, Germany*
M. SCHNEIDER, *Wuppertal, Germany*
J. SEHOULI, *Berlin, Germany*
A. SETH, *Toronto, ON, Canada*
G. V. SHERBET, *Newcastle-upon-Tyne, UK*
A. SLOMINSKI, *Birmingham, AL, USA*
G.-I. SOMA, *Kagawa, Japan*
G. S. STEIN, *Burlington, VT, USA*
T. STIGBRAND, *Umeå, Sweden*
T. M. THEOPHANIDES, *Athens, Greece*
P. M. UELAND, *Bergen, Norway*
H. VAN VLIERBERGHE, *Ghent, Belgium*
R. G. VILE, *Rochester, MN, USA*
M. WELLER, *Zurich, Switzerland*
J. WESTERMARCK, *Turku, Finland*
B. WESTERMARK, *Uppsala, Sweden*
Y. YEN, *Duarte, CA, USA*
M.R.I. YOUNG, *Charleston, SC, USA*
B. ZUMOFF, *New York, NY, USA*

G. J. DELINASIOS, *Athens, Greece*
Managing Editor and Executive Publisher

J. G. DELINASIOS, *Athens, Greece*
Managing Editor (1981-2016)

Editorial Office: International Institute of Anticancer Research, 1st km Kapandritiou-Kalamou Rd., Kapandriti, P.O. Box 22, Attiki 19014, Greece. Tel / Fax: +30-22950-53389.

U.S. Branch: Anticancer Research USA, Inc., 111 Bay Avenue, Highlands, NJ 07732, USA.

E-mails: Editorial Office: journals@iiar-anticancer.org
Managing Editor: editor@iiar-anticancer.org

ANTICANCER RESEARCH supports: (a) the establishment and the activities of the INTERNATIONAL INSTITUTE OF ANTICANCER RESEARCH (IIAR; Kapandriti, Attiki, Greece); and (b) the organization of the International Conferences of Anticancer Research. The IIAR is a member of UICC. For more information about ANTICANCER RESEARCH, IIAR and the Conferences, please visit the IIAR website: www.iiar-anticancer.org

Publication Data: ANTICANCER RESEARCH (AR) is published bimonthly from January 1981 to December 2008 and monthly from January 2009. Each annual volume comprises 12 issues. Annual Author and Subject Indices are included in the last issue of each volume. ANTICANCER RESEARCH Vol. 24 (2004) and onwards appears online with Stanford University HighWire Press from April 2009.

Copyright: On publication of a manuscript in AR, which is a copyrighted publication, the legal ownership of all published parts of the paper passes from the Author(s) to the Journal.

Annual Subscription Rates 2017 per volume: Institutional subscription US$ 1,898.00 (online) or US$ 2,277.00 (print & online). Personal subscription US$ 897.00 (online) or US$ 1,277.00 (print & online). Prices include rapid delivery and insurance. The complete previous volumes of Anticancer Research (Vol. 1-36, 1981-2016) are available at 50% discount on the above rates.

Subscription Orders: Orders can be placed at agencies, bookstores, or directly with the Publisher. (e-mail: subscriptions@iiar-anticancer.org)

Advertising: All correspondence and rate requests should be addressed to the Editorial Office.

Book Reviews: Recently published books and journals should be sent to the Editorial Office. Reviews will be published within 2-4 months.

Articles in ANTICANCER RESEARCH are regularly indexed in all bibliographic services, including Current Contents (Life Sciences), Science Citation Index, Index Medicus, Biological Abstracts, PubMed, Chemical Abstracts, Excerpta Medica, University of Sheffield Biomedical Information Service, Current Clinical Cancer, AIDS Abstracts, Elsevier Bibliographic Database, EMBASE, Compendex, GEOBASE, EMBiology, Elsevier BIOBASE, FLUIDEX, World Textiles, Scopus, Progress in Palliative Care, Cambridge Scientific Abstracts, Cancergram (International Cancer Research Data Bank), MEDLINE, Reference Update - RIS Inc., PASCAL-CNRS, Inpharma-Reactions (Datastar, BRS), CABS, Immunology Abstracts, Telegen Abstracts, Genetics Abstracts, Nutrition Research Newsletter, Dairy Science Abstracts, Current Titles in Dentistry, Inpharma Weekly, BioBase, MedBase, CAB Abstracts/Global Health Databases, Investigational Drugs Database, VINITI Abstracts Journal, Leeds Medical Information, PubsHub, Sociedad Iberoamericana de Información Científíca (SIIC) Data Bases.

Obtaining permission to reuse or reproduce our content: AR has partnered with Copyright Clearance Center (CCC) to make it easy to secure permissions to reuse its content. Please visit www.copyright.com and enter the title that you are requesting permission for in the 'Get Permission' search box. For assistance in placing a permission request, Copyright Clearance Center can be contacted directly at: Copyright Clearance Center, 222 Rosewood Drive, Danvers, MA 01923 USA. Phone: +1-978-750-8400. Fax: +1-978-646-8600. E-mail: info@copyright.com.

The Editors and Publishers of ANTICANCER RESEARCH accept no responsibility for the opinions expressed by the contributors or for the content of advertisements appearing therein.

Copyright© 2017, International Institute of Anticancer Research (Dr. George J. Delinasios), All rights reserved.

D.T.P. BY IIAR

PRINTED BY ENTYPO, ATHENS, GREECE. PRINTED ON ACID-FREE PAPER

ANTICANCER RESEARCH *37*: 2275-2288 (2017)
doi:10.21873/anticanres.11565

Genome-wide Expression Profiling (with Focus on the Galectin Network) in Tumor, Transition Zone and Normal Tissue of Head and Neck Cancer: Marked Differences Between Individual Patients and the Site of Specimen Origin

VERONIKA ZIVICOVA[1,2*], PETR BROZ[3*], ZDENEK FIK[1,2], ALZBETA MIFKOVA[1,2], JAN PLZAK[2], ZDENEK CADA[2], HERBERT KALTNER[4], JANA FIALOVA KUCEROVA[3], HANS-JOACHIM GABIUS[4] and KAREL SMETANA JR.[1,5]

[1]*Institute of Anatomy, and* [2]*Department of Otorhinolaryngology, Head and Neck Surgery, First Faculty of Medicine, Charles University, Prague, Czech Republic;*
[3]*Institute of Applied Biotechnologies, Prague, Czech Republic;*
[4]*Institute of Physiological Chemistry, Faculty of Veterinary Medicine, Ludwig Maximilian University, Munich, Germany;*
[5]*BIOCEV, First Faculty of Medicine, Charles University, Vestec, Czech Republic*

Abstract. *Background/Aim: Expression profiling was performed to delineate and characterize the impact of malignancy by comparing tissues from three sites of head and neck cancer of each patient, also determining interindividual variability. Materials and Methods: Genome-wide analysis was carried out covering the expression of 25,832 genes with quantification for each site of seven patients with tonsillar or oropharyngeal squamous cell carcinoma. Immunohistochemical analysis was performed for adhesion/growth-regulatory galectins, three pro-inflammatory chemo- and cytokines and keratins. Results: Up- and down-regulation was found for 281 (tumor vs. normal) and 276 genes (transition zone vs. normal), respectively. The profile of the transition zone had its own features, with similarity to the tumor. Galectins were affected in a network manner, with differential regulation and interindividual variability between patients, also true for keratins and the chemo- and cytokines. Conclusion: These results underline special features at each site of specimen origin as well as the importance of analyzing galectins as a network and of defining the expression status of the individual patient prior to reaching clinically relevant conclusions.*

*These Authors contributed equally to this study.

Correspondence to: Karel Smetana Jr., Institute of Anatomy, 1st Faculty of Medicine, Charles University, U Nemocnice 3, 128 00 Prague 2, Czech Republic. E-mail: karel.smetana@lf1.cuni.cz

Key Words: Adhesion, glycosylation, lectin, malignancy, proliferation.

Squamous cell carcinoma (SCC) of the head and neck continues to be a major clinical challenge (1). This tumor type is characterized by locally aggressive growth, lymph node metastasis and limited spread beyond lymph nodes (2). Radical surgery represents the main therapeutic modality but can have unfavorable consequences and reduce quality of life. Clinically, reliable independent prognostic factors can guide decisions on the strategy of therapy for the individual patient. While classical parameters such as site of tumor localization, radicality of resection and human papillomavirus status have reached a high degree of validity, current research aims to identify molecular markers reflecting potential for tumor invasiveness and spread (3, 4). Delineating and studying functionally-relevant epitopes based on a clear concept thus offers the prospect of defining functional markers whose strategic blocking or regulation is innovative and may be of therapeutic benefit. The complexity of cellular glycosylation of lipids and proteins, amenable to analysis in molecular detail by sophisticated techniques and known to be like a fingerprint for cells (5, 6), and its capacity to store information at high coding capacity (7-10) provide an incentive towards this end.

In fact, the functional pairing of glycan determinants with endogenous receptors (lectins) is being revealed to be of broad (patho)physiological significance (11-13). Figuring prominently as contact sites, the termini of glycan chains are special due to their intimately regulated profiles of expression, *e.g.* by a tumor suppressor which eventually causes lectin-triggered anoikis (14,15). Such signals are evidently read and interpreted by members of the family of adhesion/growth-

regulatory galectins (16-18), and these bioeffectors are present in SCC. Their study was initiated in cells and immunohistochemically for galectins 1 and 3 (19-24), then extended to other family members such as galectins 7, 8 and 9, indicating the presence of a galectin network (25-31). At the level of cellular activity, the demonstration that a lectin such as galectin-1 is associated to pro-inflammatory/invasive activities such as those of chemo- and cytokines, or the pro-degradative matrix metalloproteinases, points to a molecular bridge from lectins to tumor progression (32-34). These results explain the interest in monitor immune mediators such as the chemokine (C-X-C motif) ligand 1 (CXCL1) and interleukin 6 and 8 (IL6/IL8), flanked by markers of differentiation, that are keratins (35,36), concomitantly with studying the galectin network in this tumor class. The work here feared on the level of such factors in individual patients in genome-wide expression analysis, and for specimens from three different regions of each patient.

In this study, we address two issues. In the first step, we performed a genome-wide expression analysis of the tumor (SCC), the margin of surgical resection (MSR) and normal tissue (NOE) to comparatively map the influence of the site on mRNA representation. Next, mRNA quantity for seven members of the galectin family was determined, together with that for seven keratins and the three immune factors for each patient in order to characterize interindividual variability. Finally, this network analysis was taken to the level of immunohistochemistry for selected probes to visualize distribution profiles of the gene products. The observed differences between signal intensities at the mRNA level of and immunopositivity substantiate interpretation of each set of data in its own context without unwarranted extrapolations.

Materials and Methods

Characteristics of patients and tissue processing. Samples were collected from patients suffering from SCC after acquiring their informed consent and study design approval by the Local Ethical Committee of the University Hospital in Motol, Prague, Czech Republic No. MZ VES 2015, in agreement with the Declaration of Helsinki. The characteristics of patients are summarized in Table I. For each case, specimens of each of the three tissue regions, *i.e.* SCC, MSR and NOE from the contralateral cheek of each donor, were processed. Tissue specimens were routinely incubated in RNAlater® (Ambion, Foster City, CA, USA) to preclude degradation by activity of endogenous RNases, frozen in liquid nitrogen and stored at −80˚C. Frozen sections (7 μm thickness) were prepared using CryoCut-E (Reichert-Jung, Vienna, Austria) and used for extraction of RNA and for immunohistochemistry.

RNA Extraction and library preparation for sequencing. Total RNA from 30 microdissected cryosections of each sample stored in RNAlater was isolated using the reagents of the RNeasy Micro Kit (Qiagen, Hilden, Germany) according to manufacturer's instructions, including DNase I treatment. The concentration of RNA was measured with a Qubit 3.0 fluorimeter (Life Technologies, Carlsbad, CA, USA), and its quality was routinely determined by 2100 Bioanalyzer and RNA 6000 Nano kit reagents (Agilent, Santa Clara, CA, USA). A sequencing library including indices was prepared in two pools using a TruSeq Stranded mRNA LT Sample Prep Kit (Illumina, San Diego, USA). The cDNA concentration of the libraries was measured using the KAPA Library Quantification Kit (Kapa Biosystems, Wilmington, MA, USA), the size distribution was estimated by Agilent High Sensitivity DNA Kit reagents and 2100 Bioanalyzer equipment (Agilent). Clusters were generated with TruSeq Rapid Cluster Kit/cBot (Illumina) on two separate rapid flow lines using 10 pM diluted libraries, with 1% PhiX control added. Sequencing on an Illumina Hiseq 2500 instrument was performed to generate 2×50-bp paired-end exome reads using TruSeq Rapid SBS Kit chemistry.

Table I. *Characteristics of studied patients*.

Characteristic	Tumor localization, n	
	Tonsil (n=6)	Oropharynx (n=1)
Gender, n		
Male	6	0
Female	0	1
Mean age	61	68
T Classification, n		
T2	5	1
T3	1	0
N Classification, n		
N0	1	0
N1	1	0
N2	2	0
N2b	1	0
N2c	1	1
M Classification, n		
M0	6	1

Overview of primary analysis. Material from the 21 different samples from seven patients (SCC, MSR and NOE for each) was sequenced. A total of 109 cycles yielded 35.21 Gbp of raw data with 96.65% clusters passing filter for read 1 and 97.71% for read 2. The overall percentage of bases matching or being above the Q30 Illumina Sequencing Quality Score was 96.5%, and cluster density reached optimal range for both reads with 1012 and 836 K/mm^2, respectively. Aligned reads for spiked PhiX control reached 0.92% of total.

Data pre-processing and RNA-seq alignment. The raw data (BCL files) were demultiplexed using Illumina's tool bcl2fastq (version 2.17; Illumina) with default parameters. The quality of raw FASTQ files was checked using the program MultiQC (37). All reads passed the quality control (Phred Qual Score >30). Reads of the length of 50 bases were aligned to human genome hg19 reference (https://support.illumina.com/sequencing/sequencing_software/igenome.html) applying the splice junction mapper for RNA-seq reads TopHat (38). The default parameters for TopHat were used. The output was as a BAM file (39).

Table II. *List of antibodies used for immunohistochemistry.*

Primary antibody	Producer	Secondary antibody/fluorochrome	Producer
Galectin-1/P Galectin-3/P Galectin-4/P Galectin-7/P Galectin-8/P Galectin-9/P	Munich laboratory (in house)	Swine anti-rabbit/FITC	DAKO Cytomation, Glostrup, Denmark
Keratin 8/M Keratin 19/M	DAKO Cytomation, Glostrup, Denmark	Goat anti-mouse/TRITC (or FITC)	Sigma-Aldrich, Prague, Czech Republic
Keratin 14/M Keratin 17/M CD45/M	Sigma-Aldrich, Prague, Czech Republic		

P: Rabbit polyclonal, M: mouse monoclonal, FITC: fluorescein isothocyanate, TRITC: tetramethylrhodamine isothiocyanate.

RNA-seq data quantification and gene expression. Analysis was performed by Tuxedo pipeline-based processing (40). The resultant BAM files were used in Cufflinks algorithm v 2.2.1 (39). Differential expression analysis was performed by Cuffdiff v. 2.2.1 (40) based on transcript abundances. The raw output cufflinks transcripts were log2 transformed at fragments per kilobase of exon per million mapped reads (FPKM). To avoid taking log2 of zero, we routinely added a constant (0.01) to the FPKM.

Statistical analysis. Genome-wide comparisons were made to pinpoint significant differences and interindividual comparison of selected genes mentioned above (galectins, keratins and pro-tumoral chemo- and cytokines). Genes differentially expressed at a log2 fold-change value greater than 2 (based on FPKM ratio) and false discovery rates (FDR) values of less than 5% were listed. Gene ontology (GO) and pathway analysis of up- and down-regulated genes were performed using Enrichr and PANTHER (41) databases. Statistical analysis was carried out using the CummeRbund Bioconductor package within the R environment (R Development Core Team 2007).

Immunohistochemistry. Tissue sections were routinely washed in phosphate-buffered saline (PBS; pH 7.2), fixed in 5% paraformaldehyde in PBS for 5 min and extensively washed with PBS. The primary antibodies listed in Table II were diluted as recommended by the supplier or tested at 1:50 when made in-house, and the signal of immunohistochemical processing was visualized by fluorescein isothocyanate (FITC)- or tetramethylrhodamine isothiocyanate (TRITC)-labeled second-step antibodies, also diluted as recommended by the supplier (Table II). As a control for specificity, that is, to exclude antigen-independent reactions, the first-step antibody was either omitted from the protocol or replaced by an irrelevant antibody (same isotype for the monoclonals). The polyclonal antibodies to galectin were made in-house, their specificity being rigorously checked for absence of any cross-reactivity among human galectins by enzyme-linked immunosorbent assay (ELISA)//western blotting and rounds of chromatographic affinity depletion of the respective IgG fraction using resin-immobilized lectin (42-45). Nuclei were counterstained by 4',6-diamidine-2-phenylindol (DAPI) (Sigma-Aldrich, Prague, Czech Republic), and the specimens were mounted in Vectashield (Vector Laboratories, Burlingame, CA, USA). The specimens were inspected, evaluated and files stored using a Nikon-Eclipse 90i microscope equipped with the computer-assisted image analysis system LUCIA 5.1 (Laboratory Imaging, Prague, Czech Republic) and a Vosskühler VDS CCD-1300 camera (VDS Vosskühler GmbH, Osnabrück, Germany).

Results

Differential gene-expression profiling. A total of 25,832 genes was covered by this profiling. When compared in detail, the expression profile of SCC significantly differed from that of NOE in 281 genes, and MSR from NOE in 276 genes. The most highly dysregulated gene products in SCC are listed in Table III (SCC *vs*. NOE; upregulated) and Table IV (SCC *vs*. NOE; down-regulated). For comparison, Table V and Table VI list the respective information on the MSR *vs*. NOE comparison, and Table VII and Table VIII complete the pairwise comparisons by presenting the results of setting MSR and SCC data in relation. The extended version of each listing is accessible at http://www.physiolchem.vetmed.uni-muenchen.de/summary/anticancer_research/index.html

Various families of proteins appear in these lists (and the further identified cases), among them so-called glycogenes coding for lectins such as collectin-11, CD22 (siglec-2) and galectins or glycosyltransferases such as genes for β-1,4-*N*-acetyl-galactosaminyltransferase 4 (preparing the Lacdi*N*Ac epitope) or α2,6-sialyltransferase 1, the main activity of α2,6-sialylation. As graphically illustrated in the heat map with the dendrogram based on Jensen-Shannon distances, the profiles of gene expression have distinctive features (Figure 1). Of interest, the profile of MSR was revealed to be different from that for NOE, as demonstrated by principal component analysis (PCA) for dimensionality reduction and by multi-dimensional scaling for dimensionality reduction (Figure 2). Using the gene ontology (GO) and pathway analysis, respective assignment of the most dysregulated cases of gene

Table III. *The genes most up-regulated in squamous cell carcinoma compared to normal epithelium.*

Gene symbol	HGNC	Ontology	Fold-change	*p*-Value
KRT10	6413	Keratin, type I cytoskeletal 10	7.28096	0.00005
CIDEC	24229	Cell death activator CIDE-3	7.20618	0.0005
KRT31	6448	Keratin, type I cuticular Ha1	5.89646	0.00005
HHLA2	4905	HERV-H LTR-associating protein 2	4.95419	0.00005
LY6G6C	13936	Lymphocyte antigen 6 complex locus protein G6c	4.87151	0.0006
PLAC9	19255	Placenta-specific protein 9	4.57599	3.50E-004
KRTDAP	16313	Keratinocyte differentiation-associated protein	4.47024	5.00E-005
CRNN	1230	Cornulin	4.35129	6.00E-004
IL18	5986	Interleukin-18	3.23351	5.00E-005
COX7A1	2287	Cytochrome c oxidase subunit 7A1, mitochondrial	4.31603	5.00E-005
CD36	1663	Platelet glycoprotein 4	4.3085	5.00E-005
MTRNR2L10	37167	Humanin-like 10	4.20429	2.50E-004
LCE3D	16615	Late cornified envelope protein 3D	4.18008	5.00E-005
PLA2G2A	9031	Phospholipase A2, membrane associated	4.044	5.00E-005
MAL	6817	Myelin and lymphocyte protein	3.97912	5.00E-005
MIR17HG	23564	Putative microRNA 17 host gene protein	3.77539	5.00E-005
CNFN	30183	Cornifelin	3.76645	2.50E-004
ALOX12	429	Arachidonate 12-lipoxygenase, 12S-type	3.75755	5.00E-005
DCLK1	2700	Serine/threonine-protein kinase DCLK1	3.71979	2.50E-004
HSPB6	26511	Heat shock protein β6	3.61402	5.00E-005
KRT3	6440	Keratin, type II cytoskeletal 3	3.59278	5.00E-005

HGNC: Human Gene Nomenclature Committee.

Table IV. *The genes most down-regulated in squamous cell carcinoma compared to normal epithelium.*

Gene symbol	HGNC	Ontology	Fold-change	*p*-Value
SPP1	11255	Osteopontin	–8.01172	2.00E-004
MZB1	30125	Marginal zone B- and B1-cell-specific protein	–5.9354	5.00E-005
IGLL5	38476	Immunoglobulin λ-like polypeptide 5	–5.75518	5.00E-005
CLC	2014	Galectin-10	–5.71586	5.77E-002
STAG3	11356	Cohesin subunit SA-3	–5.56316	2.50E-004
DERL3	14236	Derlin-3	–5.54659	5.00E-005
SERPINE1	8583	Plasminogen activator inhibitor 1	–5.00641	5.00E-005
ALG1L	33721	Putative glycosyltransferase ALG1-like	–4.99979	2.00E-004
PRR4	18020	Proline-rich protein 4	–4.81877	5.00E-005
COLEC11	17213	Collectin-11	–4.78257	5.50E-004
PTHLH	9607	Parathyroid hormone-related protein	–4.28194	5.00E-005
MMP11	7157	Stromelysin-3	–4.28087	5.00E-005
PTGS2	9605	Prostaglandin G/H synthase 2	–4.2221	5.00E-005
IL6	6018	Interleukin-6	–4.12237	2.54E-002
CD79A	1698	B-Cell antigen receptor complex-associated protein α-chain	–4.09462	5.00E-005
MEI1	28613	Meiosis inhibitor protein 1	–4.09113	5.00E-005
UBD	18795	Ubiquitin D	–3.95711	5.00E-005
LAMC2	6493	Laminin subunit γ2	–3.93688	5.00E-005
AIM2	357	Interferon-inducible protein AIM2	–3.81255	5.00E-005
CDKN2A	1787	Cyclin-dependent kinase inhibitor 2A	–3.57499	5.00E-005

HGNC: Human Gene Nomenclature Committee.

expression in SCC in relation to NOE was performed, with indications for extracellular sites of action (Table IX).

Based on the reasoning given in the introduction, data on galectins, keratins and cytokines are presented on a patient-to-patient basis. Levels of gene expression of galectins-1, -2, -4, -8 and -9 show increases in tumors relative to NOE, with the highest difference seen in the case of galectin-4 (Figure 3A). However, individual cases showed exceptional data, *i.e.* a decrease. The same trends were seen for MSR data when compared to those for NOE (Figure 3B). The level

Table V. *The genes most up-regulated in margin of surgical resection compared to normal epithelium.*

Gene symbol	HGNC	Ontology	Fold-change	*p*-Value
PRR4	18020	Proline-rich protein 4	9.06544	0.00005
IGLL5	38476	Immunoglobulin λ-like polypeptide 5	6.35297	0.00005
MZB1	30125	Marginal zone B- and B1-cell-specific protein	6.26814	0.00005
DERL3	14236	Derlin-3	6.2189	0.00005
CD79A	1698	B-Cell antigen receptor complex-associated protein α-chain	6.08902	0.0001
FDCSP	19215	Follicular dendritic cell secreted peptide	5.34024	0.00005
SPIB	11242	Transcription factor Spi-B	4.89362	0.00005
PAX1	8615	Paired box protein Pax-1	4.82606	0.00005
FCRLA	18504	Fc receptor-like A	4.76497	0.00005
STAG3	11356	Cohesin subunit SA-3	4.41745	0.00055
LYZ	6740	Lysozyme C	4.3502	0.00005
FOSB	3797	Protein fosB	4.32308	0.00005
FAM46C	24712	Protein FAM46C	4.27245	0.00005
CXCL13	10639	C-X-C motif chemokine 13	4.17529	0.00005
POU2AF1	9211	POU domain class 2-associating factor 1	4.06358	0.00005
CD22	1643	Siglec-2; CD22	3.92959	0.00005
IL6	6018	Interleukin-6	3.8633	0.02522
ATF3	785	Cyclic AMP-dependent transcription factor ATF-3	3.42798	0.00005
CD180	6726	CD180 Antigen	3.40267	0.0001
CXCR4	2561	C-X-C Chemokine receptor type 4	3.31944	0.00005

HGNC: Human Gene Nomenclature Committee.

Table VI. *The genes most down-regulated in margination of surgical resection compared to normal epithelium.*

Gene symbol	HGNC	Ontology	Fold-change	*p*-Value
KRT1	6412	Keratin, type II cytoskeletal 1	–11.2718	5.00E-005
KRT10	6413	Keratin, type I cytoskeletal 10	–8.14347	5.00E-005
FLG	3748	Filaggrin	–8.10598	5.00E-005
ASPRV1	26321	Retroviral-like aspartic protease 1	–6.66337	5.00E-005
KRTDAP	16313	Keratinocyte differentiation-associated protein	–6.06565	5.00E-005
MTRNR2L1	37155	Humanin-like 1	–5.82079	5.00E-005
LCE3D	16615	Late cornified envelope protein 3D	–5.70158	5.00E-005
VSIG8	27647	Siglec-8; V-Set and immunoglobulin domain-containing protein 8	–5.69346	5.00E-005
RGS20	14600	Regulator of G-protein signaling 20	–5.57383	5.00E-005
SPRR2B	11262	Small proline-rich protein 2B	–5.53185	5.00E-005
LCE3E	29463	Late cornified envelope protein 3E	–5.51303	5.00E-005
KRT3	6440	Keratin, type II cytoskeletal 3	–5.2648	5.00E-005
KLK9	6370	Kallikrein-9	–4.96059	5.00E-005
LGALS12	15788	Galectin-12	–4.93873	2.46E-002
SBSN	24950	Suprabasin	–4.78284	5.00E-005
LGALS7B	34447	Galectin-7	–4.49409	5.00E-005
FLG2	33276	Filaggrin-2	–4.44255	7.00E-004
TREX2	12270	Three prime repair exonuclease 2	–4.42317	5.00E-005
SERPINB4	10570	Serpin B4	–4.14905	5.00E-005
KPRP	31823	Keratinocyte proline-rich protein	–4.08595	5.00E-005

HGNC: Human Gene Nomenclature Committee.

of galectin-7-coding mRNA was, in contrast, reduced in most cases (Figure 3). Data sets of comparisons for MSR and SCC are available online: http://www.physiolchem.vetmed.uni-muenchen.de/summary/anticancer_research/index.html. The obvious deviations underscore the patient- and site-dependent nature of the characteristics.

Expression of *CXCL1*, *IL6* and *IL8* genes was found to be up-regulated in SCC and MSR in comparison to NOE [Figure 4, with MSR having lower levels than SCC (http://www.physiolchem.vetmed.uni-muenchen.de/bilder/zivicova-et-al-suppl-fig-1.jpg)]. Concerning keratins, marked interindividual variability was

Table VII. *The genes imost up-regulated in margin of surgical resection compared to squamous cell carcinoma.*

Gene Symbol	HGNC	Ontology	Fold-change	*p*-Value
PRR4	18020	Proline-rich protein 4	4.24667	1.50E-004
CRISP3	16904	Cysteine-rich secretory protein 3	3.72177	2.50E-004
SRPX	11309	Sushi repeat-containing protein SRPX	3.42866	5.00E-005
CD22	1643	Siglec-2; B-cell receptor CD22	3.0965	1.50E-004
CXCL12	10672	Stromal cell-derived factor 1	2.78279	5.00E-005
MMRN1	7178	Multimerin-1	2.76234	5.00E-005
GFRA1	4243	GDNF family receptor α1	2.73579	5.00E-005
ABCA8	38	ATP-Binding cassette sub-family A member 8	2.71081	2.50E-004
ABI3BP	17265	Target of Nesh-SH3	2.63971	4.00E-004
ADRA2A	281	α2A adrenergic receptor	2.60041	3.00E-004
ANK2	493	Ankyrin-2	2.59542	2.50E-004
RECK	11345	Reversion-inducing cysteine-rich protein with Kazal motifs	2.5949	5.00E-005
BLK	1057	Tyrosine-protein kinase Blk	2.56796	5.00E-004
HSPB6	26511	Heat shock protein β6	2.51233	2.50E-004
VPREB3	12710	Pre-B lymphocyte protein 3	2.48558	1.00E-004
CCL21	10620	C-C motif chemokine 21	2.41223	3.00E-004
COL14A1	2191	Collagen α1(XIV)-chain	2.20506	5.00E-005
PDK4	8812	[Pyruvate dehydrogenase (acetyl-transferring)] kinase isozyme 4, mitochondrial	2.17112	4.00E-004
PTGDS	9592	Prostaglandin-H2 D-isomerase	2.15497	5.00E-005
VWA8	29071	von Willebrand factor A domain-containing protein 8	2.13467	5.00E-005

HGNC: Human Gene Nomenclature Committee.

Table VIII. *The genes most down-regulated in margin of surgical resection compared to squamous cell carcinoma.*

Gene symbol	HGNC	Ontology	Fold-change	*p*-Value
CLC	2014	Galectin-10	–5.7305	1.81E-002
KRT17	6427	Keratin, type I cytoskeletal 17	–4.76107	5.00E-005
KRT14	6416	Keratin, type I cytoskeletal 14	–4.50188	2.90E-003
CNTNAP2	13830	Contactin-associated protein-like 2	–3.85258	5.00E-005
KLK9	6370	Kallikrein-9	–3.78367	5.00E-005
EPPK1	15577	Epiplakin	–3.36048	5.00E-005
LAMC2	6493	Laminin subunit γ2	–3.34597	5.00E-005
TUBB3	20772	Tubulin β3 chain	–3.3348	5.00E-005
RBP1	16831	Peripheral-type benzodiazepine receptor-associated protein 1	–3.3028	5.00E-005
PTHLH	9607	Parathyroid hormone-related protein	–3.17485	1.00E-004
CSPG4	2466	Chondroitin sulfate proteoglycan 4	–3.16629	1.00E-004
HAP1	4812	Huntingtin-associated protein 1	–3.15833	5.00E-005
KLHDC7B	25145	Kelch domain-containing protein 7B	–3.1501	5.00E-005
IL12RB2	5972	Interleukin-12 receptor subunit β2	–3.13533	5.00E-005
IFI6	4054	Interferon α-inducible protein 6	–3.06252	5.00E-005
MMP12	7158	Macrophage metalloelastase	–2.94276	5.00E-005
S100A7	10497	Protein S100-A7	–2.92962	1.00E-004
WDR66	28506	WD Repeat-containing protein 66	–2.87516	5.00E-005
ADAM23	202	Disintegrin and metalloproteinase domain-containing protein 23	–2.71994	2.50E-004

HGNC: Human Gene Nomenclature Committee.

noted for keratin 5 and 6, their expression levels generally being lower in MSR than in NOE samples (Figure 4). Expression of keratins 8, 14, 17 and 19 was up-regulated in SCC relative to NOE, 8 and 19 were also up-regulated in MSR in comparison to NOE (Figure 4). Keratin 14 and 17 genes were expressed to a lower extent in MSR than in NOE, with exceptions (Figure 4). Transcript levels for all studied keratins except for keratin 19 were lower in MSR than in SCC (http://www.physiolchem.vetmed.uni-muenchen.de/bilder/zivicova-et-al-suppl-fig-1.jpg).

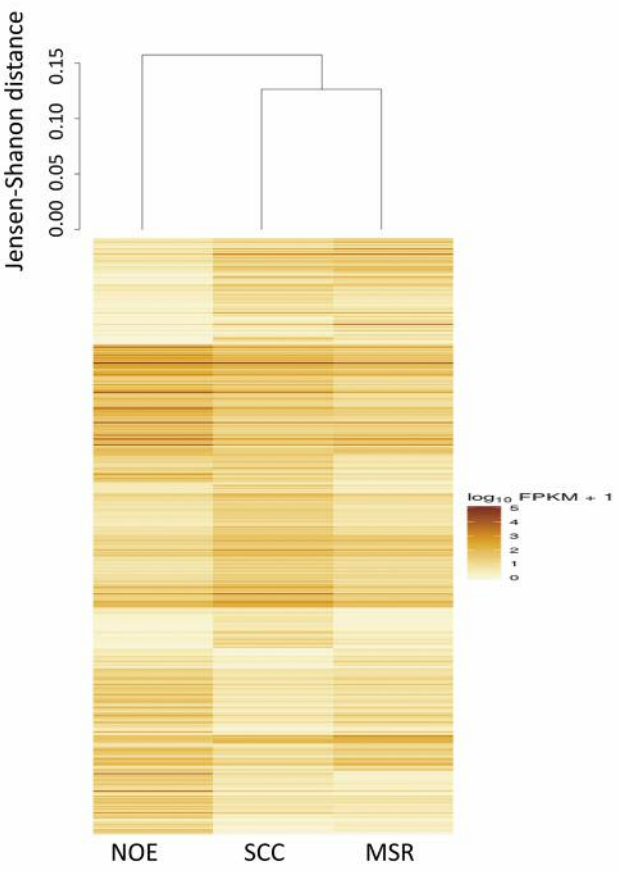

Figure 1. *Heat map showing genes differentially expressed between squamous cell carcinoma (SCC), normal epithelium (NOE) and margin of surgical resection (MSR) at a statistically significant level. Mutual relations between the three types of tested specimen are presented in the dendrogram (based on Jensen-Shannon distances) at 5% false discovery rates (FDR) and fragments per kilobase of exon per million fragments mapped (FPKM).*

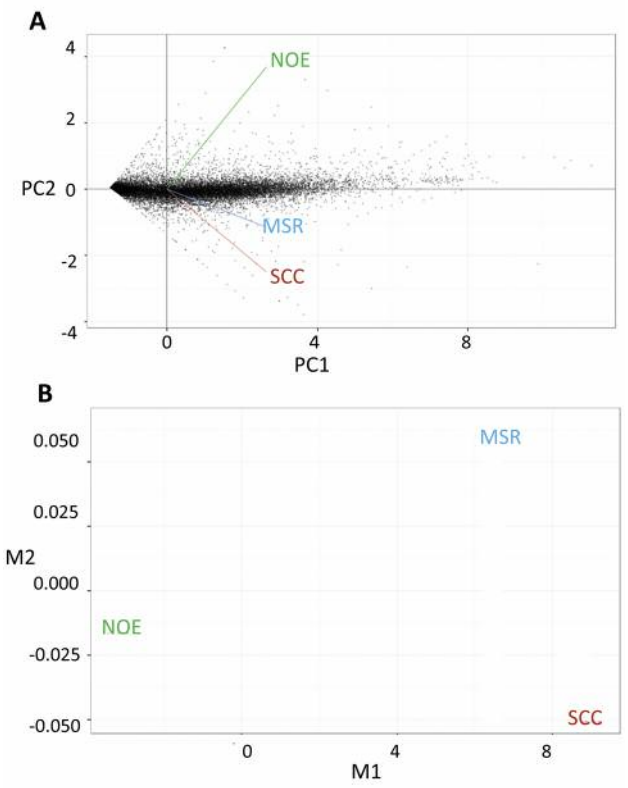

Figure 2. *Principial component analysis (PCA) for dimensionality reduction showing a strong relation between gene expression in squamous cell carcinoma (SCC) and margin of surgical resection (MSR) in comparison with normal epithelium (NOE) (A). A similar scenario is obtained by multi-dimensional scaling for dimensionality reduction (B).*

Immunohistochemical analysis. A common feature of all cases for immunopositivity was their interindividual variability. Table X gives a detailed account of this parameter for each patient, Figure 5 presents exemplary illustrations for each galectin. Galectin-1 was neither detected in SCC/NOE nor in the epithelium of the MSR, but was found in the extracellular matrix of cancer stroma (Figure 5, top panel). Galectin-3 was present in tumor stroma, namely in inflammatory leukocytes, and in malignant epithelium, in MSR samples in the epithelium, whereas staining of NOE was negative or revealing a very weak signal in the epithelium (Figure 5). No positivity for galectin-4 was observed in normal or SCC samples, a limited number of cells expressing galectin-7 were found in two cases (Figure 5). Five samples of NOE exhibited immunopositivity for galectin-7 and two samples were negative (Figure 5). Whereas galectin-8 was not detected, signals for galectin-9 were seen in the basal layer of two samples of NOE. In SCC and MSR samples, it was detected in infiltrating leukocytes, ascertained by signal overlap with positivity for CD45 (Figure 5, bottom panel).

Keratins 8, 14, 17 and 19, at a level of interindividual variability similar to galectins, were positively stained in SCC cases (Table XI, Figure 5). No signal for keratin 8 was detected in NOE, keratins 14, 17 and 19 were observed in the majority of tumors, expression of 14 and 19 was present in the basal layer of normal epithelium and also in MSR.

Discussion

Genome-wide expression profiling was applied on specimens from seven patients, for each patient from three sites. Obviously, when using normal tissue (unaffected, from the other cheek) as a reference, it was possible to compare material from the tumor and the margin. Thus, a full-scale set of pairwise comparisons between normal, margin and tumor specimens is presented. Beyond pinpointing disparities, we

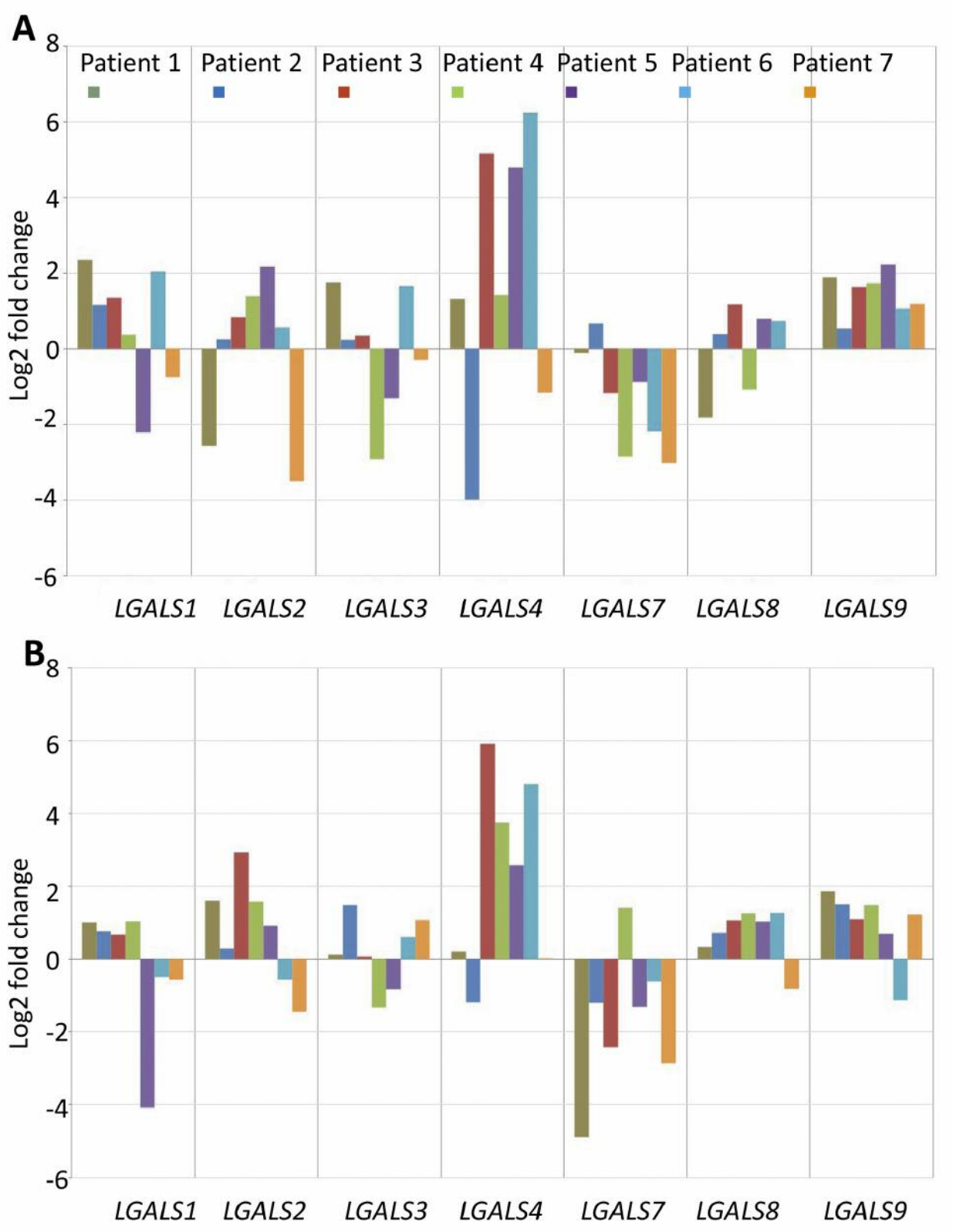

Figure 3. *Log2 fold-change as a measure of up- or down-regulation of gene expression for galectins (LGAL). Down-regulated genes have negative log2 value, positive log2 values identify gene up-regulation. Comparisons between squamous cell carcinoma (SCC) and normal epithelium (NOE) (A), and margin of surgical resection (MSR) and normal epithelium (NOE) (B) are given.*

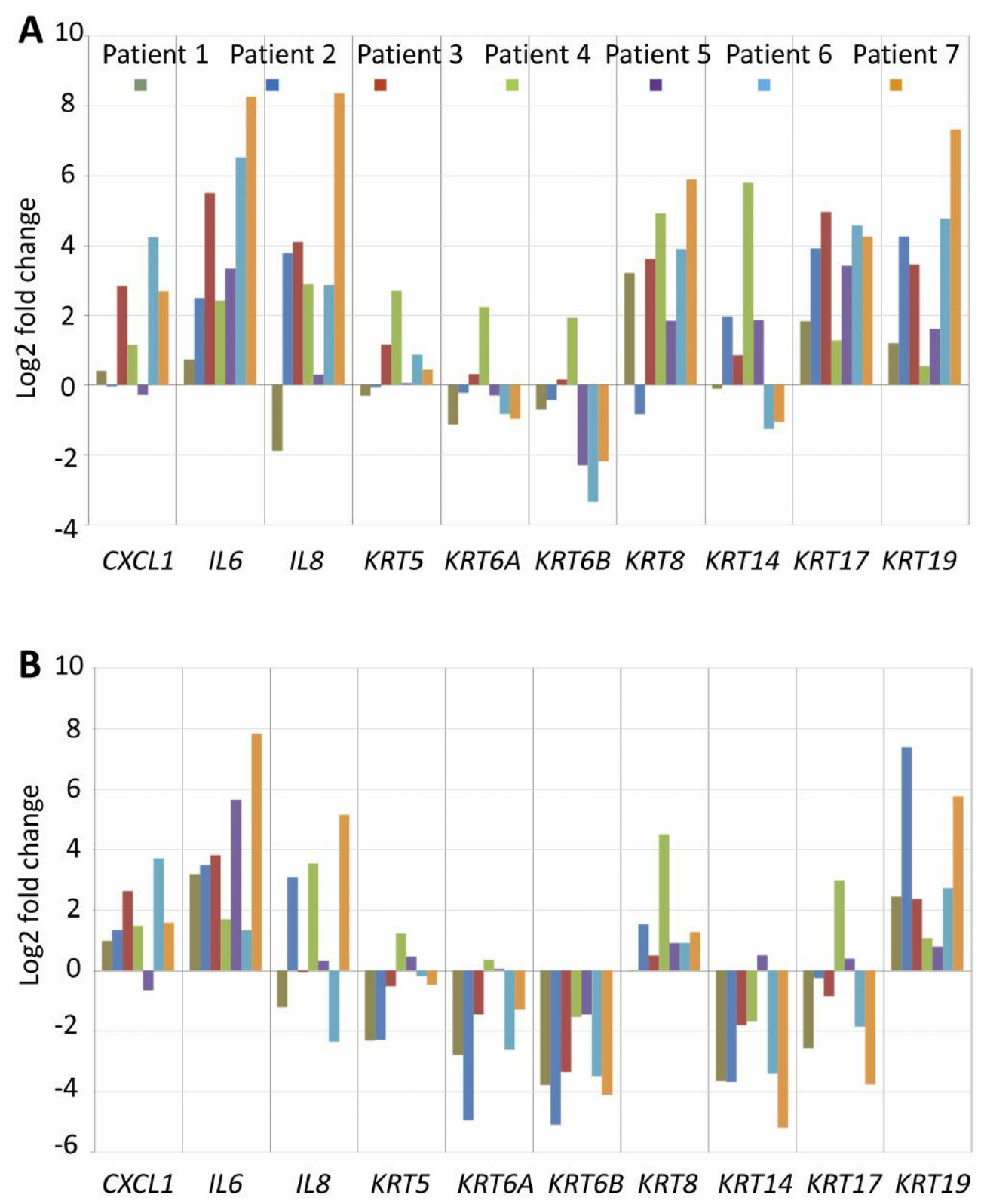

Figure 4. *Log2 fold-change for expression of genes for interleukins (IL6, IL8), for chemokine (C-X-C motif) ligand 1 (CXCL1) (A) and for keratins (KRT) (B). Down-regulated genes have negative log2 value, positive log2 values identify gene up-regulation. Comparisons between squamous cell carcinoma (SCC) and normal epithelium (NOE) (A), and margin of surgical resection (MSR) and normal epithelium (NOE) (B) are given.*

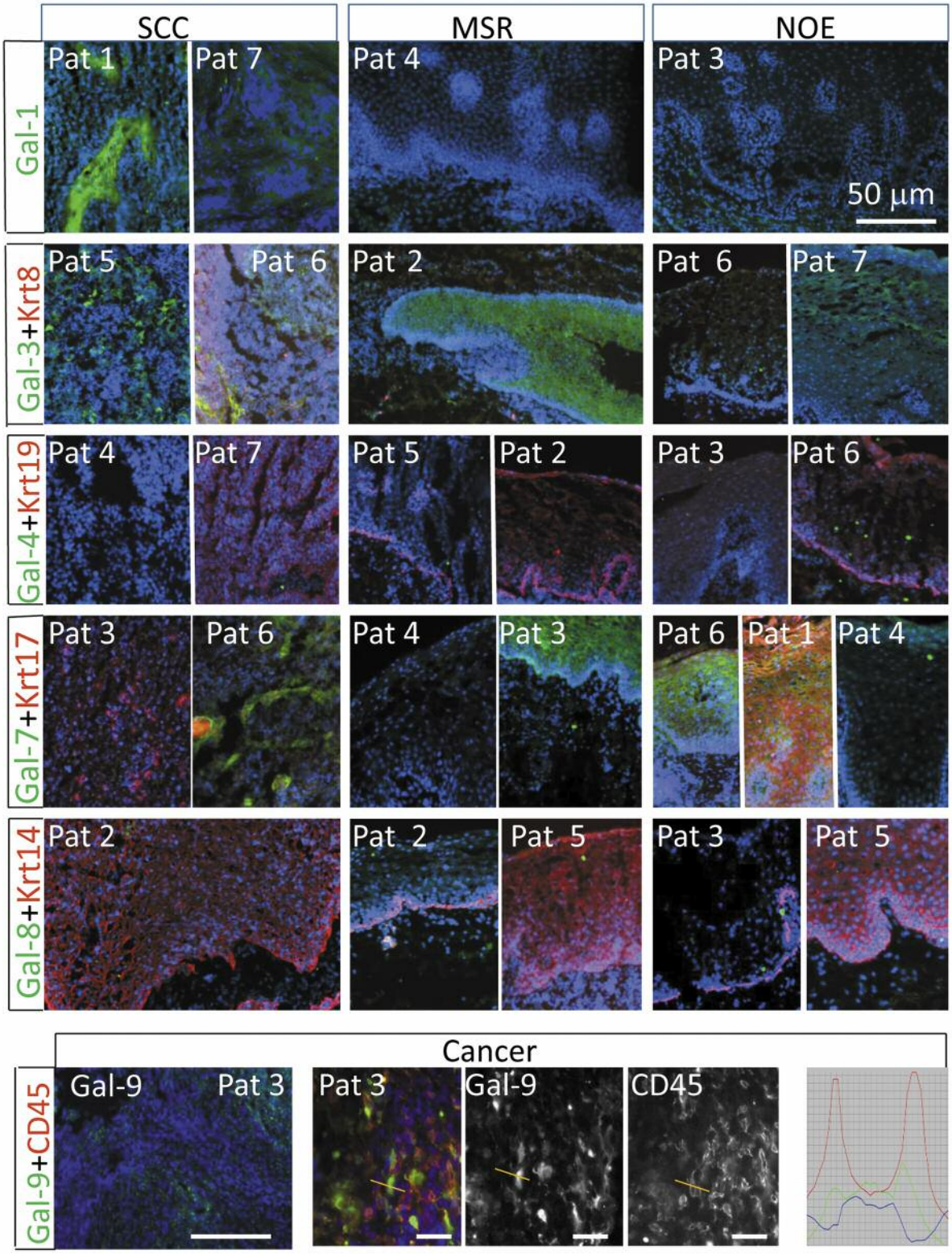

Figure 5. *Immunodetection of galectins (G, green signal): Gal-1, Gal-3, Gal-4, Gal-7, Gal-8 and Gal-9. Keratins (KRT) such as 8, 19, 17 and 14 and the leukocyte marker CD45 (red signal) were also detected in representative samples of squamous cell cancer (SCC), margin of surgical resection (MSR) and normal oral epithelium (NOE). The number of the patient is given in each panel. The fluorescence profiles of galectin-9 and CD45 provide information on co-localization (the measured cell is marked by a yellow line). Nuclei were counterstained by 4',6-diamidine-2-phenylindole.*

Table IX. *Gene Ontology (GO) biological process classification for the genes most up-regulated between squamous cell carcinoma and normal epithelium (log2 fold-change >2, p<0.05).*

Term	Overlap	*p*-Value	*p*-Value	Z-Score	Combined score
Extracellular region (GO:0005576)	11/1585	0.0040136377	0.2107604977	–2.6323608589	4.0986723883
Collagen trimer (GO:0005581)	3/91	0.0021218384	0.2107604977	–2.1962328608	3.4196067589
Endoplasmic reticulum lumen (GO:0005788)	3/154	0.0092105819	0.2107604977	–2.1804963949	3.3951045642
Extracellular matrix (GO:0031012)	4/348	0.0162722728	0.2107604977	–2.1565801777	3.3578662278
Extracellular space (GO:0005615)	8/1120	0.0122587112	0.2107604977	–2.1529752424	3.352253225
Heterochromatin (GO:0000792)	2/68	0.0155862027	0.2107604977	–2.1291495068	3.3151557715
Potassium channel complex (GO:0034705)	2/71	0.0169120267	0.2107604977	–1.9838354847	3.0888970623
Voltage-gated potassium channel complex (GO:0008076)	2/70	0.0164648846	0.2107604977	–1.9741441399	3.0738073199
Chromatin (GO:0000785)	3/289	0.047243783	0.2189756086	–1.9563400033	2.9712792812
Late endosome (GO:0005770)	2/107	0.0362100659	0.2115430167	–1.8277730107	2.8391290074
Nuclear chromosome part (GO:0044454)	3/327	0.0636854817	0.2215358089	–1.8234538826	2.7482568793
Extracellular matrix part (GO:0044420)	2/127	0.0493188308	0.2189756086	–1.6694709902	2.5355840781
Early endosome (GO:0005769)	2/141	0.0593625463	0.2215358089	–1.645528775	2.4800933105
Cation channel complex (GO:0034703)	2/147	0.0638661791	0.2215358089	–1.5737064331	2.3718447569

Combined score >2 according to (57) is shown.

Table X. *Immunopositivity for galectins.*

Patient no.	Tumor site	Type of tissue	Gal-1[x]	Gal-3*	Gal-4	Gal-7	Gal-8	Gal-9*
1	Tonsills	NOE	–	–	–	+	–	+
		MSR	–	–	–	+	–	–
		SCC	+	+	–	–/+	–	–
2	Oropharynx	NOE	–	–	–	+	–	–
		MSR	–	+	–	+	–	–
		SCC	+	–	–	–	–	–
3	Tonsills	NOE	–	–	–	+	–	–
		MSR	–	–	–	–	–	–
		SCC	+	–	–	–	–	–
4	Tonsills	NOE	–	–	–	–	–	–
		MSR	–	–	–	–	–	–
		SCC	–	–	–	–	–	–
5	Tonsills	NOE	–	–	–	+	–	+
		MSR	–	–	–	+	–	–
		SCC	–	+	–	–	–	–
6	Tonsills	NOE	–	+	–	+	–	–
		MSR	–	–	–	+	–	–
		SCC	+	+	–	–/+	–	–
7	Tonsiils	NOE	–	+	–	–	–	–
		MSR	–	+	–	+	–	–
		SCC	–	–	–	–	–	–

NOE: Normal epithelium, MSR: margin of surgical resection, SCC: squamous cell carcinoma. [x]Extracellular matrix, *positive leukocytes, –/+ positivity confined to few cells.

focused on a class of emerging bioeffectors to investigate their significance of this factor, *i.e.* site of specimen, at the level of the individual patient. Of note, special attention is given to the question of whether, in this group, the interindividual variability could even reach divergent patterns of up- and down-regulation instead of quantitative differences.

Galectins form a family of tissue lectins, which share reactivity to β-galactosides and the capacity to trigger post-binding effects. Intriguingly, these can be additive or antagonistic, as the examples of galectins-1 and -3 in osteoarthritis progression or in anoikis induction in pancreatic carcinoma cells attest (46-49). Moreover, an inducer of differentiation (butyrate) revealed differences in responsiveness

between family members (50), and galectins can alter the proteomic profile of tumor cells, demonstrating an impact of galectin presence on expression (51). As consequence, it appears to make sense to proceed from recording the expression profile of a single or few proteins to a network analysis. On the histopathological side, this study was deliberately designed to include normal tissue from each patient. In addition to a comparison between tumor and normal tissue from the same patient, we also included a specimen of the surgical margin in order to address the issue as to whether and to what extent expression characteristics in this region deviate from that of tumor/normal tissue. Given the possibility that the studied gene products may have potential for therapeutic innovation, the application of the same protocol to specimens from several patients enables estimation of the extent of interindividual variations. In this sense, we obtained a fingerprint for galectin expression from three different sites for clinical specimens.

Our data revealed differential regulation among the galectin family with up- and down-regulation and interindividual variability. The resection margin can still show features of the SCC region that may signal the presence of tumor cells. The MSR zone appeared macro- and microscopically normal, whereas its gene-expression profile presented similarities to the cancer specimen. Because individual patients in this group presented exceptional behavior, a verification of expression at the protein (effector) level seems to be necessary before any decision on tumor management may be considered. Thus, salient lessons arising from the present results on galectins are that gene regulation is different for different galectin family numbers in SCC and among patients. Having tested antibody preparations applied in previous studies on head and neck SCCs (22-26), the possibility for false-negativity in staining is excluded, as confirmed by flanking immunohistochemical keratin localization. Given the possibility for applying human galectins as tools in tumor pathology (52, 53), such work can extend the given scope of analysis.

As a consequence of the reported expression of several galectins, it is advised that histopathological studies on galectins be carried out as a network analysis, as illustrated by this report and previously by respective mapping during development in a phylogenetic model (53-56). The possibility of functional antagonism and cooperation among galectin family members should be followed-up by experimental studies. Clinically, the noted interindividual variability calls for thorough analysis of each case prior to reaching clinically relevant conclusions.

Table XI. *Immunopositivity for selected keratins.*

Patient no.	Tumor site	Type of tissue	KRT8	KRT14	KRT17	KRT19
1	Tonsills	NOE	–	+*	+	+
		MSR	+	+*	–	+*
		SCC	+	+	–	+
2	Oropharynx	NOE	–	+*	–	–
		MSR	–	+	–	–
		SCC	–	+	+	+
3	Tonsills	NOE	–	+	–	–
		MSR	+	+	–	–
		SCC	+	+	+	+
4	Tonsills	NOE	–	+	–	–
		MSR	–	+	–	–
		SCC	+	+	–	–
5	Tonsills	NOE	–	+*	–	+
		MSR	+	+*	–	+
		SCC	+	–	+	+
6	Tonsills	NOE	–	+	–	+
		MSR	+	+	–	–
		SCC	+	+	–	+
7	Tonsills	NOE	–	+	–	–
		MSR	+	+	–	–
		SCC	+	–/+	–	+

NOE: Normal epithelium, MSR: margin of surgical resection, SCC: squamous cell carcinoma. *Positivity in suprabasal leukocytes.

Acknowledgements

The Authors are grateful for funding by the Ministry of Health of the Czech Republic, project No. 15-28933A, the Charles University, projects PROGRES Q28/1LF, UNCE 204013 and Specific University Research, as well as by the Ministry of Education, Youth and Sports of the Czech Republic within the National Sustainability Program II (project BIOCEV-FAR reg. no. LQ1604) and project BIOCEV (CZ.1.05/1.1.00/02.0109). This publication is a result of the project implementation, covering expenses for equipment for bioanalyses (No CZ.1.05/2.1.00/19.0400), supported by the Research and Development for Innovations Operational Program (RDIOP) co-financed by European Regional Development Fund and the state budget of the Czech Republic. The Authors thank to Radana Kavková, M.Sc. and Marie Jindráková for excellent technical assistance.

References

1 Marur S and Forastiere AA: Head and neck squamous cell carcinoma: update on epidemiology, diagnosis, and treatment. Mayo Clin Proc *91*: 386-396, 2016.

2 Gumusay O, Ozet A, Buyukberber S, Baykara M, Coskun U, Cetin B, Uner A, Aydil U and Benekli M: Factors predicting the development of distant metastases in patients with head and neck squamous cell carcinoma: a retrospective study from a single centre. J BUON *20*: 521-526, 2015.

3 Barber BR, Biron VL, Klimowicz AC, Puttagunta L, Côté DW and Seikaly H: Molecular predictors of locoregional and distant metastases in oropharyngeal squamous cell carcinoma. J Otolaryngol Head Neck Surg *16*: 42-53, 2013.

4 Taghavi N and Yazdi I: Prognostic factors of survival rate in oral squamous cell carcinoma: clinical, histologic, genetic and molecular concepts. Arch Iran Med *18*: 314-319, 2015.

5 Corfield A: Eukaryotic protein glycosylation: a primer for histochemists and cell biologists. Histochem Cell Biol *147*: 119-147, 2017.

6 Kopitz J: Lipid glycosylation: a primer for histochemists and cell biologists. Histochem Cell Biol *147*: 175-198, 2017.

7 Solís D, Bovin NV, Davis AP, Jiménez-Barbero J, Romero A, Roy R, Smetana K Jr. and Gabius H-J: A guide into glycosciences: how chemistry, biochemistry and biology cooperate to crack the sugar code. Biochim Biophys Acta *1850*: 186-235, 2015.

8 Gabius H-J: The magic of the sugar code. Trends Biochem Sci *40*: 341, 2015.

9 Gabius H-J, Kaltner H, Kopitz J and André S: The glycobiology of the CD system: a dictionary for translating marker designations into glycan/lectin structure and function. Trends Biochem Sci *40*: 360-376, 2015.

10 Gabius H-J and Roth J: An introduction to the sugar code. Histochem Cell Biol *147*: 111-117, 2017.

11 Gabius H-J, Manning JC, Kopitz J, André S and Kaltner H: Sweet complementarity: the functional pairing of glycans with lectins. Cell Mol Life Sci *73*: 1989-2016, 2016.

12 Manning JC, Romero A, Habermann F, García Caballero G, Kaltner H and Gabius H-J: Lectins: a primer for histochemists and cell biologists. Histochem Cell Biol *147*: 199-222, 2017.

13 Roth J and Zuber C: Quality control of glycoprotein folding and ERAD: the role of N-glycan handling, EDEM1 and OS-9. Histochem Cell Biol *147*: 269-284, 2017.

14 Amano M, Eriksson H, Manning JC, Detjen KM, André S, Nishimura S-I, Lehtiö J and Gabius H-J: Tumour suppressor $p16^{INK4a}$: anoikis-favouring decrease in *N*/*O*-glycan/cell surface sialylation by down-regulation of enzymes in sialic acid biosynthesis in tandem in a pancreatic carcinoma model. FEBS J *279*: 4062-4080, 2012.

15 Bhide GP and Colley KJ: Sialylation of *N*-glycans: mechanism, cellular compartmentalization and function. Histochem Cell Biol *147*: 149-174, 2017.

16 Gabius HJ, Engelhardt R and Cramer F: Endogenous tumor lectins: overview and perspectives. Anticancer Res *6*: 573-578, 1986.

17 Kaltner H and Gabius H-J: A toolbox of lectins for translating the sugar code: the galectin network in phylogenesis and tumors. Histol Histopathol *27*: 397-416, 2012.

18 Kaltner H, Toegel S, García Caballero G, Manning JC, Ledeen RW and Gabius H-J: Galectins: their network and roles in immunity/tumor growth control. Histochem Cell Biol *147*: 239-256, 2017.

19 Gillenwater A, Xu XC, El-Naggar AK, Clayman GL and Lotan R: Expression of galectins in head and neck squamous cell carcinoma. Head & Neck *18*: 422-432, 1996.

20 Gillenwater A, Xu X-C, Estrov Y, Sacks PG, Lotan D and Lotan R: Modulation of galectin-1 content in human head and neck squamous carcinoma cells by sodium butyrate. Int J Cancer *75*: 217-224, 1998.

21 Piantelli M, Iacobelli S, Almadori G, Iezzi M, Tinari N, Natoli C, Cadoni G, Lauriola L and Ranelletti FO: Lack of expression of galectin-3 is associated with a poor outcome in node-negative patients with laryngeal squamous cell carcinoma. J Clin Oncol *20*: 3850-3856, 2002.

22 Saussez S, Decaestecker C, Lorfevre F, Cucu D-R, Mortuaire G, Chevalier D, Wacreniez A, Kaltner H, André S, Toubeau G, Camby I, Gabius H-J and Kiss R: High level of galectin-1 expression is a negative prognostic predictor of recurrence in laryngeal squamous cell carcinomas. Int J Oncol *30*: 1109-1117, 2007.

23 Saussez S, Decaestecker C, Mahillon V, Cludts S, Capouillez A, Chevalier D, Vet HK, André S, Toubeau G, Leroy X and Gabius H-J: Galectin-3 up-regulation during tumor progression in head and neck cancer. Laryngoscope *118*: 1583-1590, 2008.

24 Saussez S, Decaestecker C, Cludts S, Ernoux P, Chevalier D, Smetana K Jr, André S, Leroy X and Gabius H-J: Adhesion/growth-regulatory tissue lectin galectin-1 in relation to angiogenesis/lymphocyte infiltration and prognostic relevance of stromal up-regulation in laryngeal carcinomas. Anticancer Res *29*: 59-65, 2009.

25 Saussez S, Cucu D-R, Decaestecker C, Chevalier D, Kaltner H, André S, Wacreniez A, Toubeau G, Camby I, Gabius H-J and Kiss R: Galectin-7 (p53-induced gene-1): a new prognostic predictor of recurrence and survival in stage IV hypopharyngeal cancer. Ann Surg Oncol *13*: 999-1009, 2006.

26 Cludts S, Decaestecker C, Mahillon V, Chevalier D, Kaltner H, André S, Remmelink M, Leroy X, Gabius H-J and Saussez S: Galectin-8 up-regulation during hypopharyngeal and laryngeal tumor progression and comparison with galectin-1, -3 and -7. Anticancer Res *29*: 4933-4940, 2009.

27 Dong GW, Kim J, Park JH, Choi JY, Cho SI and Lim SC: Galectin-8 expression in laryngeal squamous cell carcinoma. Clin Exp Otorhinolaryngol *2*: 13-19, 2009.

28 Alves PM, Godoy GP, Gomes DQ, Medeiros AM, de Souza LB, da Silveira EJ, Vasconcelos MG and Queiroz LM: Significance of galectin-1, -3, -4 and -7 in the progression of squamous cell carcinoma of the tongue. Pathol Res Pract *207*: 236-240, 2011.

29 Fík Z, Valach J, Chovanec M, Mazánek J, Kodet R, Kodet O, Tachezy R, Foltynova E, André S, Kaltner H, Gabius H-J and Smetana K Jr: Loss of adhesion/growth-regulatory galectin-9 from squamous cell epithelium in head and neck carcinomas. J Oral Pathol Med *42*: 166-173, 2013.

30 Matsukawa S, Morita K, Negishi A, Harada H, Nakajima Y, Shimamoto H, Tomioka H, Tanaka K, Ono M, Yamada T and Omura K: Galectin-7 as a potential predictive marker of chemo- and/or radio-therapy resistance in oral squamous cell carcinoma. Cancer Med *3*: 349-361, 2014.

31 Muniz JM, Bibiano Borges CR, Beghini M, de Araujo MS, Miranda Alves P, de Lima LM, Pereira SA, Nogueira RD, Napimoga MH, Rodrigues V Jr and Rodrigues DB: Galectin-9 as an important marker in the differential diagnosis between oral squamous cell carcinoma, oral leukoplakia and oral lichen planus. Immunobiology *220*: 1006-1011, 2015.

32 Wu MH, Hong TM, Cheng HW, Pan SH, Liang YR, Hong HC, Chiang WF, Wong TY, Shieh DB, Shiau AL, Jin YT and Chen YL: Galectin-1-mediated tumor invasion and metastasis, up-regulated matrix metalloproteinase expression, and reorganized actin cytoskeletons. Mol Cancer Res *7*: 311-318, 2009.

33 Valach J, Fík Z, Strnad H, Chovanec M, Plzák J, Cada Z, Szabo P, Sáchova J, Hroudová M, Urbanová M, Steffl M, Pačes J, Mazanek J, Vlček C, Betka J, Kaltner H, André S, Gabius H-J, Kodet R, Smetana K Jr, Gál P and Kolár M: Smooth muscle actin-expressing stromal fibroblasts in head and neck squamous cell carcinoma: increased expression of galectin-1 and induction of poor prognosis factors. Int J Cancer *131*: 2499-2508, 2012.

34 Rizqiawan A, Tobiume K, Okui G, Yamamoto K, Shigeishi H, Ono S, Shimasue H, Takechi M, Higashikawa K and Kamata N: Autocrine galectin-1 promotes collective cell migration of squamous cell carcinoma cells through up-regulation of distinct integrins. Biochem Biophys Res Commun *441*: 904-910, 2013.

35 Moll R, Divo M and Langbein L: The human keratins: biology and pathology. Histochem Cell Biol *129*: 705-733, 2008.
36 Kurokawa I, Takahashi K, Moll I and Moll R: Expression of keratins in cutaneous epithelial tumors and related disorders: distribution and clinical significance. Exp Dermatol *20*: 217-228, 2011.
37 Ewels P, Magnusson M, Lundin S and Käller M: MultiQC: Summarize analysis results for multiple tools and samples in a single report. Bioinformatics *32*: 3047-3048, 2016.
38 Trapnell C, Pachter L and Salzberg S: TopHat: discovering splice junctions with RNA-Seq. Bioinformatics *25*: 1105-1111, 2009.
39 Trapnell C, Roberts A, Goff L, Pertea G, Kim D, Kelley DR, Pimentel H, Salzberg SL, Rinn JL and Pachter L: Differential gene and transcript expression analysis of RNA-seq experiments with TopHat and Cufflinks. Nat Protoc *7*: 562-578, 2012.
40 Goff L, Trapnell C and Kelley D: cummeRbund: analysis, exploration, manipulation, and visualization of Cufflinks high-throughput sequencing data. R package version 2.14.0. 2013.
41 Mi H, Huang X, Muruganujan A, Tang H, Mills C, Kang D and Thomas PD: PANTHER version 11: expanded annotation data from Gene Ontology and Reactome pathways, and data analysis tool enhancements. Nucleic Acids Res *45*: D183-D189, 2017.
42 Kaltner H, Seyrek K, Heck A, Sinowatz F and Gabius H-J: Galectin-1 and galectin-3 in fetal development of bovine respiratory and digestive tracts. Comparison of cell type-specific expression profiles and subcellular localization. Cell Tissue Res *307*: 35-46, 2002.
43 Purkrábková T, Smetana K Jr, Dvoránková B, Holíková Z, Böck C, Lensch M, André S, Pytlík R, Liu F-T, Klíma J, Smetana K, Motlík J and Gabius H-J: New aspects of galectin functionality in nuclei of cultured bone marrow stromal and epidermal cells: biotinylated galectins as tool to detect specific binding sites. Biol Cell *95*: 535-545, 2003.
44 Čada Z, Smetana K Jr., Lacina L, Plzáková Z, Stork J, Kaltner H, Russwurm R, Lensch M, André S and Gabius H-J: Immunohistochemical fingerprinting of the network of seven adhesiongrowth-regulatory lectins in human skin and detection of distinct tumour-associated alterations. Folia Biol *55*: 145-152, 2009.
45 Čada Z, Chovanec M, Smetana K Jr, Betka J, Lacina L, Plzák J, Kodet R, Stork J, Lensch M, Kaltner H, André S and Gabius H-J: Galectin-7: Will the lectin's activity establish clinical correlations in head and neck squamous cell and basal cell carcinomas? Histol Histopathol *21*: 41-48, 2009.
46 Sanchez-Ruderisch H, Fischer C, Detjen KM, Welzel M, Wimmel A, Manning JC, André S and Gabius H-J: Tumor suppressor *p16^{INK4a}*: down-regulation of galectin-3, an endogenous competitor of the pro-anoikis effector galectin-1, in a pancreatic carcinoma model. FEBS J *277*: 3552-3563, 2010.
47 Toegel S, Weinmann D, André S, Walzer SM, Bilban M, Schmidt S, Chiari C, Windhager R, Krall C, Bennani-Baiti IM and Gabius H-J: Galectin-1 couples glycobiology to inflammation in osteoarthritis through the activation of an NF-κB-regulated gene network. J Immunol *196*: 1910-1921, 2016.
48 Toegel S, Bieder D, André S, Kayser K, Walzer SM, Hobusch G, Windhager R and Gabius H-J: Human osteoarthritic knee cartilage: fingerprinting of adhesion/growth-regulatory galectins *in vitro* and *in situ* indicates differential upregulation in severe degeneration. Histochem Cell Biol *142*: 373-388, 2014.
49 Weinmann D, Schlangen K, André S, Schmidt S, Walzer SM, Kubista B, Windhager R, Toegel S and Gabius H-J: Galectin-3 induces a pro-degradative/inflammatory gene signature in human chondrocytes, teaming up with galectin-1 in osteoarthritis pathogenesis. Sci Rep *6*: 39112, 2016.
50 Katzenmaier E-M, André S, Kopitz J and Gabius H-J: Impact of sodium butyrate on the network of adhesion/growth-regulatory galectins in human colon cancer *in vitro*. Anticancer Res *34*: 5429-5438, 2014.
51 Michalak M, Warnken U, André S, Schnölzer M, Gabius H-J and Kopitz J: Detection of proteome changes in human colon cancer induced by cell surface binding of growth-inhibitory human galectin-4 using quantitative SILAC-based proteomics. J Proteome Res *15*: 4412-4422, 2016.
52 Plzák J, Betka J, Smetana K Jr, Chovanec M, Kaltner H, André S, Kodet R and Gabius H-J: Galectin-3: an emerging prognostic indicator in advanced head and neck carcinoma. Eur J Cancer *40*: 2324-2330, 2004.
53 Dawson H, André S, Karamitopoulou E, Zlobec I and Gabius H-J: The growing galectin network in colon cancer and clinical relevance of cytoplasmic galectin-3 reactivity. Anticancer Res *33*: 3053-3059, 2013.
54 Kaltner H, Singh T, Manning JC, Raschta A-S, André S, Sinowatz F and Gabius H-J: Network monitoring of adhesion/growth-regulatory galectins: localization of the five canonical chicken proteins in embryonic and maturing bone and cartilage and their introduction as histochemical tools. Anat Rec *298*: 2051-2070, 2015.
55 García Caballero G, Kaltner H, Michalak M, Shilova N, Yegres M, André S, Ludwig AK, Manning JC, Schmidt S, Schnölzer M, Bovin NV, Reusch D, Kopitz J and Gabius H-J: Chicken GRIFIN: A homodimeric member of the galectin network with canonical properties and a unique expression profile. Biochimie *128-129*: 34-47, 2016.
56 Kaltner H, García Caballero G, Sinowatz F, Schmidt S, Manning JC, André S and Gabius H-J: Galectin-related protein: an integral member of the network of chicken galectins. 2. From expression profiling to its immunocyto- and histochemical localization and application as tool for ligand detection. Biochim Biophys Acta *1860*: 2298-2312, 2016.
57 Chen EY, Tan CM, Kou Y, Duan Q, Wang Z, Meirelles GV, Clark NR and Ma'ayan A: Enrichr: interactive and collaborative HTML5 gene list enrichment analysis tool. BMC Bioinformatics *14*: 128, 2013.

Received March 25, 2017
Revised April 11, 2017
Accepted April 19, 2017

Instructions for Authors 2017

General Policy. ANTICANCER RESEARCH (AR) will accept original high quality works and reviews on all aspects of experimental and clinical cancer research. The Editorial Policy suggests that priority will be given to papers advancing the understanding of cancer causation, and to papers applying the results of basic research to cancer diagnosis, prognosis, and therapy. AR will also accept the following for publication: (a) Abstracts and Proceedings of scientific meetings on cancer, following consideration and approval by the Editorial Board; (b) Announcements of meetings related to cancer research; (c) Short reviews (of approximately 120 words) and announcements of newly received books and journals related to cancer, and (d) Announcements of awards and prizes.

The principal aim of AR is to provide prompt publication (print and online) for original works of high quality, generally within 1-2 months from final acceptance. Manuscripts will be accepted on the understanding that they report original unpublished works in the field of cancer research that are not under consideration for publication by another journal, and that they will not be published again in the same form. All authors should sign a submission letter confirming the approval of their article contents. All material submitted to AR will be subject to peer-review, when appropriate, by two members of the Editorial Board and by one suitable outside referee. All manuscripts submitted to AR are urgently treated with absolute confidence, with access restricted to the Managing Editor, the journal's secretary, the reviewers and the printers.The Editors reserve the right to improve manuscripts on grammar and style.

The Editors and Publishers of AR accept no responsibility for the contents and opinions expressed by the contributors. Authors should warrant due diligence in the creation and issuance of their work.

NIH Open Access Policy. The journal acknowledges that authors of NIH-funded research retain the right to provide a copy of the published manuscript to the NIH four months after publication in ANTICANCER RESEARCH, for public archiving in PubMed Central.

Copyright. Once a manuscript has been published in ANTICANCER RESEARCH, which is a copyrighted publication, the legal ownership of all published parts of the paper has been transferred from the Author(s) to the journal. Material published in the journal may not be reproduced or published elsewhere without the written consent of the Managing Editor or Publisher.

Format. Two types of papers may be submitted: (i) Full papers containing completed original work, and (ii) review articles concerning fields of recognisable progress. Papers should contain all essential data in order to make the presentation clear. Reasonable economy should be exercised with respect to the number of tables and illustrations used. Papers should be written in clear, concise English. Spelling should follow that given in the "Shorter Oxford English Dictionary".

Manuscripts. Submitted manuscripts should not exceed fourteen (14) pages (approximately 250 words per double – spaced typed page), including abstract, text, tables, figures, and references (corresponding to 4 printed pages). Papers exceeding 4 printed pages will be subject to excess page charges. All manuscripts should be divided into the following sections: (a) *First page* including the title of the presented work [not exceeding fifteen (15) words], full names and full postal addresses of all Authors, name of the Author to whom proofs are to be sent, key words, an abbreviated running title, an indication "review", "clinical", "epidemiological", or "experimental" study, and the date of submission. (Note: The order of the Authors is not necessarily indicative of their contribution to the work. Authors may note their individual contribution(s) in the appropriate section(s) of the presented work); (b) *Abstract* not exceeding 150 words, organized according to the following headings: Background/Aim – Materials and Methods/Patients and Methods – Results – Conclusion; (c) *Introduction;* (d) *Materials and Methods/Patients and Methods;* (e) *Results;* (f) *Discussion;* (g) *Acknowledgements;* (h) *References*. All pages must be numbered consecutively. Footnotes should be avoided. Review articles may follow a different style according to the subject matter and the Author's opinion. Review articles should not exceed 35 pages (approximately 250 words per double-spaced typed page) including all tables, figures, and references.

Figures. All figures should appear at the end of the submitted document file. Once a manuscript is accepted all figures and graphs should be submitted separately in either jpg, tiff or pdf format and at a minimum resolution of 300 dpi. Graphs must be submitted as pictures made from drawings and must not require any artwork, typesetting, or size modifications. Symbols, numbering and lettering should be clearly legible. The number and top of each figure must be indicated. Pages that include color figures are subject to color charges..

Tables. All tables should appear at the end of the submitted document file. Once a manuscript is accepted, each table should be submitted separately, typed double-spaced. Tables should be numbered with Roman numerals and should include a short title.

References. Authors must assume responsibility for the accuracy of the references used. Citations for the reference sections of submitted works should follow the standard form of "Index Medicus" and must be numbered consecutively. In the text, references should be cited by number. Examples: 1 Sumner AT: The nature of chromosome bands and their significance for cancer research. Anticancer Res 1: 205-216, 1981. 2 McGuire WL and Chamnes GC: Studies on the oestrogen receptor in breast cancer. In: Receptors for Reproductive Hormones (O' Malley BW, Chamnes GC (eds.). New York, Plenum Publ Corp., pp 113-136, 1973.

Nomenclature and Abbreviations. Nomenclature should follow that given in "Chemical Abstracts", "Index Medicus", "Merck Index", "IUPAC -IUB", "Bergey's Manual of Determinative Bacteriology", The CBE Manual for Authors, Editors and Publishers (6th edition, 1994), and MIAME Standard for Microarray Data. Human gene symbols may be obtained from the HUGO Gene Nomenclature Committee (HGNC) (http://www.gene.ucl.ac.uk/). Approved mouse nomenclature may be obtained from http://www.informatics.jax.org/. Standard abbreviations are preferable. If a new abbreviation is used, it must be defined on first usage.

Clinical Trials. Authors of manuscripts describing clinical trials should provide the appropriate clinical trial number in the correct format in the text.

For International Standard Randomised Controlled Trials (ISRCTN) Registry (a not-for-profit organization whose registry is administered by Current Controlled Trials Ltd.) the unique number must be provided in this format: ISRCTNXXXXXXXX (where XXXXXXXX represents the unique number, always prefixed by "ISRCTN"). Please note that there is no space between the prefix "ISRCTN" and the number. Example: ISRCTN47956475.

For Clinicaltrials.gov registered trials, the unique number must be provided in this format: NCTXXXXXXXX (where XXXXXXXX represents the unique number, always prefixed by 'NCT'). Please note that there is no space between the prefix 'NCT' and the number. Example: NCT00001789.

Ethical Policies and Standards. ANTICANCER RESEARCH agrees with and follows the "Uniform Requirements for Manuscripts Submitted to Biomedical Journals" established by the International Committee of Medical Journal Editors in 1978 and updated in October 2001 (www.icmje.org). Microarray data analysis should comply with the "Minimum Information About Microarray Experiments (MIAME) standard". Specific guidelines are provided at the "Microarray Gene Expression Data Society" (MGED) website. Presentation of genome sequences should follow the guidelines of the NHGRI Policy on Release of Human Genomic Sequence Data. Research involving human beings must adhere to the principles of the Declaration of Helsinki and Title 45, U.S. Code of Federal Regulations, Part 46, Protection of Human Subjects, effective December 13, 2001. Research involving animals must adhere to the Guiding Principles in the Care and Use of Animals approved by the Council of the American Physiological Society. The use of animals in biomedical research should be under the careful supervision of a person adequately trained in this field and the animals must be treated humanely at all times. Research involving the use of human foetuses, foetal tissue, embryos and embryonic cells should adhere to the U.S. Public Law 103-41, effective December 13, 2001.

Submission of Manuscripts. Please follow the Instructions for Authors regarding the format of your manuscript and references.
Manuscripts must be submitted only through our online submission system at: http://www.iiar-submissions.com/login.html
In case a submission is incomplete, the corresponding Author will be notified accordingly. Questions regarding difficulties in using the online submission system should be addressed to: email: journals@iiar-anticancer.org

Galley Proofs. Unless otherwise indicated, galley proofs will be sent to the corresponding Author of the submission. Corrections of galley proofs should be limited to typographical errors. Reprints, PDF files, and/or Open Access may be ordered after the acceptance of the paper. Authors of online open access articles are entitled to a complimentary online subscription to Anticancer Research for the current year and all previous digital content since 2004. Requests should be addressed to the Editorial Office. Galley proofs should be returned corrected to the Editorial Office by email within two days.

Specific information and additional instructions for Authors

1. Anticancer Research (AR) closely follows the new developments in all fields of experimental and clinical cancer research by (a) inviting reviews on topics of immediate importance and substantial progress in the last three years, and (b) providing the highest priority for rapid publication to manuscripts presenting original results judged to be of exceptional value. Theoretical papers will only be considered and accepted if they bear a significant impact or formulate existing knowledge for the benefit of research progress.

2. Anticancer Research will consider the publication of conference proceedings and/or abstracts provided that the material submitted fulfils the quality requirements and instructions of the journal, following the regular review process by two suitable referees.

3. An acknowledgement of receipt, including the article number, title and date of receipt is sent to the corresponding author of each manuscript upon receipt. If this receipt is not received within 20 days from submission, the author should call or write to the Editorial Office to ensure that the manuscript (or the receipt) was not lost in the mail or during electronic submission.

4. Each manuscript submitted to AR is sent for review in confidence to two suitable referees with the request to return the manuscript with their comments to the Editorial Office within 12 days from receipt. If reviewers need a longer time or wish to send the manuscript to another expert, the manuscript may be returned to the Editorial Office with a delay. All manuscripts submitted to AR, are treated in confidence, without access to any person other than the Managing Editor, the journal's secretary, the reviewers and the printers.

5. All accepted manuscripts are peer-reviewed and carefully corrected in style and language, if necessary, to make presentation clear. (There is no fee for this service). Every effort is made (a) to maintain the personal style of the author's writing and (b) to avoid change of meaning. Authors will be requested to examine carefully manuscripts which have undergone language correction at the pre-proof or proof stage.

6. Authors should pay attention to the following points when writing an article for AR:
   - The Instructions to Authors must be followed in every detail.
   - The presentation of the experimental methods should be clear and complete in every detail facilitating reproducibility by other scientists.
   - The presentation of results should be simple and straightforward in style. Results and discussion should not he combined into one section, unless the paper is short.
   - Results given in figures should not be repeated in tables.
   - Figures (graphs or photographs) should be prepared at a width of 8 or 17 cm with legible numbers and lettering.
   - Photographs should be clear with high contrast, presenting the actual observation described in the legend and in the text. Each legend should provide a complete description, being self-explanatory, including technique of preparation, information about the specimen and magnification.
   - Statistical analysis should be elaborated wherever it is necessary. Simplification of presentation by giving only numerical or % values should be avoided.
   - Fidelity of the techniques and reproducibility of the results, should be points of particular importance in the discussion section. Authors are advised to check the correctness of their methods and results carefully before writing an article. Probable or dubious explanations should be avoided.
   - Authors should not cite results submitted for publication in the reference section. Such results may be described briefly in the text with a note in parenthesis (submitted for publication by… authors, year).
   - The References section should provide as complete a coverage of the literature as possible including all the relevant works published up to the time of submission.
   - By following these instructions, Authors will facilitate a more rapid review and processing of their manuscripts and will provide the readers with concise and useful papers.

7. Following review and acceptance, a manuscript is examined in language and style, and galley proofs are rapidly prepared. Second proofs are not sent unless required.

8. Authors should correct their galley proofs very carefully and preferably twice. An additional correction by a colleague always proves to be useful. Particular attention should be paid to chemical formulas, mathematical equations, symbols, medical nomenclature etc. Any system of correction marks can be used in a clear manner, preferably with a red pen. Additions or clarifications are allowed provided that they improve the presentation but do not bring new results (no fee).

9. Articles submitted to AR may be rejected without review if:
   - they do not fall within the journal's policy.
   - they do not follow the instructions for authors.
   - language is unclear.
   - results are not sufficient to support a final conclusion.
   - results are not objectively based on valid experiments.
   - they repeat results already published by the same or other authors before the submission to AR.
   - plagiarism is detected by plagiarism screening services.

   (Rejection rate (2016): 66%).

10. Authors who wish to prepare a review should contact the Managing Editor of the journal in order to get confirmation of interest in the particular topic of the review. The expression of interest by the Managing Editor does not necessarily imply acceptance of the review by the journal.

11. Authors may inquire information about the status of their manuscript(s) by calling the Editorial Office at +30-22950-53389, Monday to Friday 9.00-16.00 (Athens time), or by sending an e-mail to journals@iiar-anticancer.org

12. Authors who wish to edit a special issue on a particular topic should contact the Managing Editor.

13. Authors, Editors and Publishers of books are welcome to submit their books for immediate review in AR. There is no fee for this service.

(This text is a combination of advice and suggestions contributed by Editors, Authors, Readers and the Managing Editor of AR).

Copyright© 2017 - International Institute of Anticancer Research (G.J. Delinasios). All rights reserved (including those of translation into other languages). No part of this journal may be reproduced, stored in a retrieval system, or transmitted in any form or by any means, electronic, mechanical, photocopying, microfilming, recording or otherwise, without written permission from the Publisher.

ANTICANCER RESEARCH *38*: 1279-1290 (2018)
doi:10.21873/anticanres.12350

Detection of Distinct Changes in Gene-expression Profiles in Specimens of Tumors and Transition Zones of Tenascin-positive/-negative Head and Neck Squamous Cell Carcinoma

VERONIKA ZIVICOVA[1,2], PETER GAL[3,4], ALZBETA MIFKOVA[1,2], STEPAN NOVAK[1,2], HERBERT KALTNER[5], MICHAL KOLAR[6], HYNEK STRNAD[6], JANA SACHOVA[6], MILUSE HRADILOVA[6], MARTIN CHOVANEC[7], HANS-JOACHIM GABIUS[5], KAREL SMETANA JR.[1,8] and ZDENEK FIK[1,2]

[1]*Institute of Anatomy, 1st Faculty of Medicine, Charles University, Prague, Czech Republic;*
[2]*Department of Otorhinolaryngology, Head and Neck Surgery, 1st Faculty of Medicine, Charles University and University Hospital Motol, Prague, Czech Republic;*
[3]*Department of Biomedical Research, East-Slovak Institute of Cardiovascular Diseases, Inc., Kosice, Slovak Republic;*
[4]*Department of Pharmacology, Faculty of Medicine, Pavol Jozef Šafárik University in Košice, Kosice, Slovak Republic;*
[5]*Institute of Physiological Chemistry, Faculty of Veterinary Medicine, Ludwig-Maximilians University, Munich, Germany;*
[6]*Laboratory of Genomics and Bioinformatics, Institute of Molecular Genetics, Academy of Sciences of the Czech Republic, Prague, Czech Republic;*
[7]*Department of Otorhinolaryngology and Head and Neck Surgery, 3rd Faculty of Medicine, University Hospital Královské Vinohrady, Charles University Prague, Prague, Czech Republic;*
[8]*BIOCEV, Charles University, 1st Faculty of Medicine, Charles University, Vestec, Czech Republic*

Abstract. *Background/Aim: Having previously initiated genome-wide expression profiling in head and neck squamous cell carcinoma (HNSCC) for regions of the tumor, the margin of surgical resecate (MSR) and normal mucosa (NM), we here proceed with respective analysis of cases after stratification according to the expression status of tenascin (Ten). Materials and Methods: Tissue specimens of each anatomical site were analyzed by immunofluorescent detection of Ten, fibronectin (Fn) and galectin-1 (Gal-1) as well as by microarrays. Results: Histopathological examination demonstrated that $Ten^{+}Fn^{+}Gal\text{-}1^{+}$ co-expression occurs more frequently in samples of HNSCC (55%) than in NM (9%; $p<0.01$). Contrary, the $Ten^{-}Fn^{+}Gal\text{-}1^{-}$ (45%) and $Ten^{-}Fn^{-}Gal\text{-}1^{-}$ (39%) status occurred with significantly ($p<0.01$) higher frequency than in HNSCC (3% and 4%, respectively). In MSRs, different immunophenotypes were distributed rather equally ($Ten^{+}Fn^{+}Gal\text{-}1^{+}$=24%; $Ten^{-}Fn^{+}Gal\text{-}1^{-}$=36%; $Ten^{-}Fn^{-}Gal\text{-}1^{-}$=33%), differing to the results in tumors ($p<0.05$). Absence/presence of Ten was used for stratification of patients into cohorts without a difference in prognosis, to comparatively examine gene-activity signatures. Microarray analysis revealed i) expression of several tumor progression-associated genes in Ten^{+} HNSCC tumors and ii) a strong up-regulation of gene expression assigned to lipid metabolism in MSRs of Ten^{-} tumors, while NM profiles remained similar. Conclusion: The presented data reveal marked and specific changes in tumors and MSR specimens of HNSCC without a separation based on prognosis.*

This article is freely accessible online.

Correspondence to: Dr. Zdeněk Fík, Department of Otorhinolaryngology, Head and Neck Surgery, First Faculty of Medicine, Charles University and University Hospital Motol V Úvalu 84, 150 06 Prague 5, Czech Republic. Tel: +420 224434301, Fax: +420 22443430, e-mail: zdenek.fik@lf1.cuni.cz; and Dr. Peter Gál, Department of Biomedical Research, East-Slovak Institute of Cardiovascular Diseases Inc., Ondavská 8, 040 11 Košice, Slovak Republic. Tel: +421 552343251, Fax: +421 557891613, e-mail: pgal@vusch.sk or galovci@yahoo.com

Key Words: Extracellular matrix, fibronectin, galectin, tenascin, tumor, stroma.

Faced with the enormous quantity of details on cell features, it is tempting to relate cases of differential expression to clinically-relevant properties. Conceptually, however, it could be possible that dysregulation occurs in such RNA

profiles without any association to, most importantly, prognosis. Thus, it is an open question to what extent these profiles are similar or different in tissue specimens of tumors classified according to a certain immunophenotypical parameter. In our recent pilot study, we initiated a comparison of tumor, margin and normal tissue specimen in head and neck squamous cell carcinoma (HNSCC) (1). Building on the previously detected relationship of presence of a member of the family of adhesion/growth-regulatory galectins, a reader of the sugar code (2, 3), *i.e.* galectin-1 (Gal-1), with tumor invasiveness (4) and its activity to promote fibronectin (Fn) expression and fibroblast conversion to α-smooth muscle actin (α-SMA) expressing myofibroblasts (5) as well as the significance of tenascin (Ten) expression (6), we here examine a panel of HNSCC cases always with specimen of the margin of surgical resecate (MSR) and normal mucosa (NM) according to presence of these three extracellular matrix (ECM) effectors.

Of fundamental importance, tumors of diverse metastatic potential and progression status differ in the composition of both tumor- and stroma-derived ECM components (7, 8). In this study, we first ask the question whether detection of the three proteins, expressed individually and/or in combination, provides prognostic information in the studied cohort of HNSCC patients. Following the immunohistochemical part that results in stratification according to the status of Ten expression, microarray analysis between Ten^+/Ten^- cases was performed in order to answer the question on occurrence of differences on the level of RNA presence. In addition to tumor tissues from specimens stratified according to Ten presence, we also ran array-based RNA profiling of MSR and NM of the two patient groups differing in Ten expression.

Materials and Methods

Tissue samples. The set of tissue specimen of i) HNSCC (n=80; for details on classification, see Table I; for details on anatomical localization of analyzed tumors, see Table II), of ii) normal oral mucosa (NM) contralaterally to the primary tumor (NE – normal epithelium; n=47), and of iii) margin of surgical resecate (MSR, macroscopically healthy mucosa up to 1 cm to the tumor margin; n=45) was obtained from the Charles University, 1st Faculty of Medicine, Department of Otorhinolaryngology, Head and Neck Surgery. All tissue samples were collected with informed consent of patients and approval of local ethical committee according to the Helsinki Declaration.

Tissue processing – immunohistochemistry. Tissue specimen of NE, HNSCC and MSR were cryoprotected by Tissue-Tek (Sakkura, Zoeterwoude, The Netherlands) and frozen in liquid nitrogen. Frozen sections, 7 μm thick, were prepared by a Cryocut-E microtome (Reichert-Jung, Vienna, Austria).

Immunofluorescent detection of Ten, Fn and Gal-1. Frozen sections were carefully washed with phosphate-buffered saline (PBS, pH 7.2) and fixed by exposure to 2% (w/v) buffered paraformaldehyde in PBS for five minutes. After extensive washing in PBS (three times for 10 minutes), the specimens were treated with PBS containing 0.2 % (v/v) Triton X-100 (Sigma-Aldrich, St. Louis, MO, USA) and then washed in PBS. Antigen-independent binding of antibody *via* the Fc part was precluded by preincubation of specimens with porcine serum (DAKO, Glostrup, Denmark) diluted as recommended by the supplier. A murine monoclonal antibody against Ten-C and a rabbit polyclonal antibody against Fib (both from Sigma-Aldrich St. Louis, MO, USA) were applied as recommended by the supplier. Home-made rabbit polyclonal antibody against Gal-1 (9) that had thoroughly been tested for any cross-reactivity against other members of the galectin family, was used at a dilution of 1:50 (v/v). The specificity of immunodetection was ascertained by replacing the first-step antibodies by an irrelevant antibody of the same isotype (in the case of monoclonal antibody) or by omitting the first-step polyclonal antibody from pocessing. DNA was visualized by 4',6-diamidino-2-phenylindole (DAPI) (Vector-Laboratories, Burlingame, CA, USA). All preparations were analyzed by a fluorescence microscope Eclipse 90i (Nikon, Tokyo, Japan) equipped with filter blocks for FITC, TRITC and DAPI and a Cool-1300Q CCD camera (Vosskühler, Osnabrück, Germany). Data were processed using the LUCIA 5.1 computer-assisted image analysis system (Laboratory Imaging, Prague, Czech Republic).

Microarray analysis. Material from a subset of 26 patients was processed using microarray techniques. Anatomical sites of specimens used for gene profiling are given in Table I. Briefly, total RNA was isolated using RNeasy Micro Kit reagents (QIAGEN, Germantown, MD, USA) from cryostat sections, following the procedure optimized for animal cells. The quantity and quality of RNA were determined using a NanoDrop ND-1000 spectrophotometer (NanoDrop Technologies LLC, Wilmington, DE,

Table I. *TNM classification*.

	G	T	N	S
0	-	-	24	-
1	14	16	15	4
2	39	36	38	8
3	27	17	3	21
4	-	11	-	47

G: Grade; T: size of the primary tumor; N: degree of spread to regional lymph nodes; M: presence of distant metastasis; S: stage.

Table II. *Anatomical sites of the primary tumors analyzed in the present study*.

Primary site	Number of patients/microarray
Oral cavity	11/4
Oropharynx	51/13
Hypopharynx	5/1
Larynx	13/8

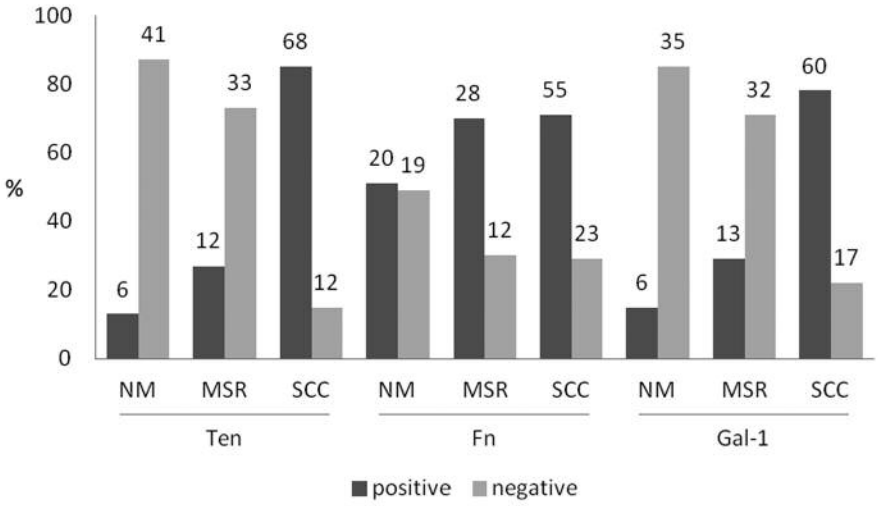

Figure 1. *Distribution (%) of specimen according to the category of immunohistochemical negativity/positivity for the studied ECM proteins, i.e. tenascin (Ten), fibronectin (Fn) and galectin-1 (Gal-1), in tissue sections of normal mucosa (NM), margin of surgical resecate (MSR) and squamous cell carcinoma (SCC). Number of evaluated patients is provided above each column.*

USA) and an Agilent 2100 Bioanalyzer (Agilent Technologies, Santa Clara, CA, USA). Illumina HumanWG-6 V3 chips (Illumina, San Diego, CA, USA) were used for microarray analysis following a standard protocol: total RNA (150 ng) was amplified using an Illumina TotalPrep RNA Amplification Kit (Ambion™; Thermo Fisher Scientific, Waltham, MA, USA), and 1,500 ng of the amplified RNA was hybridized to oligonucleotides presented on the chips according to the manufacturer's protocol. Including several technical replicates, 26 samples of tumor tissue (four Ten^- tumors; 22 Ten^+ tumors), 22 samples of stromal tissue (four samples of Ten^- tumors and 18 samples of Ten^+ tumors), and 25 specimen of normal tissue (four samples of Ten^- tumors and 21 of Ten^+ tumors) were processed. To control the quality of the microarray analysis, we analyzed several samples in technical replicates.

The raw data were pre-processed using Genome Studio software (version 1.9.0.24624; Illumina) and further analyzed using the packages oligo (10) and limma (11) of the Bioconductor (12) within the R environment (R Foundation for Statistical Computing, Vienna, Austria; http://www.R-project.org/). In brief, transcription profiles were background corrected using a normal-exponential model, quantile normalized and variance stabilized using base 2 logarithmic transformation. A moderated *t*-test was used to detect differentially expressed transcripts after fitting the linear model I ~ Tissue * Presence of Ten in Tumor Stroma. Storey's q-value less than 0.25 (13) and a minimally 1.5-fold change in expression intensity were required to consider genes as being differentially transcribed. The MIAME compliant data was deposited to the Array Express database (E-MTAB- E-MTAB-5852 and E-MTAB-6364).

Gene set enrichment analysis (GSEA) was performed using Fisher's exact test on KEGG pathways (14) and Gene Ontology (15). To consider the gene set significantly enriched by differentially expressed genes and to account for possible multiple testing issues, statistical significance of the test was set to $p<0.005$, enrichment odds ratio to at least two and at least three genes shared by the gene set and the set of differentially transcribed genes.

Results

Histology. Immunohistochemical detection of presence of the ECM proteins in sections of HNSCC, MSR and NM is exemplarily illustrated in Figures 1 and 2. There is an apparent similarity between the frequency of Ten and Gal-1 presence. These two proteins were consistently absent in NM and in MSR, but strongly expressed in HNSCC (NM or MSR *vs*. HNSCC; $p<0.01$). Fn expression in NM showed almost equal distribution between positive and negative samples. In MSR and HNSCC, a shift to positive cases was seen (NM *vs*. MSR or HNSCC; $p<0.01$).

Co-expression of markers to establish the $Ten^+Fn^+Gal\text{-}1^+$ status occurred more frequently in samples of HNSCC (n=42; 55%) than in NM (n=3; 9%; $p<0.01$). The most common combinations of marker parameters observed in NM were $Ten^-Fn^+Gal\text{-}1^-$ (n=15; 45%) and $Ten^-Fn^+Gal\text{-}1^-$ (13; 39%). Of note, they were rather rare in HNSCC (3% and 4%, respectively; $p<0.01$). Interestingly, all three combinations occurred with rather similar frequency in MSR, *i.e.* $Ten^+Fn^+Gal\text{-}1^+$ (n=8; 24%), $Ten^-Fn^+Gal\text{-}1^-$ (n=12; 36%) and $Ten^-Fn^-Gal\text{-}1^-$ (11; 33%) ($p=0.568$). Of note, the difference of frequency values between HNSCC and MSR samples was statistically significant ($p<0.05$) (Figure 3).

Considering association of positivity for Ten, FN or Gal-1 with clinical characteristics, no significant correlation between immunopositivity and nodal stage of tumors (Ten: $p=0.0715$; Fn: $p=0.906$; Gal-1: $p=0.963$) was found in the present study, Figure 4 illustrating data for Ten. The data on the other histopathological parameters, too, revealed no correlations to the status of expression of these three proteins.

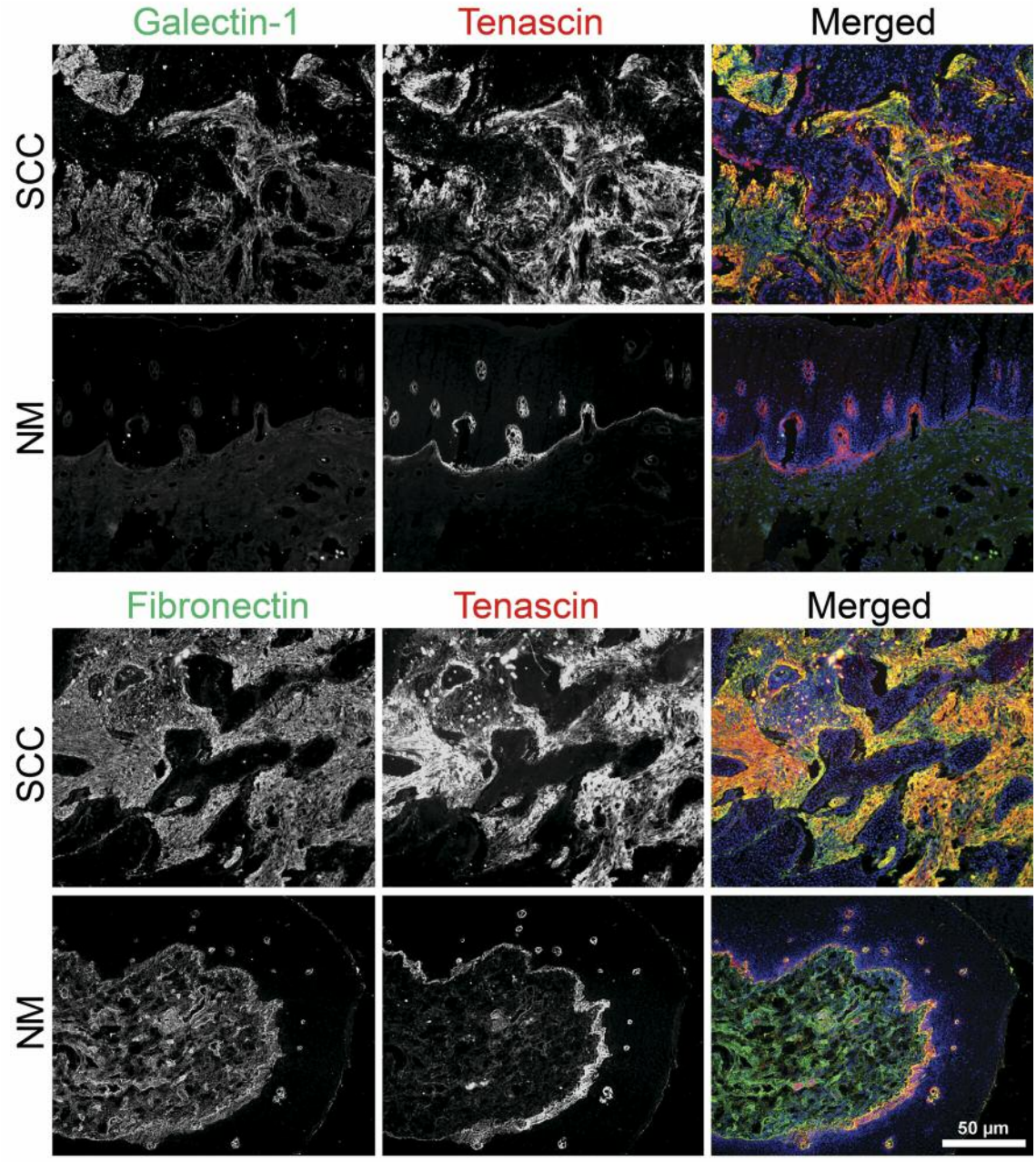

Figure 2. *Immunofluorescent detection of pairs of galectin-1 (green signal) and tenascin (red signal) in the top part and of fibronectin (green signal) and tenascin (red signal) in the bottom part in frozen sections of normal mucosa (NM) and squamous cell carcinoma (SCC). Nuclei were counterstained with DAPI (scale bar 50 µm).*

Prognostic correlations. Ten: No tendency for improved prognosis in short-term 2-year follow-up for patients with Ten^+ tumor stroma in both overall survival (OS) and disease-free survival (DFS) was observed. The difference was not statistically significant (Figure 5; OS: p=0.245; DFS: p=0.369). After 5-year follow-up, no difference was found between Ten^+ and Ten^- samples (in both OS and DFS).

Positivity in MSR was likewise related to prognosis (2- and 5-year OS and DFS). The obtained data did not reach the level of statistical significance (2-year OS: p=0.168; 5-year OS: p=0.218; 2y DFS: p=0.0742; 5y DFS: p=0.122). Respective data on 5-year OS and DFS were significantly higher in patients with Ten^+ NE (p<0.05) (Figure 5 and Figure 6).

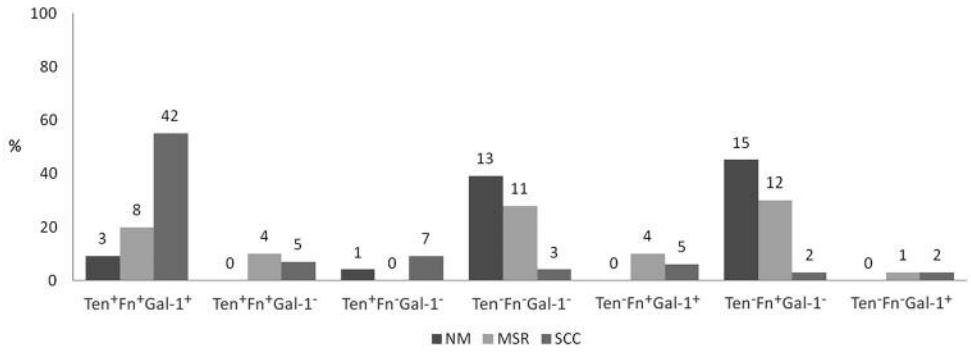

Figure 3. *Distribution (%) of specimen according to the categories of immunohistochemical negativity (–)/positivity (+) for tenascin (Ten), fibronectin (Fn) and galectin-1 (Gal-1) in tissue sections of normal mucosa (NM), margin of surgical resecate (MSR) and squamous cell carcinoma (SCC). Number of evaluated patients is provided above each column.*

Fib: No correlation between Fn expression and patients' prognosis was delineated.

Gal-1: Although 2-year OS indicated that Gal-1$^+$ tumors may have a relatively unfavorable prognosis, this correlation did not reach the threshold for statistical significance. Similarly, no association between Gal-1 expression and prognosis was found in peritumoral and normal tissues.

These immunohistochemical data thus document differences between HNSCC and NM but did not uncover a prognostically relevant association of Ten presence/absence. In the concept of our study design, we proceeded to map gene-expression profiles to answer the questions whether and which profile changes can occur.

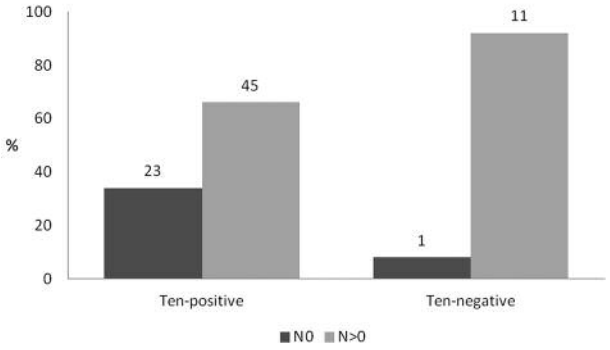

Figure 4. *Distribution (%) of specimen according to the categories of immunohistochemical Ten negativity/positivity based on lymph node staging (N0, absence of regional lymph node metastasis; N>0, presence of regional lymph node metastasis). Number of evaluated patients is provided above each column.*

Microarray analysis: a) RNA profiles differ between Ten$^-$ and Ten$^+$ tumors. When comparing RNA preparations from Ten$^+$ and Ten$^-$ tumors, changes in 115 genes were detected. They are compiled in the Table III and Supplementary Table I (available at http://www.physiolchem.vetmed.uni-muenchen.de/summary/anticancer_research/index.html) for the cases of most significant differences. The GSEA analysis of the Biological Process GO ontology terms (Table IV and Supplementary Table II available at http://www.physiolchem. vetmed.uni-muenchen.de/summary/anticancer_research/index.html) revealed an association of differentially transcribed genes with the JAK-STAT signaling cascade (GO:0046427), with expression of several genes down-regulated in Ten$^+$ tumors (JAK2, LIF, and CYP1B1) and that of the NOTCH1 gene down-regulated in Ten$^-$ tumors. Also, a strong up-regulation of expression of genes involved in ncRNA processing (GO:0034470) in the Ten$^+$ tumors was seen. A gene belonging to this section is argonaute 2 (AGO2), whose transcriptions appear to be significantly up-regulated in Ten$^+$ tumors compared to Ten$^-$ tumors, MSR, and NE, as also seen for the gene for pseudouridylate synthase 7 (PUS7), while gene expression for integrator complex subunit 1 (INTS1) is significantly down-regulated in Ten$^-$ tumors in comparison to Ten$^+$ tumors, MSR, and NE. GSEA of the Cellular Compartment GO ontology resulted in strong enrichment of the genes associated with components of the ECM and microenvironment (GO:0044421). Among them are lysyl oxidase-like 1 (LOXL1), whose expression is up-regulated in Ten$^-$ tumors, C1q and TNF related 1 (C1QTNF1), up-regulation seen in Ten$^-$ tumors and related MSR, and basal cell adhesion molecule (BCAM), up-regulation detected in Ten$^-$ tumors-derived MSR and normal tissues. There were no Molecular Function GO ontology terms found among the genes differentially expressed between Ten$^+$ and Ten$^-$ tumors (Figure 7).

Cases of gene dysregulation between Ten$^+$ *vs.* Ten$^-$ tumors furthermore include PRAME (preferentially expressed antigen in melanoma) strongly up-regulated in Ten$^+$ tumors, G6PC3 (glucose-6-phosphatase catalytic subunit 3) and IDUA, α-L-

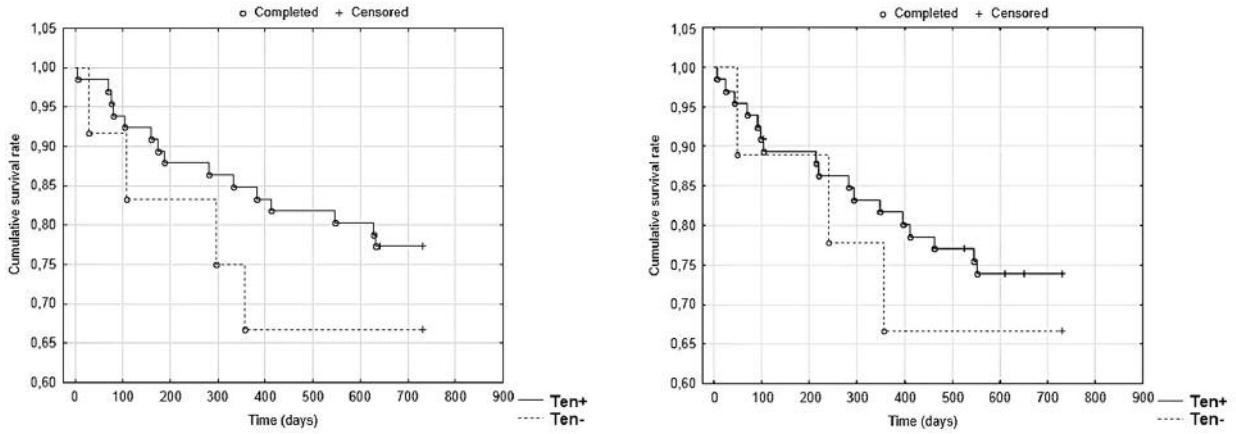

Figure 5. *2-year overall (left) and disease-free (right) survival in tenascin (Ten)-positive/negative tumors (completed – patients' data available during the whole evaluated interval or patient died during the evaluated interval; censored – patients' data are only partially available).*

iduronidase, which are up-regulated in all Ten$^-$ samples, and also LIF, an interleukin 6 family cytokine, which is specifically up-regulated in Ten$^-$ tumors (for the most deregulated genes in this comparison, see Supplementary Table I).

Microaray analysis: b) RNA profiles of MSR differ between Ten$^-$ and Ten$^+$ tumors. Comparing RNA preparations of MSR of patients with either Ten$^+$ or Ten$^-$ tumors, dysregulation of 154 genes was found (Table V and Supplementary Table I). GSEA analyses revealed that major changes occured in the metabolism of lipids (Table VI and Supplementary Table II). The most prominently enriched KEGG signaling pathway is the PPAR signaling pathway (hsa03320), with up-regulation of genes coding for peroxisome proliferator activated receptor gamma (PPARG), aquaporin 7 (AQP7), adiponectin ADIPOQ, perilipins 1 and 4 (PLIN1, PLIN4), lipoprotein lipase (LPL), and fatty acid desaturase 2 (FADS2) in MSR of patients with Ten$^-$ tumors. The glycerophosphatidyl metabolic pathway (hsa00561) also came up to be significantly enriched for up-regulated genes. Consistently, many GO terms associated with lipid metabolism are in the list of genes whose activity was enhanced in MSR of patients with Ten$^-$ tumors. These include cellular compartment lipid droplet (GO:0005811), lipid metabolic process (GO:0006629) and transferase activity (transferring acyl groups other than amino-acyl groups, GO:0016747). Other genes that showed significantly increased representation in the MSR of the patients with Ten$^-$ tumors are leptin (LEP) and galectin-12 (Gal-12; LGALS12) (for the most deregulated genes in this comparison, see Figure 8 and Supplementary Table I).

Microarray analysis: c) RNA profiles of NM of the patients with Ten$^-$ and Ten$^+$ tumors are similar. The profiles of normal tissues of the cohorts of patients with Ten$^-$/Ten$^+$ tumors were very similar. In cases appearing to differ in expression activity such as genes for RAB11B, a member RAS oncogene family, and pancreatic progenitor cell differentiation and proliferation factor (PPDPF), no statistical significance (p=0.21) was reached. Obviously, MSR characteristics appeared to be more susceptible to an influence by the tumor than NM features, based on array-based RNA profiling.

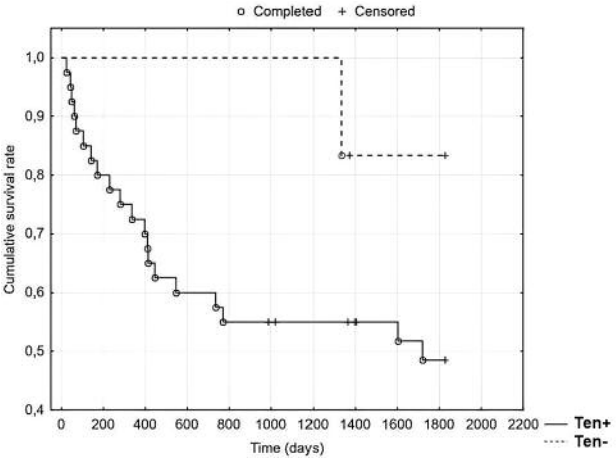

Figure 6. *5-year disease-free survival in tenascin-positive/negative normal mucosae (for explanation of completed/censored, see legend to Figure 5).*

Discussion

In the immunohistochemical part of our study, we revealed the possibility for a stratification according to the absence/presence of Ten. With relevance to prognosis, no

Table III. *Genes differentially transcribed after comparison of Ten$^+$ and Ten$^-$ tumors (|logFC|>1, Storey's q<0.1).*

Entrez gene Id	Gene symbol	Definition	logFC	q-Value
Up-regulated in Ten$^+$ tumors				
23532	PRAME	Preferentially expressed antigen in melanoma	1.74	0.08
27161	AGO2	Argonaute 2, RISC catalytic component	1.65	0.0386
54517	PUS7	Pseudouridylate synthase 7 (putative)	1.15	0.062
Down-regulated in Ten$^+$ tumors				
128434	VSTM2L	V-set and transmembrane domain containing 2 like	–1.72	0.03
3425	IDUA	Iduronidase, alpha-L-	–1.36	0.062
51733	UPB1	Beta-ureidopropionase 1	–1.34	0.0375
147381	CBLN2	Cerebellin 2 precursor	–1.31	0.03
10398	MYL9	Myosin light chain 9	–1.22	0.062
4059	BCAM	Basal cell adhesion molecule (Lutheran blood group)	–1.19	0.00674
114897	C1QTNF1	C1q and TNF related 1	–1.16	0.0364
92579	G6PC3	Glucose-6-phosphatase catalytic subunit 3	–1.14	0.0798
51208	CLDN18	Claudin 18	–1.12	0.0832
4016	LOXL1	Lysyl oxidase like 1	–1.07	0.00485
22977	AKR7A3	Aldo-keto reductase family 7 member A3	–1.06	0.0832
1510	CTSE	Cathepsin E	–1.05	0.061
3976	LIF	LIF, interleukin 6 family cytokine	–1.04	0.0832
441518	RTL8B	Retrotransposon Gag like 8B	–1.01	0.0422

Table IV. *GSEA analysis on GO Biological process ontology for the genes that are differentially expressed (DEG) between Ten$^+$ and Ten$^-$ tumors (p<0.005, odds ratio > 4, and at least 3 DEG in the gene set).*

Go Id	GO term	No. of genes with term	No. of DEG with term	Odds ratio	*p*-Value
GO:0007214	Gamma-aminobutyric acid signaling pathway	23	3	25.5	0.000345
GO:0034470	ncRNA processing	392	9	4.17	0.000597
GO:0046427	Positive regulation of JAK-STAT cascade	73	4	9.92	0.000984
GO:1904894	Positive regulation of STAT cascade	73	4	9.92	0.000984

correlation between Ten expression and grade, TNM stage and primary site of examined tumors, respectively, was discerned. Of particular note, no significant prognostic correlations was disclosed in all three groups of patients. A lack of association between Ten expression and histopathological features has previoulsy been reported in oral and pharyngeal cancers (16). Considering cell types other than tumor cells, Ten expression in cancer-associated fibroblasts was associated with patient age, tumor stage, lymph node metastasis, clinical stage, cancer recurrence and positively correlated with the presence of platelet-derived growth factor-α/-β and α-SMA. Furthermore, its expression in cancer cells correlated with an increase in the population of tumor-associated macrophages, cancer recurrence and expression of hypoxia inducible factor-1α (17).

The following comparison of gene expression profiles of Ten$^+$ and Ten$^-$ tumors by whole-genome transcriptome analysis led to detection of marked differences. The systematic comparison of profiles identified several genes that code for kinases and receptors relevant in tumor development that are transcriptionally dysregulated in Ten$^-$ tumor samples. Janus kinase 2 (JAK2), a case of down-regulation, is a non-receptor tyrosine kinase associated with cytokine receptors and involved in cell growth, development, differentiation or histone modifications and its overexpression predicts unfavorable prognosis for nasopharyngeal carcinoma (18). *Notch1*, the second prominent example of a down-regulated gene in Ten$^-$ tumors, controls cell-fate decisions including epithelial-to-mesenchymal transition and can hereby be involved a variety of developmental processes, mutations associated with several types of leukemia and HNSCC (19, 20). Leukemia inhibitory factor (LIF) can mediate pro-invasive activation of stromal fibroblasts in cancer (21). Cytochrome *P450* CYP1B1 is involved in an NADPH-

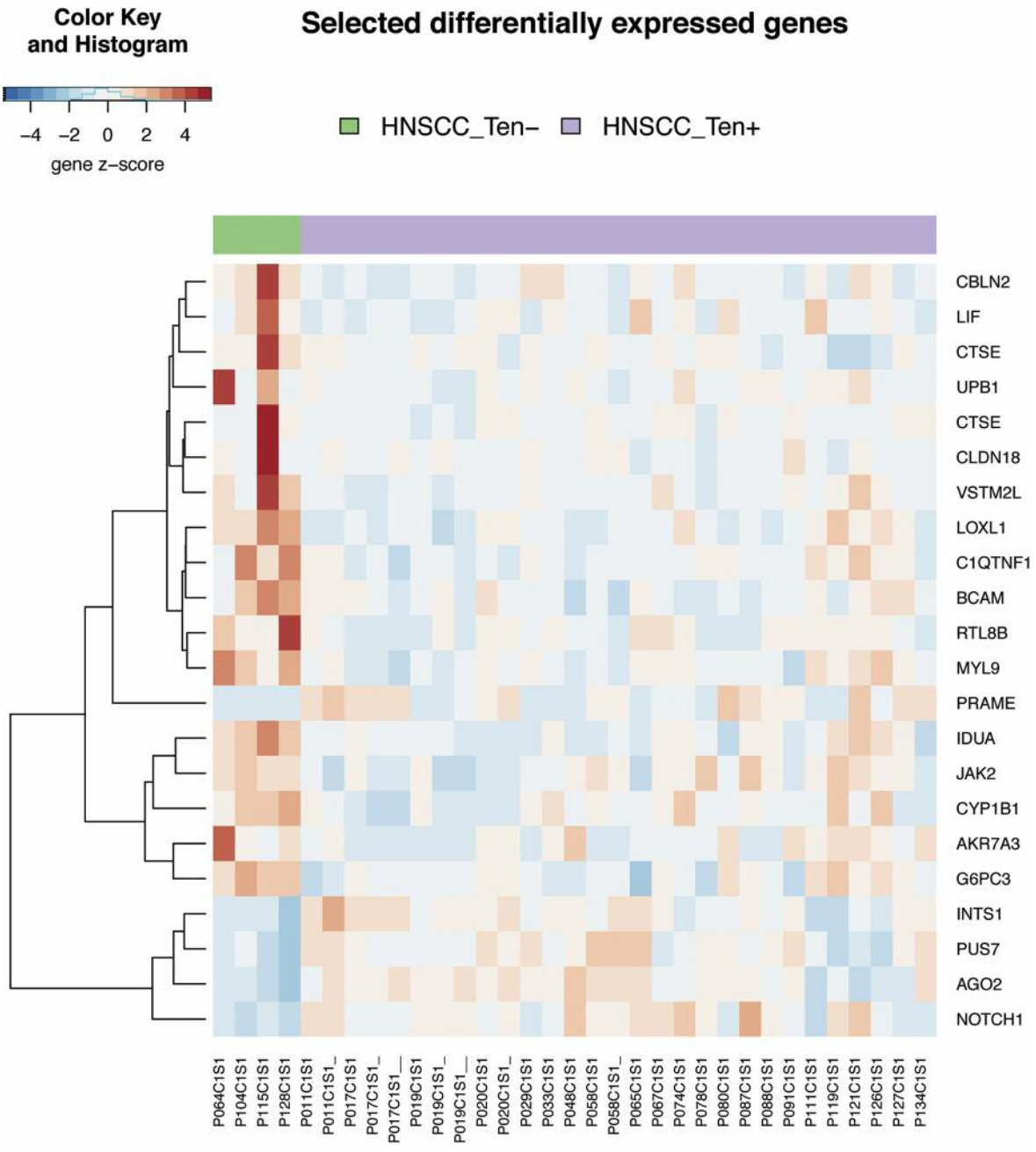

Figure 7. *Transcriptome data on selected genes in preparations of tenascin-positive/negative (Ten$^+$/Ten$^-$) tissue (n=26; for details, see Table II) of head and neck squamous cell carcinoma (HNSCC).*

dependent electron transport pathway, oxidizing a variety of structurally unrelated compounds and promoting angiogenesis. Our data set on Ten$^+$/Ten$^-$ tumors furthermore revealed strong enrichment of factors of the extracellular region. Among these, BCAM was found to be up-regulated in Ten$^-$ tumors, their stroma and matching normal tissues. Its expression is associated with immature states of human keratinocytes and it is induced in epithelial skin tumors and inflammatory epidermis (22, 23).

In this study, we next turned to the comparison of MSR specimens separated according to Ten expression of the tumor. Intriguingly, monitoring the MSR surrounding the

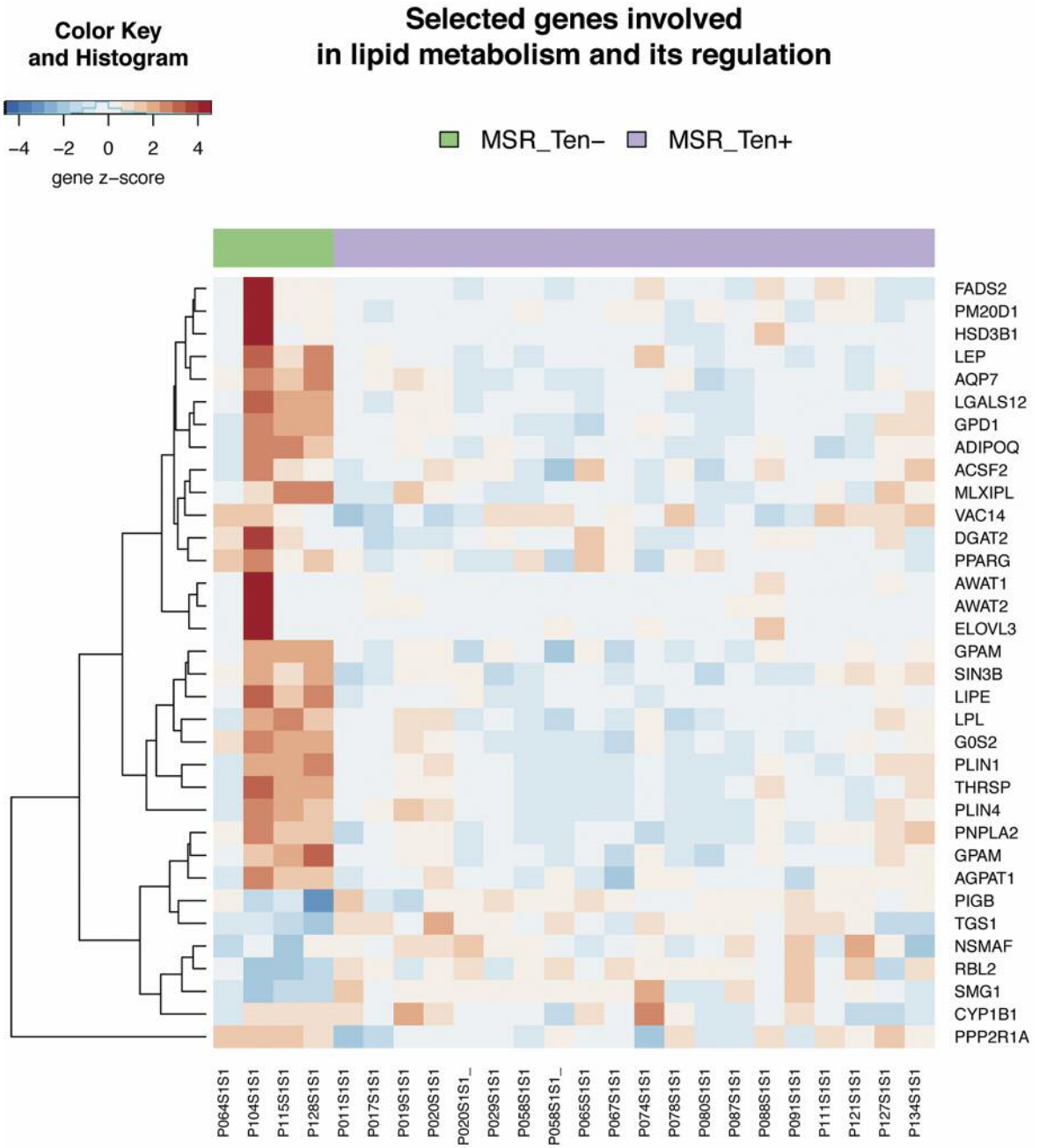

Figure 8. *Transcriptome data on selected genes involved in lipid metabolism and its regulation in margin of surgical reseacate (MSR) preparations of tenascin-positive/negative (Ten$^+$/Ten$^-$) tumors.*

Ten$^-$ tumors found a strong up-regulation of transcription of genes within the lipid metabolism. A prominent gene on this list is LEP. It is a key player in the regulation of energy balance and body weight (24). Moreover, LEP has also been described as a tumor-promoting gene for example in breast (25) and liver cancers (26). In addition, the multifunctional LEP is involved in the regulation of the ERK signaling (27) and can be apoptotic *via* the JAK2-STAT3 pathway and up-regulation of BIRC5 expression, as well as regulates presence of matrix metalloproteinases (MMPs) and tissue inhibitors of MMPs (28, 29).

Multifunctionality, too, holds true for the adhesion/growth-regulatory galectins (2, 30-32), Gal-12 expression exhibiting a similar increase as LEP does (see Supplementary Figure 1).

Table V. *Genes differentially transcribed in margin of surgical resecates (MSR) of Ten+ and Ten− tumors (|logFC|>1, Storey's q<0.1, best 20 by |logFC|).*

Entrez gene Id	Gene symbol	Definition	logFC	q-Value
Up-regulated in MSR of patients with Ten+ tumors				
6726	*SRP9*	Signal recognition particle 9	1.23	0.003
Down-regulated in MSR of patients with Ten+ tumors				
7069	*THRSP*	Thyroid hormone responsive	–3.33	<0.001
729359	*PLIN4*	Perilipin 4	–3.03	0.09
50486	*G0S2*	G0/G1 switch 2	–2.64	0.02
5346	*PLIN1*	Perilipin 1	–2.47	0.08
4023	*LPL*	Lipoprotein lipase	–2.07	0.09
6649	*SOD3*	Superoxide dismutase 3	–2.04	0.008
5997	*RGS2*	Regulator of G protein signaling 2	–1.92	0.09
3991	*LIPE*	Lipase E, hormone sensitive type	–1.8	<0.001
56246	*MRAP*	Melanocortin 2 receptor accessory protein	–1.8	0.008
9370	*ADIPOQ*	Adiponectin, C1Q and collagen domain containing	–1.78	0.009
2819	*GPD1*	Glycerol-3-phosphate dehydrogenase 1	–1.7	0.01
83483	*PLVAP*	Plasmalemma vesicle associated protein	–1.56	0.02
84870	*RSPO3*	R-spondin 3	–1.51	0.1
3952	*LEP*	Leptin	–1.39	0.008
85329	*LGALS12*	Galectin 12	–1.38	0.005
57678	*GPAM*	Glycerol-3-phosphate acyltransferase, mitochondrial	–1.31	0.08
57104	*PNPLA2*	Patatin like phospholipase domain containing 2	–1.3	0.02
375719	*AQP7P1*	Aquaporin 7 pseudogene 1	–1.28	0.01
364	*AQP7*	Aquaporin 7	–1.27	<0.001

Table VI. *GSEA analysis on GO Biological process ontology for the genes that are differentially expressed (DEG) between MSR of patients with Ten+ and Ten− tumors (p<0.005, odds ratio>10, and at least 3 DEG in the gene set).*

Go Id	GO term	No. of genes with term	No. of DEG with term	Odds ratio	*p*-Value
GO:0036155	Acylglycerol acyl-chain remodeling	7	3	104	<0.0001
GO:0010889	Regulation of sequestering of triglyceride	11	3	52	<0.0001
GO:0019915	Lipid storage	60	5	12.8	<0.0001
GO:0019432	Triglyceride biosynthetic process	32	4	20	<0.0001
GO:0055089	Fatty acid homeostasis	13	3	41.6	0.0001
GO:0046460	Neutral lipid biosynthetic process	34	4	18.6	0.0001
GO:0046463	Acylglycerol biosynthetic process	34	4	18.6	0.0001
GO:0030730	Sequestering of triglyceride	14	3	37.8	0.0001
GO:0050873	Brown fat cell differentiation	37	4	16.9	0.0002
GO:0010883	Regulation of lipid storage	40	4	15.5	0.0002
GO:0010888	Negative regulation of lipid storage	17	3	29.7	0.0002
GO:0031116	Positive regulation of microtubule polymerization	21	3	23.1	0.0005
GO:0031112	Positive regulation of microtubule polymer./depolymer.	24	3	19.8	0.0007
GO:0014823	Response to activity	59	4	10.2	0.0009

This galectin's impact on growth control accounts for its current status as candidate tumor suppressor (33), in line with epigenetic gene silencing by promoter methylation and induction by butyrate in colorectal carcinoma lines (34, 35). The herein reported up-regulation thus gives incentive to extend the immunohistochemical analysis of the galectin network in cancer, as described for example for colon cancer (36), and its surrounding tissue to this so far not studied

family member, flanked by monitoring galectin binding using the labeled tissue lectin, an approach complementary to immunohistochemical monitoring (37-39). In this sense, determining this protein's presence, prompted by the array data presented herein, is likely to add to the evidence for galectin involvement in processes related to malignancy, as assumed following the detection of expression of tissue lectins in cancer more than 30 years ago (40).

In summary, our results reveal marked disparities of gene-expression signatures between i) tumor specimens stratified according to matrix glycoprotein without prognostic relevance and ii) MSR specimens in the formal category of lipid metabolism. These data point to plasticity of gene-expression profiles without necessarily bearing prognostic relevance and are relevant in principle for considerations of relating differences detected on this level to clinical parameters.

Conflicts of Interest

The Authors declare no potential conflicts of interest.

Acknowledgements

This work was supported by Progres Q28, GAUK 165015, and the Ministry of Health of the Czech Republic (Grant no. 15-28933A). The present study was also supported in part by the Agency for Science and Research under the contract no. APVV-0408-12, APVV-14-0731, APVV-16-0446, and APVV-16-0207). Support was also provided by Ministry of Education, Youth and Sports of CR within the National Sustainability Program II (project BIOCEV-FAR; registration no. LQ1604) and project BIOCEV (grant no. CZ.1.05/1.1.00/02.0109). The present study usedthe equipment for metabolomics and cell analyses (grant no. CZ.1.05/2.1.00/19.0400) supported by the Research and Development for Innovations Operational Program, co-financed by the European regional development fund and the state budget of the Czech Republic. Inspiring discussions with Drs. B. Friday and A. Leddoz are gratefully acknowledged.

References

1 Zivicova V, Broz P, Fik Z, Mifkova A, Plzak J, Cada Z, Kaltner H, Kucerova JF, Gabius H-J and Smetana K Jr.: Genome-wide expression profiling (with focus on the galectin network) in tumor, transition zone and normal tissue of head and neck cancer: marked differences between individual patients and the site of specimen origin. Anticancer Res *37*: 2275-2288, 2017.

2 Kaltner H, Toegel S, Caballero GG, Manning JC, Ledeen RW and Gabius H-J: Galectins: their network and roles in immunity/tumor growth control. Histochem Cell Biol *147*: 239-256, 2017.

3 Gabius H-J: How to crack the sugar code. Folia Biol (Praha) *63*: 121-131, 2017.

4 Valach J, Fík Z, Strnad H, Chovanec M, Plzák J, Cada Z, Szabo P, Sáchová J, Hroudová M, Urbanová M, Steffl M, Pačes J, Mazánek J, Vlček C, Betka J, Kaltner H, André S, Gabius H-J, Kodet R, Smetana K Jr, Gál P and Kolář M: Smooth muscle actin-expressing stromal fibroblasts in head and neck squamous cell carcinoma:increased expression of galectin-1 and induction of poor prognosis factors. Int J Cancer *131*: 2499-2508, 2012.

5 Dvořánková B, Szabo P, Lacina L, Gal P, Uhrova J, Zima T, Kaltner H, André S, Gabius H-J, Sykova E and Smetana K Jr: Human galectins induce conversion of dermal fibroblasts into myofibroblasts and production of extracellular matrix: potential application in tissue engineering and wound repair. Cells Tissues Organs *194*: 469-480, 2011.

6 Guttery DS, Shaw JA, Lloyd K, Pringle JH and Walker RA: Expression of tenascin-C and its isoforms in the breast. Cancer Metastasis Rev *29*: 595-606, 2010.

7 Nguyen-Ngoc KV, Cheung KJ, Brenot A, Shamir ER, Gray RS, Hines WC, Yaswen P, Werb Z and Ewald AJ: ECM microenvironment regulates collective migration and local dissemination in normal and malignant mammary epithelium. Proc Natl Acad Sci USA *109*: E2595-2604, 2012.

8 Pickup MW, Mouw JK and Weaver VM: The extracellular matrix modulates the hallmarks of cancer. EMBO Rep *15*: 1243-1253, 2014.

9 Kaltner H, Seyrek K, Heck A, Sinowatz F and Gabius H-J: Galectin-1 and galectin-3 in fetal development of bovine respiratory and digestive tracts. Comparison of cell type-specific expression profiles and subcellular localization. Cell Tissue Res *307*: 35-46, 2002.

10 Carvalho BS and Irizarry RA: A framework for oligonucleotide microarray preprocessing. Bioinformatics 26: 2363-2367, 2010.

11 Ritchie ME, Phipson B, Wu D, Hu Y, Law CW, Shi W and Smyth GK: Limma powers differential expression analyses for RNA-sequencing and microarray studies. Nucleic Acids Res *43*: e47, 2015.

12 Huber W, Carey VJ, Gentleman R, Anders S, Carlson M, Carvalho BS, Bravo HC, Davis S, Gatto L, Girke T, Gottardo R, Hahne F, Hansen KD, Irizarry RA, Lawrence M, Love MI, MacDonald J, Obenchain V, Oleś AK, Pagès H, Reyes A, Shannon P, Smyth GK, Tenenbaum D, Waldron L and Morgan M: Orchestrating high-throughput genomic analysis with bioconductor. Nature Methods *12*: 115-121, 2015.

13 Storey JD and Tibshirani R: Statistical significance for genomewide studies. Proc Natl Acad Sci USA *100*: 9440-9445, 2003.

14 Kanehisa M and Goto S: KEGG: Kyoto encyclopedia of genes and genomes. Nucleic Acids Res *28*: 27-30, 2000.

15 Ashburner M, Ball CA, Blake JA, Botstein D, Butler H, Cherry JM, Davis AP, Dolinski K, Dwight SS, Eppig JT, Harris MA, Hill DP, Issel-Tarver L, Kasarskis A, Lewis S, Matese JC, Richardson JE, Ringwald M, Rubin GM and Sherlock G: Gene ontology: tool for the unification of biology. The Gene Ontology Consortium. Nature Genet *25*: 25-29, 2000.

16 Atula T, Hedstrom J, Finne P, Leivo I, Markkanen-Leppanen M and Haglund C: Tenascin-C expression and its prognostic significance in oral and pharyngeal squamous cell carcinoma. Anticancer Res *23*: 3051-3056, 2003.

17 Yang ZT, Yeo SY, Yin YX, Lin ZH, Lee HM, Xuan YH, Cui Y and Kim SH: Tenascin-C, a prognostic determinant of esophageal squamous cell carcinoma. PLoS One *11*: e0145807, 2016.

18 He HL, Lee YE, Liang PI, Lee SW, Chen TJ, Chan TC, Hsing CH, Chang IW, Shiue YL and Li CF: Overexpression of JAK2: a predictor of unfavorable prognosis for nasopharyngeal carcinoma. Future Oncol *12*: 1887-1896, 2016.

19 Leong KG, Niessen K, Kulic I, Raouf A, Eaves C, Pollet I and Karsan A: Jagged1-mediated Notch activation induces epithelial-to-mesenchymal transition through Slug-induced repression of E-cadherin. J Exp Med *204*: 2935-2948, 2007.
20 Cancer Genome Atlas Network: Comprehensive genomic characterization of head and neck squamous cell carcinomas. Nature *517*: 576-582, 2015.
21 Albrengues J, Bourget I, Pons C, Butet V, Hofman P, Tartare-Deckert S, Feral CC, Meneguzzi G and Gaggioli C: LIF mediates proinvasive activation of stromal fibroblasts in cancer. Cell Rep *7*: 1664-1678, 2014.
22 Schon M, Klein CE, Hogenkamp V, Kaufmann R, Wienrich BG and Schon MP: Basal-cell adhesion molecule (B-CAM) is induced in epithelial skin tumors and inflammatory epidermis, and is expressed at cell-cell and cell-substrate contact sites. J Invest Dermatol *115*: 1047-1053, 2000.
23 Schon M and Schon MP: Expression of basal-cell adhesion molecule (B-CAM) is associated with immature states of human keratinocytes. J Invest Dermatol *117*: 995-997, 2001.
24 Mechanick JI, Zhao S and Garvey WT: Leptin, an adipokine with central importance in the global obesity problem. Glob Heart, 2017. doi: 10.1016/j.gheart.2017.10.003. [Epub ahead of print].
25 Barone I, Catalano S, Gelsomino L, Marsico S, Giordano C, Panza S, Bonofiglio D, Bossi G, Covington KR, Fuqua SA and Andò S: Leptin mediates tumor-stromal interactions that promote the invasive growth of breast cancer cells. Cancer Res *72*: 1416-1427, 2012.
26 Xiong Y, Zhang J, Liu M, An M, Lei L and Guo W: Human leptin protein activates the growth of HepG2 cells by inhibiting PERK-mediated ER stress and apoptosis. Mol Med Rep *10*: 1649-1655, 2014.
27 Jiang L, Li Z and Rui L: Leptin stimulates both JAK2-dependent and JAK2-independent signaling pathways. J Biol Chem *283*: 28066-28073, 2008.
28 Park HY, Kwon HM, Lim HJ, Hong BK, Lee JY, Park BE, Jang Y, Cho SY and Kim HS: Potential role of leptin in angiogenesis: leptin induces endothelial cell proliferation and expression of matrix metalloproteinases *in vivo* and *in vitro*. Exp Mol Med *33*: 95-102, 2001.
29 Jiang H Yu J, Guo H, Song H and Chen S: Up-regulation of survivin by leptin/STAT3 signaling in MCF-7 cells. Biochem Biophys Res Commun *368*: 1-5, 2008.
30 Kaltner H and Gabius H-J: A toolbox of lectins for translating the sugar code: the galectin network in phylogenesis and tumors. Histol Histopathol *27*: 397-416, 2012.
31 Smetana K Jr., André S, Kaltner H, Kopitz J and Gabius H-J: Context-dependent multifunctionality of galectin-1: a challenge for defining the lectin as therapeutic target. Expert Opin Ther Targets *17*: 79-392, 2013.
32 Solís D, Bovin NV, Davis AP, Jiménez-Barbero J, Romero A, Roy R, Smetana K Jr. and Gabius H-J: A guide into glycosciences: How chemistry, biochemistry and biology cooperate to crack the sugar code. Biochim Biophys Acta *1850*: 186-235, 2015.
33 Yang RY, Hsu DK, Yu L, Ni J and Liu FT: Cell cycle regulation by galectin-12, a new member of the galectin superfamily. J Biol Chem *276*: 20252-20260, 2001.
34 Katzenmaier EM, André S, Kopitz J and Gabius H-J: Impact of sodium butyrate on the network of adhesion/growth-regulatory galectins in human colon cancer *in vitro*. Anticancer Res *34*: 5429-5438, 2014.
35 Katzenmaier EM, Kloor M, Gabius H-J, Gebert J and Kopitz J: Analyzing epigenetic control of galectin expression indicates silencing of galectin-12 by promoter methylation in colorectal cancer. IUBMB Life *69*: 962-970, 2017.
36 Dawson H, André S, Karamitopoulou E, Zlobec I and Gabius H-J: The growing galectin network in colon cancer and clinical relevance of cytoplasmic galectin-3 reactivity. Anticancer Res *33*: 3053-3059, 2013.
37 Plzák J, Betka J, Smetana K Jr., Chovanec M, Kaltner H, André S, Kodet R and Gabius H-J: Galectin-3 - an emerging prognostic indicator in advanced head and neck carcinoma. Eur J Cancer *40*: 2324-2330, 2004.
38 Manning JC, García Caballero G, Knospe C, Kaltner H and Gabius H-J: Network analysis of adhesion/growth-regulatory galectins and their binding sites in adult chicken retina and choroid. J Anat *231*: 23-37, 2017.
39 Roy R, Cao Y, Kaltner H, Kottari N, Shiao TC, Belkhadem K, André S, Manning JC, Murphy PV and Gabius H-J: Teaming up synthetic chemistry and histochemistry for activity screening in galectin-directed inhibitor design. Histochem Cell Biol *147*: 285-301, 2017.
40 Gabius H-J, Engelhardt R and Cramer F: Endogenous tumor lectins: overview and perspectives. Anticancer Res *6*: 573-578, 1986.

Received January 17, 2018
Revised January 30, 2018
Accepted February 1, 2018

Histochemistry and Cell Biology (2018) 149:503–516
https://doi.org/10.1007/s00418-018-1650-4

ORIGINAL PAPER

Fibroblasts potentiate melanoma cells in vitro invasiveness induced by UV-irradiated keratinocytes

Njainday Pulo Jobe[1,2,8] · Veronika Živicová[3,4] · Alžběta Mifková[3,4] · Daniel Rösel[1,2] · Barbora Dvořánková[2,3] · Ondřej Kodet[2,3,5] · Hynek Strnad[6] · Michal Kolář[6] · Aleksi Šedo[7] · Karel Smetana Jr.[2,3] · Karolina Strnadová[2,3] · Jan Brábek[1,2] · Lukáš Lacina[2,3,5]

Accepted: 6 February 2018 / Published online: 12 February 2018
© Springer-Verlag GmbH Germany, part of Springer Nature 2018

Abstract

Melanoma represents a malignant disease with steadily increasing incidence. UV-irradiation is a recognized key factor in melanoma initiation. Therefore, the efficient prevention of UV tissue damage bears a critical potential for melanoma prevention. In this study, we tested the effect of UV irradiation of normal keratinocytes and their consequent interaction with normal and cancer-associated fibroblasts isolated from melanoma, respectively. Using this model of UV influenced microenvironment, we measured melanoma cell migration in 3-D collagen gels. These interactions were studied using DNA microarray technology, immunofluorescence staining, single cell electrophoresis assay, viability (dead/life) cell detection methods, and migration analysis. We observed that three 10 mJ/cm^2 fractions at equal intervals over 72 h applied on keratinocytes lead to a 50% increase ($p < 0.05$) in in vitro invasion of melanoma cells. The introduction cancer-associated fibroblasts to such model further significantly stimulated melanoma cells in vitro invasiveness to a higher extent than normal fibroblasts. A panel of candidate gene products responsible for facilitation of melanoma cells invasion was defined with emphasis on IL-6, IL-8, and CXCL-1. In conclusion, this study demonstrates a synergistic effect between cancer microenvironment and UV irradiation in melanoma invasiveness under in vitro condition.

Keywords Cancer-associated fibroblasts · Keratinocytes · Cancer microenvironment · Cytokine · Chemokine · Melanoma

Introduction

The incidence of malignant melanoma is increasing globally. Despite the remarkable progress in melanoma research, the options of treatment in advanced stages of the disease are still very limited (Rastrelli et al. 2014). This can be linked to either primary resistance or to the frequently occurring phenomenon of acquired resistance to the therapy. Extensive UV light exposure is considered to be the most critical risk factors in cutaneous melanoma initiation due to the acquisition of mutations (D´Orazio

Njainday Pulo Jobe and Veronika Živicová contributed equally.

✉ Lukáš Lacina
lukas.lacina@lf1.cuni.cz

1 Department of Cell Biology, Faculty of Sciences, Charles University in Prague, Viničná 7, 120 00 Prague 2, Czech Republic

2 Biotechnology and Biomedicine Center of the Academy of Sciences and Charles University in Vestec (BIOCEV), Průmyslová 595, Vestec u Prahy, Prague, Czech Republic

3 Institute of Anatomy, 1st Faculty of Medicine, Charles University, U Nemocnice 3, Prague 2, Czech Republic

4 Department of Otorhinolaryngology, Head and Neck Surgery, 1st Faculty of Medicine, Charles University, V Úvalu 5, Prague 5, Czech Republic

5 Department of Dermatovenereology, 1st Faculty of Medicine, Charles University, U Nemocnice 2, Prague 2, Czech Republic

6 Institute of Molecular Genetics, Academy of Sciences of the Czech Republic vvi, Vídeňská 1083, Prague 4, Czech Republic

7 Institute of Biochemistry and Experimental Oncology, 1st Faculty of Medicine, Charles University, U Nemocnice 5, Prague 2, Czech Republic

8 Present Address: Cell and Experimental Pathology, Department of Translational Medicine, Lund University, Clinical Research Centre, Skåne University Hospital, Jan Waldenströms gata 35, 21421 Malmö, Sweden

et al. 2013; Lo and Fisher 2014; Brash 2015; Rünger 2016). The skin in childhood seems to be more vulnerable to UV. However, the incidence of malignant melanoma is rare. Therefore, the childhood represents a susceptible life stage for adult-onset UV radiation late effects. UV exposure leads to accumulation of resulting irreversible DNA alterations in the skin which can be manifested after several decades (Volkmer and Greinert 2011). On the other hand, the occurrence of melanoma in sun-protected sites such as mucosal or subungual regions indicates that previous extensive sun exposition is not always a necessary condition for the formation of this type of a tumour (Merkel and Gerami 2017).

Similarly, to other types of tumours, the microenvironment is a very important factor for malignant melanoma progression and spreading (Lacina et al. 2015, 2017; Wang et al. 2016; Dvořánková et al. 2017). Cancer-associated fibroblasts isolated from melanoma (mCAFs) significantly influence not only the phenotype of melanoma cells per se but they influence also the phenotype of normal surrounding keratinocytes (Kodet et al. 2013; Kučera et al. 2015). Furthermore, they can influence the phenotype of various other co-cultured epithelial cell types, e.g., breast cancer cells (Dvořánková et al. 2012). These fibroblasts also influence in vitro invasiveness of melanoma and other cancerous (e.g., glioblastoma) cells. This mechanism seems to be dependent on the production of IL-6 and IL-8 (Trylčová et al. 2015; Jobe et al. 2016).

In the context of normal epidermis, melanocytes and keratinocytes represent a functional unit requiring multiple mutual interactions of both cell types (Kondo and Hearing 2011). Such tightly regulated interaction is a prerequisite for the proper physiological functions of the epidermis, namely the melanisation and melanogenesis. The epidermal re-pigmentation after cutaneous injury also consists of several highly orchestrated events, such as keratinocyte and melanocyte proliferation, migration of both cell types into the wound site, melanin production and transfer to the neighbouring keratinocytes (Chou et al. 2013). Both epidermal and neural crest-derived stem cells exit their niche in the hair follicle and contribute to the newly reconstituted epidermal layer. This provides an excellent example of how stem cells located in the bulge region of the hair follicle cope with sudden requirements for their differentiation and also their own maintenance. Any impairment during this period (e.g., excessive and prolonged inflammatory responses) may lead to abnormal pigmentation, both hypopigmentation and hyperpigmentations are possible. However, the molecular signals responsible for these pathological responses to injury remain, in detail, unknown.

In the context of cutaneous pathology relevant for this article, keratinocytes seem to stimulate spreading of melanoma cells via deregulation of MiTF (Golan et al. 2015) resulting in the increased aggressive behaviour of melanoma cells (Cheli et al. 2011).

Melanocyte biology studies focusing on intercellular interactions have already acknowledged the importance of keratinocytes, the principal and the most numerous population of the epidermal compartment. Despite the great difference in population numbers, this interaction is certainly not unidirectional and melanocytes are not the only subject of regulation. Melanoma cells and melanocytic precursors (represented by neural crest-originated stem cells isolated from in the bulge region of the hair follicle) can influence the maintenance of low differentiation status of human keratinocytes observed in vitro and also contribute to highly aberrant epidermal architecture observed in melanoma biopsies in vivo (Kodet et al. 2015).

On the other hand, as keratinocyte–melanocyte interaction via direct cell-to-cell contact or via paracrine factors seems to be obvious, growing evidence suggests that also dermal fibroblasts modulate melanocyte behaviour, presumably in a paracrine manner. Recent evidence indicates melanocyte being active in the modulation of angiogenesis, inflammation, and fibroplasia after injury (Catania 2007; Adini et al. 2014, 2015). Similar reciprocal interaction in the case of melanoma and mCAFs seems to be likely.

As mentioned above, UV irradiation is a key factor responsible for carcinogenesis in normal melanocytes, converting them after the acquisition of a critical set of mutations in malignant melanoma cells. Notably, one of the earliest responses of viable keratinocytes to the UV-related damage is the formation of an inflammasome within their cytoplasm. Exposure to the UV light thus induces sterile inflammation associated with the production of a broad spectrum of cytokines/chemokines that influence epidermal homeostasis and can be important for melanoma cell invasion in the skin (Kim et al. 2011). In such case, UVB seems to be the relevant part of UV spectra. UVB primarily affects keratinocytes of the epidermal basal layer, leaving fibroblasts below the basement membrane relatively unaffected. This study presents data demonstrating the synergistic effect of UV-irradiated microenvironment represented by irradiated keratinocytes with either normal as well as cancer-associated fibroblasts on invasiveness of melanoma cells in 3-D collagen gels.

Materials and methods

Cell donors

Normal human dermal fibroblasts (HFs), as well as keratinocytes, were isolated from the residual tissue after mammoplasty from Department of Esthetic Surgery, 3rd Faculty of Medicine, Charles University, Prague. mCAFs

were isolated from melanoma patients (Table 1) treated at Department of Dermatovenereology, 1st Faculty of Medicine, Charles University, Prague. All tissues were acquired with the written informed consent approved by local ethical committees of abovementioned clinical centres with full respect to Declaration of Helsinki. Highly metastatic BLM melanoma cell line was kindly provided by L. van Kempen and J.H.J.M. van Krieken, Department of Pathology, Radboud University, Nijmegen Medical Centre, the Netherlands. Commercially available A2058 melanoma cells were purchased from ATCC® HTB-43™ (Teddington, UK).

Fibroblast cultivation

mCAFs and HF were isolated as described previously by tissue explant method (Trylcova et al. 2015). Briefly, the small pieces of melanoma metastasis and human dermis, respectively, were transferred to the CellBind 6-well plate (Corning, Schiphol Rijk, the Netherlands) and cultured in Dulbecco's Modified Eagle Medium (DMEM) (Biochrom) with antibiotics and 10% Foetal Bovine Serum (FBS, all Biochrom) at 37 °C and 5% CO_2. The cells outgrowing from the explants were harvested by trypsinization (0.25% trypsin and 0.02% EDTA 1:1, Biochrom) and expanded after initial confirmation of phenotype by means of immunocytochemistry. Low passage fibroblasts (below P5) of three independent strains (coded as VEM, MAM, ZAM) were used for this study.

Keratinocyte cultivation and co-culture of keratinocytes with fibroblasts

Dermo-epidermal sheets were harvested from the residual skin from aesthetic breast surgery of otherwise healthy female donors. Small pieces of tissue were cut and treated overnight in 0.3% trypsin solution at 4 °C. The epidermis was peeled off next day and the suspension of keratinocytes was prepared by careful mechanical disintegration using syringes. Obtained keratinocyte suspension was seeded on the subconfluent Mitomycin C (Sigma-Aldrich, Prague, Czech Republic) treated monolayer of 3T3 mice fibroblasts. Cultures were maintained in keratinocyte medium (Krejčí et al. 2015) at 37 °C and 5% CO_2. Low passage keratinocytes (P1, P2) were used for this study.

Consequently, using HF or mCAFs as a feeder layer, keratinocytes were cultured on these coverslips for 7 days in keratinocyte medium. The co-cultures on coverslips were used for immunocytochemical analysis.

Immunocytochemistry

HF as well as mCAFs and their co-cultures with HK were briefly fixed in paraformaldehyde, permeabilized with 0.1% Tween-20, blocked by 10% serum in PBS, and used for immunocytochemical studies according to the standard Abcam ICC/IF protocol (http://www.abcam.com/protocols/immunocytochemistry-immunofluorescence-protocol). The primary antibody dilution was according to the recommendation of the suppliers (Table 2). The specificity of the immunocytochemical reaction was tested by use of isotype controls or tissue-irrelevant antibodies instead of specific

Table 1 Characteristic of the patients from which cancer-associated fibroblasts were isolated

CAFs	Birth	Sex	Primary melanoma, year	Breslow (mm), clark	CAFs isolation from skin metastasis	Localisation of metastasis	Death
VEM	1923	Male	Back, 2010	9.3; V	2010	Left arm	2015
ZAM	1954	Male	Chest, 2009	2.3; III	2010	Chest	2011
MAM	1947	Female	Chest, 2007	2.8; IV	2010	Abdomen	2014

Table 2 Antibodies used in immunocytochemical analyses

Primary antibody	Supplier (location)	Secondary antibody/fluorochrome	Supplier (location)
Nestin/M	Merck-Millipore (Prague, Czech Republic)	Goat anti-mouse/TRITC	Sigma-Aldrich (Prague, Czech Republic)
CD 45/M	DAKO (Glostrup, Denmark)		
Vimentin/M			
Smooth muscle actin/M			
CD34/M			
Melan A (MART-1)/M	Invitrogen, ThermoFisher Scientific (Waltham, MA, USA)		
HMB-45 (Anti-Melanosome)/M			
Wide spectrum Cytokeratin/P	Abcam, (Cambridge, UK)	Swine anti-rabbit/FITC	DAKO (Glostrup, Denmark)

antibodies. Cell nuclei were counterstained with 4′,6-diamidino-2-phenylindole (DAPI, Sigma-Aldrich), mounted in Vectashield (Vector Laboratories, Peterborough, UK) and analysed using an Eclipse 90i fluorescence microscope (Nikon, Prague, Czech Republic) equipped with a ProgRes MF Cool camera (Jenoptik Optical Systems, Jena, Germany) and NIS-ElementsAR4.40.00 computer-assisted image analysis system (Laboratory Imaging, Prague, Czech Republic).

UV irradiation of keratinocytes and conditioned media preparation

Low passage keratinocytes (P2) were seeded into the CellBind 6-well plate at the density 50,000 cells/cm^2 and cultured without feeder in keratinocyte medium for 7 days. On the day 7, the subconfluent layers of keratinocytes were treated with different single doses of UVB radiation (10, 50 and 100 mJ/cm^2, respectively) using CL-1000 Ultraviolet Crosslinker (UVP, LLC Upland, Canada) with an integrated UV-B dosimetric device. The control cells were not irradiated. Conditioned media were prepared by addition of 2 ml of DMEM to each well and the cells were cultured for the next 2 days. After 24 h, conditioned media were aspirated, filtered through 0.2 µm microfilter (Corning, NY, USA), aliquoted and frozen at − 80 °C for later use. These media were labelled as 24H media.

For the study of repeated low doses of UV-B in the presence of fibroblasts, the subconfluent cultures keratinocytes were irradiated either by a single dose of 100 or by 10 mJ/cm^2 for three consecutive days. After irradiation, HF or mCAFs in the culture inserts (seeded at the density 10,000 cells/cm^2) were placed into the wells with 2 ml of fresh DMEM. The conditioned media were prepared from this experiment as described above. In a parallel experiment, keratinocytes were cultured on cover glasses under the same conditions and used for life/dead cell assay.

Detection of percentage of viable cells

To determine levels of life and dead cells in the culture, commercial staining kit Live/Dead Viability/Cytotoxicity Kit (Invitrogen, Oregon, USA) was used according to the instructions of the supplier.

Evaluation of DNA damage by single cell gel electrophoresis (comet assay) and data analysis

The single cell gel electrophoresis was performed on UVB-irradiated keratinocytes according to standard Alkaline Comet Assay guidelines (Tice et al. 2000). Briefly, the cells were irradiated as described above. The irradiated cells were embedded in low melting point agarose and poured on negatively charged glass slides at density 20,000/slide. After the cell lysis and alkaline treatment (pH 13), the electrophoresis was performed in a light protected Comet Assay Tank (Cleaver Scientific, Rugby, United Kingdom) at 25 V for 30 min in the cold room at 4 °C. The nuclei were finally counterstained with 4′,6-diamidino-2-phenylindole and imaged as described above on fluorescence microscope. The acquired images were analysed using ImageJ with bundled OpenComet plug-in (v 1.3.1) validated (Schneider et al. 2012; Gyori et al. 2014) for alkaline comet assay. The Olive moment (calculated as DNA percentage and the distance between the intensity-weighted centroids of head and tail) of at least 100 comets for each experiment was calculated. All experiments were performed in doublets. Statistical analysis was performed using Past3 package (version 3.15) (Hammer et al. 2001), the Kruskal–Wallis test for equality of medians and Mann–Whitney test with Bonferroni serial correction of p values were performed.

Spheroid invasion assay and statistical analysis

The study was performed as described in details previously (Jobe et al. 2016). Briefly, BLM and A2058 melanoma cells were cultured as spheroids in Microtissues® 3D Petri Dish® (Sigma-Aldrich) according to manufacturer's instructions. Spheroids were then embedded in Collagen R (Serva, Heidelberg, Germany) solution, containing DMEM, 5% $NaHCO_3$ and 10% FBS (Biochrom). Using a 48-well plate, one spheroid was placed per well, and collagen was polymerized. DMEM or conditioned medium was added to the wells. Images were taken immediately, and after 48 h using a Nikon-Eclipse TE2000-S (4×/0.13 PHL objective, 10×/0.13 PHL objective) (Nikon) and analysed by NIS-Elements software (Laboratory Imaging). The data were analysed with ANOVA followed by Tukey's honest significant difference test.

Microarray analysis

The cells of each fibroblast population were seeded at a density of 1000 cells/cm^2 into two 6-cm diameter Petri dishes (Corning, NY, USA) and cultured for 7 days (95–100% confluence). Culture medium was changed every 2 days and 24 h before harvest. For cell lysis, RLT buffer (Qiagen GmbH, Hilden, Germany) with 2-Mercaptoethanol (Sigma-Aldrich, Prague, Czech Republic) was used. The cell lysates (two technical replicates of each population) were collected to small Eppendorf tubes, frozen, and stored at − 80 °C.

Total RNA was isolated using RNeasy Micro Kit (Qiagen, MD, USA) according to manufacturer's protocol. Quality and concentration of RNA were measured with a NanoDrop 2000 spectrophotometer (Thermo Fisher Scientific, MA, USA). The RNA integrity was analysed by

Agilent Bioanalyzer 2100 (Agilent). Only samples with intact RNA profile were used for expression profiling analyses (RIN > 9).

Illumina HumanHT-12 v4 Expression BeadChips (Illumina, CA, USA) were used for the microarray analysis following the standard protocol. In brief, 200 ng RNA was amplified with Illumina TotalPrep RNA Amplification Kit (Ambion, TX, USA) and 750 ng of labelled RNA was hybridized on the chip according to the manufacturer's protocol. The analysis was performed in two biological replicates per group. The raw data were preprocessed using GenomeStudio software (version 1.9.0.24624; Illumina, CA, USA) and the limma package (Smyth 2006) of the Bioconductor (Gentleman et al. 2004), as described elsewhere (Mateu et al. 2016): the transcription profiles were background corrected using normal-exponential model, quantile normalized and variance stabilized using base 2 logarithmic transformation.

A moderated t test was used to detect transcripts differentially expressed between the treated samples and controls (within limma) (Smyth 2006). False discovery rate values were used to select significantly differentially transcribed genes (FDR < 0.05). The transcription data are MIAME (Minimum Information about a Microarray Experiment) compliant and have been deposited in the ArrayExpress database (Accession number E-MTAB-5973).

Results

Immunocytochemical analysis of keratinocytes and fibroblasts

Human keratinocytes from interfollicular epidermis were positive for keratins as expected (data not shown). Primary cultures of HFs and mCAFs, respectively, were negative for the leukocyte CD45 marker, endothelial marker CD34, melanocytic markers MELAN-A, HMB-45, S100 protein, tyrosinase, and epithelial keratins. All HFs, as well as mCAFs from the cutaneous metastases of melanoma from all three different donors (coded as VEM, MAM, ZAM), revealed typical spindle-shaped fibroblastoid morphology and they were positive for typical mesenchymal marker intermediate filament vimentin. The cultures prepared from one of the mCAFs (coded as ZAM) cells also contained spontaneously in high numbers the myofibroblasts positive for α-smooth muscle actin, the hallmark of CAFs (Fig. 1).

Expression profiles of HF and mCAFs

mCAFs prepared from three melanoma patients were collectively different (FDR < 0.05 and fold change two times) from normal HFs in the expression of 402 genes. While VEM and MAM mCAFs significantly differed from normal fibroblasts in 564 genes and 623 genes, respectively, ZAM mCAFs were different in outstanding 1157 genes (from

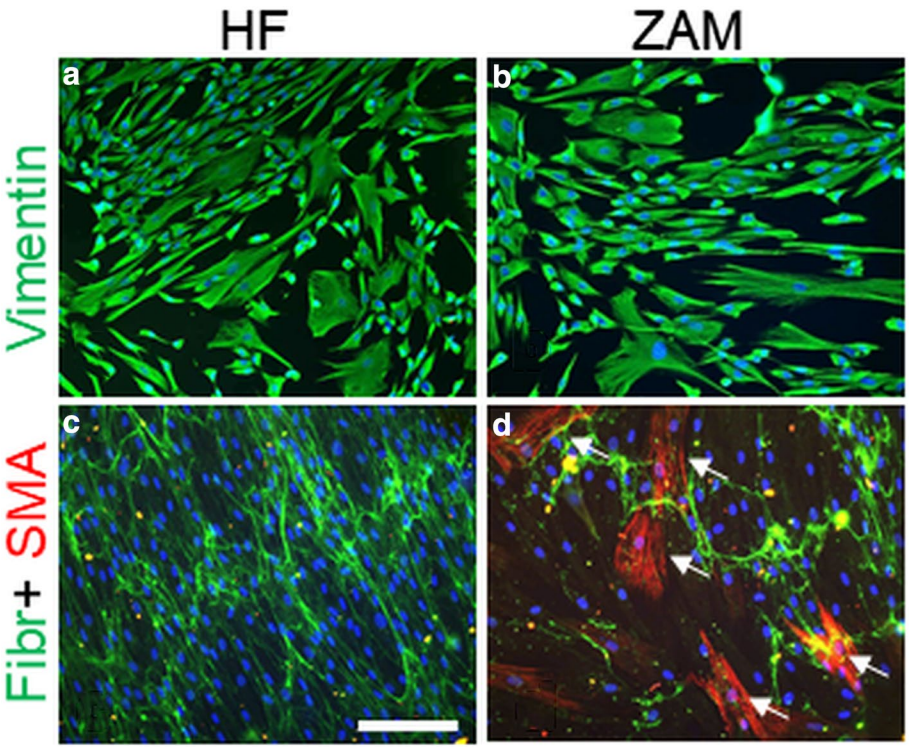

Fig. 1 Detection of vimentin (green signal, **a, b**), fibronectin (Fibr, green signal, **c, d**), and α smooth muscle actin (SMA, the red signal, **c, d**) in normal human dermal fibroblasts—HF (**a, c**) and cancer-associated fibroblasts—ZAM (**b, d**). Nuclei are counterstained with DAPI, the bar represents 100 μm

normal HFs, Fig. 2). This situation is also clearly depicted by the heat map (Fig. 3). The list of selected upregulated genes in ZAM coding extracellularly released factors (compared here to HF) with potential to influence keratinocytes and melanoma cells via paracrine interaction is shown in Table 3. Selected genes for extracellular products were also significantly upregulated in ZAM cells in comparison to mCAFs from two other donors (VEM, MAM) (Table 4). Genes coding IL6, IL8, and CXCL1 were upregulated in mCAFs from all three donors (see Tables 1, 4, respectively). Based on these indications, highly active ZAM cells were selected for further experiments as the representatives of mCAFs.

Effect of HF and ZAM on normal keratinocyte phenotype

Human keratinocytes cultured with normal HF and ZAM mCAFs formed distinct colonies. While keratinocytes cultured in the presence of HF exhibited no signal for vimentin, keratinocytes co-cultured with ZAM cells frequently coexpressed of keratins together with vimentin (Fig. 4).

Effect of keratinocyte irradiation on melanoma in vitro invasiveness in 3-D collagen gels

Keratinocytes alone stimulate invasiveness of melanoma cells almost 1.5 times in BLM and 3 times in A2058 melanoma cells using 3-D collagen migration assay. This baseline finding was compared after UV treatment of keratinocytes. Low dose UV-irradiation (10 mJ/cm^2) of keratinocytes revealed the only a very mild stimulatory effect on migration of both types of melanoma cells. More extensive UV-irradiation (50 and 100 mJ/cm^2) minimise the observed effect of keratinocytes on melanoma cells migration (Fig. 5).

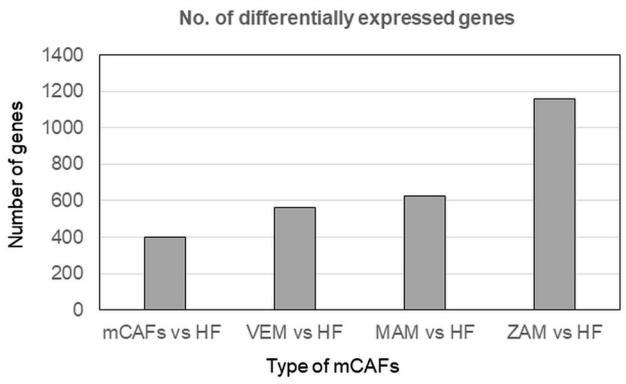

Fig. 2 The number of differentially expressed genes between cancer-associated fibroblasts (CAFs) isolated from all three donors and normal dermal fibroblasts (HF) and separately from each donor of CAF and HF

Normal HF introduced to the co-culture of keratinocytes irradiated by 3×10 mJ/cm^2 strongly stimulated invasiveness of BLM melanoma cells, however, it did not enhance invasiveness in A2058 cells.

When ZAM mCAFs were introduced to the co-culture system, the effect on the in vitro invasion in collagen gels was enhanced in both tested melanoma cell lines (Fig. 6).

The introduction of either HF or ZAM mCAFs to co-cultures after keratinocyte irradiation by 100 mJ/cm^2 was also effective in terms of melanoma enhanced invasiveness, but it did not reach extents observed in the case of the irradiation by 3×10 mJ/cm^2 (Fig. 6).

Effect of UV irradiation on DNA integrity of keratinocytes

An evident DNA damage was clearly documented in keratinocytes immediately after either 10 or 100 mJ/cm^2 UVB dose administration using Single Cell Gel Electrophoresis (Fig. 6). However, the low dose (10 mJ/cm^2) damage was readily repaired after 24 h, with or without fibroblast of any type ($p > 0.05$, no statistical significance). Keratinocytes irradiated at the high dose level (100 J/cm^2) were more seriously damaged immediately after UV irradiation ($p < 0.001$, statistical significance) and this detrimental damage could not be repaired after 24 h. Thus, single cell electrophoresis after high dose treatment could not be evaluated after 24 h in any case because only negligible numbers of keratinocytes maintained sufficient DNA and cellular integrity (Fig. 7).

Effect of HF and ZAM on normal keratinocyte: detection of life/dead cells

Non-irradiated keratinocytes, as well as keratinocytes irradiated by 3×10 mJ/cm^2, were practically without any signal of the presence of dead cells without and after the treatment with HF and ZAM CAFs. High-dose UVB irradiation (100 mJ/cm^2) was lethal for the majority of keratinocytes. After the introduction of either HF or ZAM to the culture of lethally irradiated keratinocytes, the cells formed clusters of shrinking cells with green cytoplasm (life cells) and red nuclei that are typical for dead cells (Fig. 8).

Discussion

The main finding of this study is the observation that even partial UV irradiation damage of tissue microenvironment supports in vitro invasion of melanoma cells on the 3D model. The compound model of tissue microenvironment consisting from insert co-culture of UV-irradiated keratinocytes and unirradiated fibroblasts allows collection of the conditioned medium after selective damage of a particular

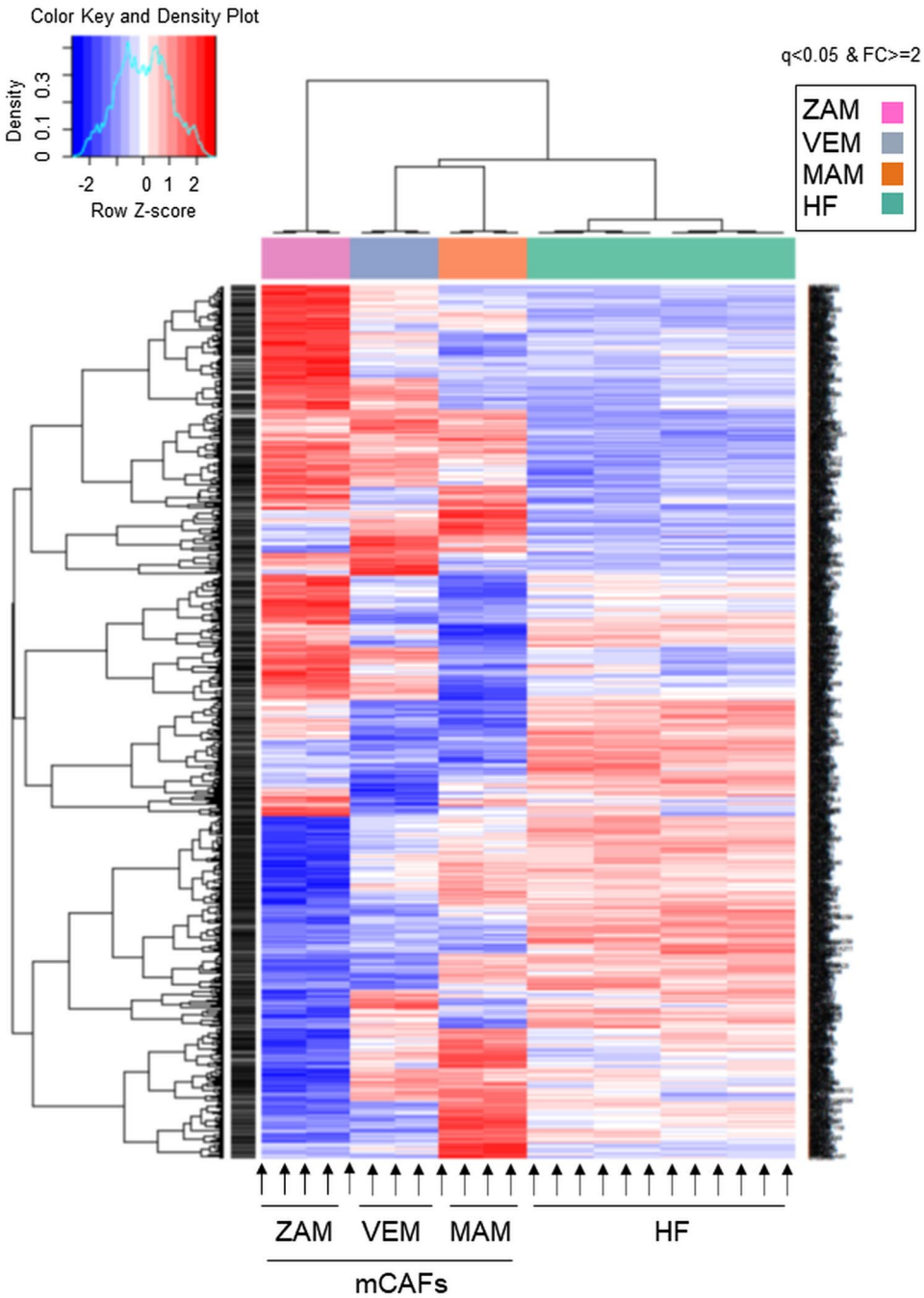

Fig. 3 Heat map demonstrates differential expression of genes in cancer-associated fibroblasts (ZAM, VEM, MAM) and normal dermal fibroblasts (HF)

component. The UVB seems to be a highly relevant component of UV light because it is causing a predominantly epidermal damage. UVB is linked to epidermal carcinogenesis. However, the selected energy of 10 mJ/cm^2 represents a low dose. It is lower than the minimal erythematous dose for fair skin (Dornelles et al. 2004). Such irradiation would not be associated with any immediate visible tissue response in vivo. However, there is a well-recognized relationship between chronic UVB-induced damage and the development of non-melanoma skin cancer. The protection mechanisms against UV-induced DNA damage have been extensively studied after subjecting cells or animal models with single acute UVB irradiation (Jackson and Bartek 2009). Until now, very little is known about how those mechanisms are influenced by chronic exposure to UVB light (Drigeard Desgarnier et al. 2017).

The dermal component of skin should be relatively unaffected by UVB irradiation, as only UVA irradiation significantly penetrates deeper into the dermis. UVA therefore potentially causes more widespread alterations in the dermis contributing to photoaging. On the other hand, acute low-level UVB irradiation upregulates matrix metalloproteinase

Table 3 Selected genes upregulated in ZAM compared to HF

Symbol	Gene name	LFC	FDR	Kerat	Melanoma
IL8	Interleukin 8	5.5	2.6e−06	+	+
ACAN	Aggrecan	4.27	3.6e−07	+	+
IL6	Interleukin 6 (interferon, beta 2)	3.87	7.5e−13	+	+
IL1B	Interleukin 1, beta	2.52	3.6e−08		
CXCL1	Chemokine (C–C–C motif) ligand 1 (melanoma growth stimulating activity, alpha)	2.49	0.0045	+	+
HBEGF	Heparin-binding EGF-like growth factor	1.74	8.5e−06	+	
BDNF	Brain-derived neurotrophic factor	1.46	5.3e−06		+
TGFB2	Transforming growth factor, beta 2	1.23	0.00017		+
IGFBP7	Insulin-like growth factor binding protein 7	1.23	0.00012	+	
GAP43	Growth associated protein 43	1.21	2.3e−05	+	
CXCL16	Chemokine (C–X–C motif) ligand 16	1.17	8.3e−05		+
BMP6	Bone morphogenetic protein 6	1.11	0.0032		
KAZALD1	Kazal-type serine peptidase inhibitor domain 1	1.03	0.016		
VEGFC	Vascular endothelial growth factor C	1.02	0.0066	+	+
CTGF	Connective tissue growth factor	0.95	0.022		+
PDGFRL	Platelet-derived growth factor receptor-like	0.93	0.055		+
LEPREL1	Leprecan-like 1	0.91	0.017		
IL17D	Interleukin 17D	0.88	0.00021		+
VEGFA	Vascular endothelial growth factor A	0.82	0.029	+	+
BMP2	Bone morphogenetic protein 2	0.73	0.028		+
LEPRE1	Leucine proline-enriched proteoglycan (leprecan) 1	0.72	0.0011		

LFC binary logarithm of the fold change in expression intensity, *FDR* false discovery rate, *Kerat* keratinocytes, *Melanoma* melanoma cells, +: genes with stimulatory effect on keratinocytes or melanoma cells according to literature data (for references see "Discussion")

Table 4 Selected genes upregulated in ZAM compared to other CAFs

Symbol	Gene name	LFC	FDR
IL8	Interleukin 8	3.87	0.00032
IL6	Interleukin 6 (interferon, beta 2)	2.61	9.8e−10
BDNF	Brain-derived neurotrophic factor	1.48	4.1e−05
HBEGF	Heparin-binding EGF-like growth factor	2.17	3.2e−07
IL1B	Interleukin 1, beta	1.95	2.7e−06
CSPG4	Chondroitin sulphate proteoglycan 4	1.77	9.1e−0.5
VEGFC	Vascular endothelial growth factor C	1.51	0.00013
KCTD10	Potassium channel tetramerisation domain containing 10	1.17	8.1e−06
TGFB2	Transforming growth factor, beta 2	1.15	0.00042
CXCL1	Chemokine (C-C-C motif) ligand 1 (melanoma growth stimulating activity, alpha)	1.06	0.42
NTF3	Neurotrophin 3	0.96	2e−05
GAP43	Growth associated protein 43	0.91	0.00094
EPS15	Epidermal growth factor receptor pathway substrate 15	0.78	0.044
CTGF	Connective tissue growth factor	0.72	0.13
BMP2	Bone morphogenetic protein 2	0.71	0.044
PDGFRL	Platelet-derived growth factor receptor-like	0.93	0.055
LEPREL1	Leprecan-like 1	0.91	0.017
VEGFA	Vascular endothelial growth factor A	0.82	0.029
BMP2	Bone morphogenetic protein 2	0.73	0.028
FGF5	FIBROBLAST growth factor 5	0.68	0.37

LFC binary logarithm of the fold change in expression intensity, *FDR* false discovery rate

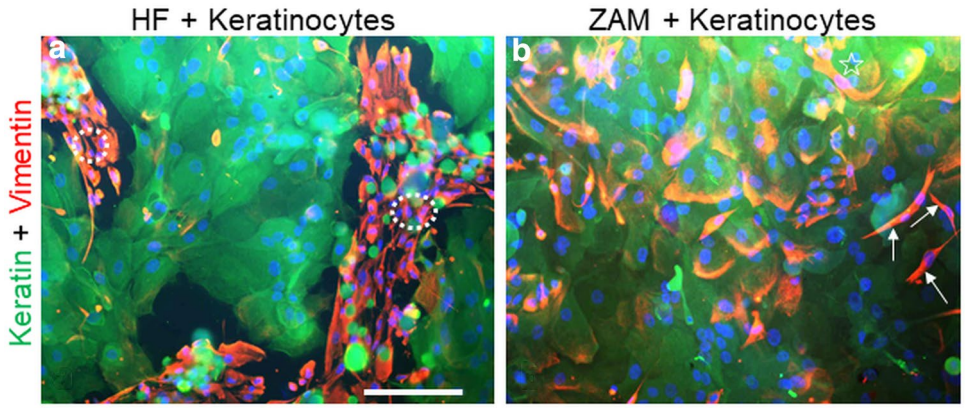

Fig. 4 Co-culture of human keratinocytes (**a, b**) with normal dermal fibroblasts (HF, **a**) and ZAM cancer-associated fibroblasts (**b**). While keratinocytes with HF exhibited only keratins (green signal, **a**), keratinocytes co-cultured with ZAM (**b**) exhibited both keratins (green signal) and vimentin (red signal). Vimentin positivity in double positive keratinocytes indicates their polarization. Vimentin-positive HFs are marked by white circles and vimentin-positive ZAM with white arrows. Nuclei are counterstained with DAPI, the bar represents 100 µm

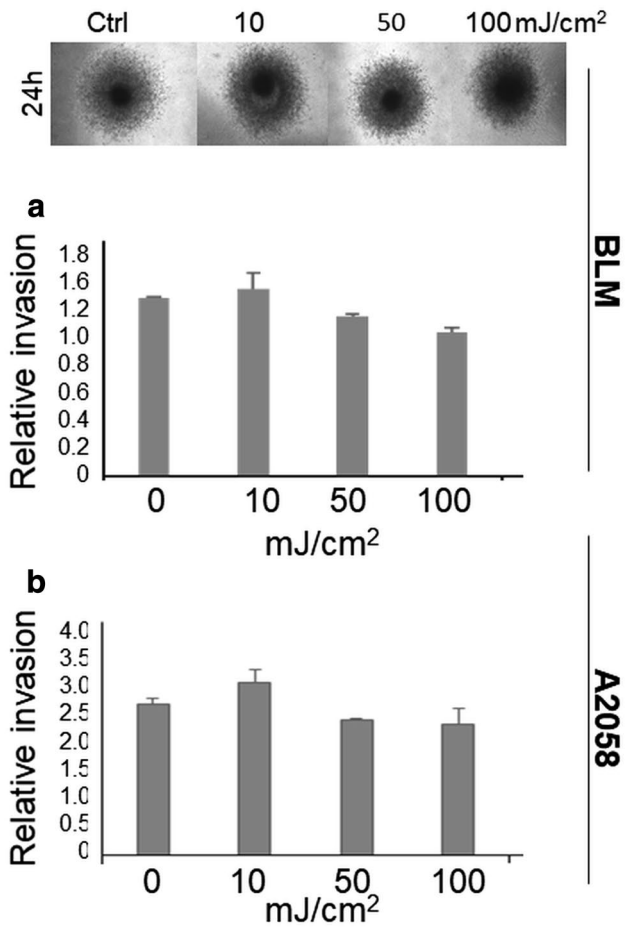

Fig. 5 Influence of UV-irradiated keratinocytes on relative invasion of BLM (**a**) and A2058 (**b**) melanoma cells. As the control, the conditioned medium from non-irradiated keratinocytes was used. The introduction of non-irradiated keratinocytes to system influences the melanoma cell invasiveness more in A2058 than in BLM cells

1 (Fisher et al. 1996) which consequently initiates collagen I fibril degradation. Ultraviolet B irradiation also suppresses procollagen I synthesis, thereby promoting further loss of collagen I fibrils (Fisher et al. 2000). Surprisingly, it was suggested that the MMPs induced by low-dose UV irradiation might be derived from the epidermis, and only to a lesser extent, from the dermis (Brennan et al. 2003; Quan et al. 2009). This clearly highlights the importance of epithelial–mesenchymal interaction in the maintenance of the epidermal structure.

Despite the increasing insight into various events in photoaging, the specific molecular pathogenesis of changes in the photodamaged dermis and their relation to various processes, such as cellular senescence, remains poorly understood. Compelling evidence about senescence in cultured cells has been gathered over the past decades. However, the senescence in living organisms is enigmatic, largely because of technical limitations relating to the identification and characterization of senescent cells in tissues and organs (Childs et al. 2015).

The autocrine and paracrine properties of senescent cells can play an important role in the contexts of ageing and age-related diseases, including cancer (Smetana et al. 2016a, b). There is convincing evidence associating senescent cells with the malignant progression of tumours. Of note, the senescence-associated secretory phenotype includes multiple pro-inflammatory cytokines, and IL-6 and IL-8 are consistently present in this repertoire (Ortiz-Montero et al. 2017).

On the other hand, the population of stromal fibroblast in malignant tumours (the CAFs) also produces a broad panel of growth factors/cytokines/chemokines broadly overlapping with the repertoire of senescence-associated secretome. As we know from our previous research (Kolář

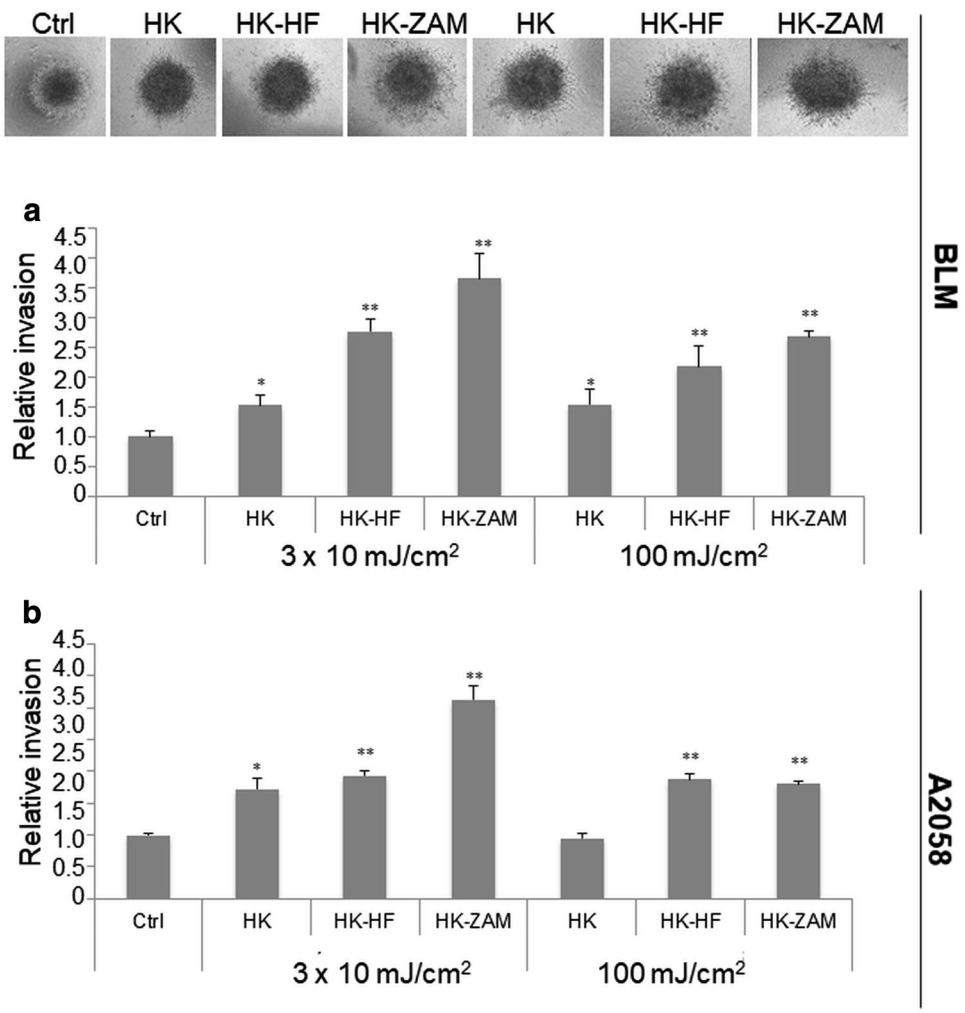

Fig. 6 Normal dermal fibroblasts (HF) and namely cancer-associated fibroblasts ZAM increased the effect of UV-irradiated keratinocytes (HK) and stimulated invasion of BLM (**a**) and A2058 (**b**) melanoma cells. Mild fractionated irradiation (3×10 mJ/cm^2) was more efficient than lethal irradiation of keratinocytes (100 mJ/cm^2)

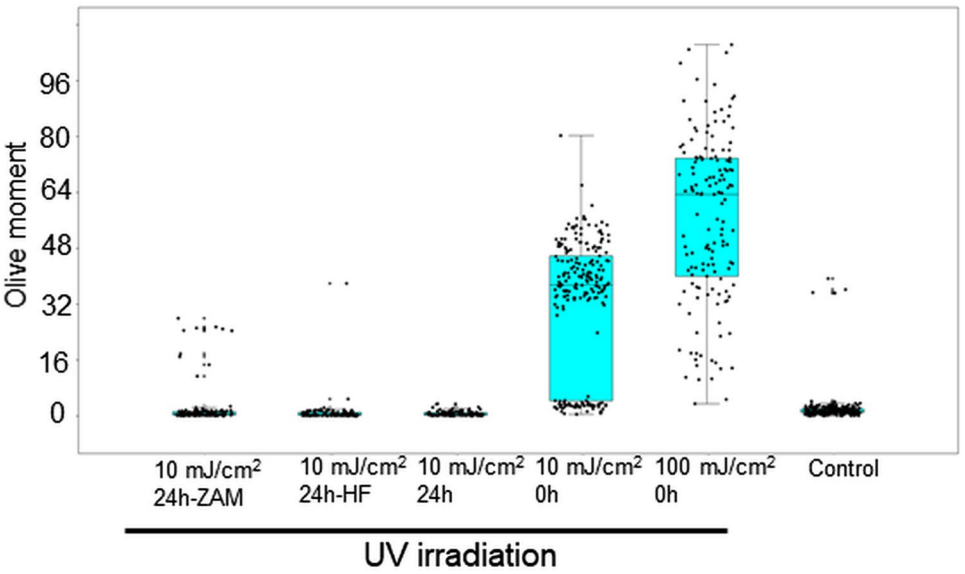

Fig. 7 Significant damage to DNA assessed by single cell gel electrophoresis (comet assay) was detected immediately after 10 and 100 mJ/cm^2 dose, respectively ($p < 0.01$). However, keratinocytes were able to repair DNA damage after 24 h in case of low dose (10 mJ/cm^2) irradiation with or without co-cultured cancer-associated fibroblasts isolated from melanoma (mCAFs) or normal fibroblasts (HF) (no significant differences, $p > 0.05$)

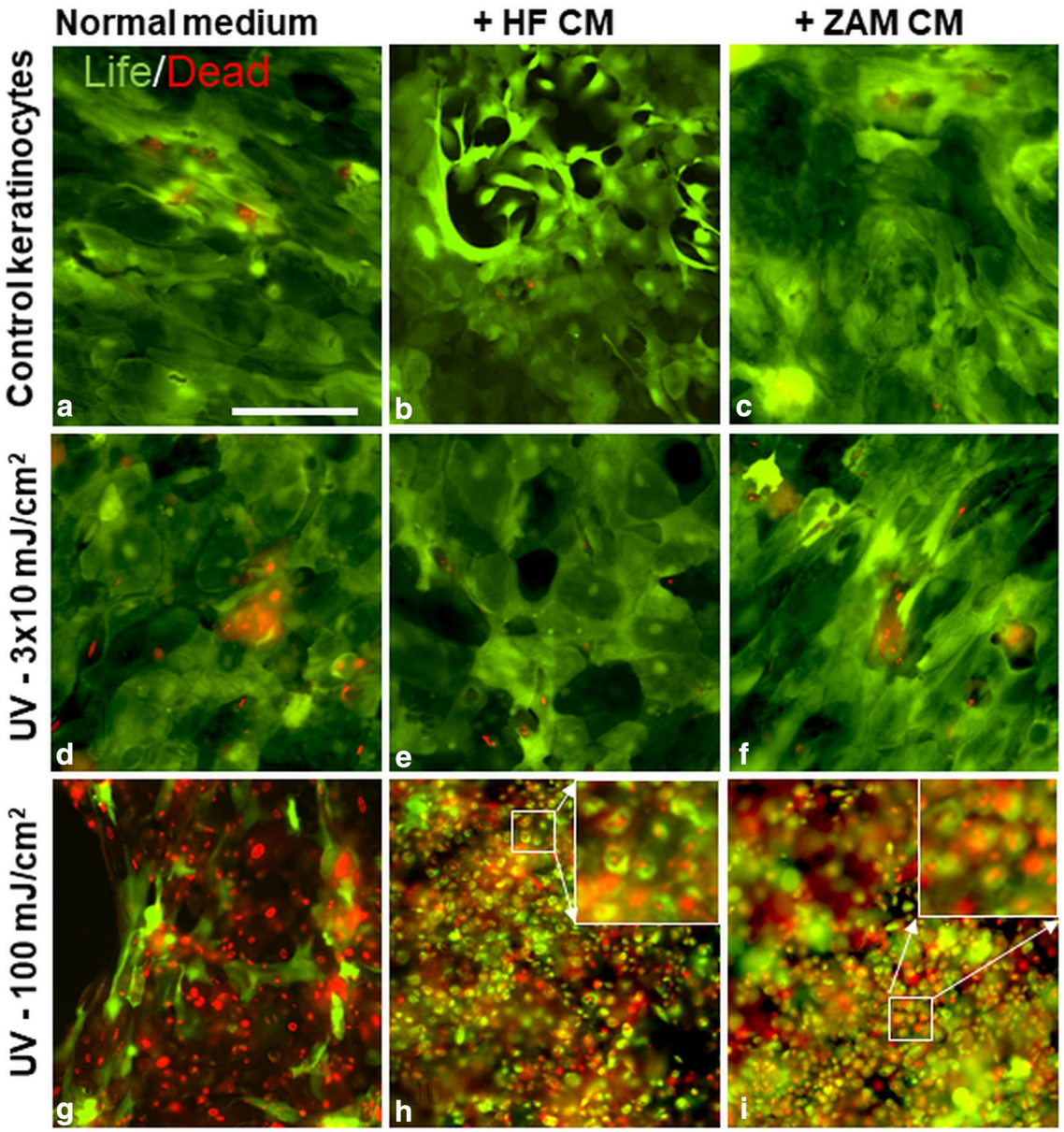

Fig. 8 Control keratinocytes (**a**–**c**) as well as keratinocytes after fractionated mild irradiation (3×10 mJ/cm^2) (**d**–**f**) exhibited the low occurrence of dead cells (red nuclei) without (**a, d**), or with normal fibroblasts (**b, e**) and with ZAM cancer-associated fibroblasts (**c, f**). High dose UV irradiation (100 mJ/cm^2) significantly increased the number of dead cells (**g**). Interestingly that introduction of HF or ZAM to the system increased a number of green cells (signal for living elements), although the number of dead nuclei was not affected (**h, i**). These green cells are very small with shrunk cytoplasm. The bar represents 100 µm

et al. 2012), IL-6, IL-8 and CXCL-1 can be produced by CAFs in a paracrine manner and these cytokines can significantly influence the maintenance of low differentiation status of keratinocytes. Besides that, IL-6 and IL-8 also potentiate invasiveness of melanoma cells in vitro (Jobe et al. 2016). The differences between the real senescence-associated secretory phenotype and its counterpart in malignant tumours are subtle, if any, and still elusive (Ghosh and Capell 2016).

Assuming that we are physiologically exposed to a repeated chronic low dose of UV radiation, it becomes crucial to understand how molecular mechanisms in skin tissue respond to these minor recurrent irradiation doses. Repeated mild UV irradiation of keratinocytes thus resembles the situation in the light-unprotected human skin. It has no detrimental effect on keratinocyte viability in contrast to high-dose (100 mJ/cm^2) with lethal effect on treated keratinocytes. However, even this low dose treatment can

cause DNA damage. Mesenchymal cells in the dermal compartment, either HF or mCAFs, respond to and interact with the UV-damaged keratinocytes via paracrine production of bioactive factors. This UV damage in keratinocytes, in fact, triggers multilateral intercellular interaction. Notably, UV-irradiated keratinocytes (and fibroblasts) secrete molecules also important for melanoma progression such as bFGF, endothelin-1, TGF-β1, TNF-α, IL-11, IL-1α, and PDGF (platelet-derived growth factor and hepatocyte growth factor) even in monoculture (Brenner et al. 2005).

Normal HF and mCAFs seem to be able to influence UV-damaged epidermal keratinocytes by the paracrine production of numerous bioactive factors that we selected from their expression profile analysis in the present study. In addition to others, aggrecan (Shafritz et al. 1994), HBEGF (Johnson and Wang 2013), IGFBP-7 (Hochberg et al. 2013), GAP-43 (Kant et al. 2015), CTGF (Barrientos et al. 2008), VEGF-C (Benke et al. 2010), PDGFRL (Kamp et al. 2003), VEGF-A (Wu et al. 2014), IL-6, IL-8 and CXCL-1 (Kolář et al. 2012) stimulate proliferation and/or migration of keratinocytes (Table 3). Moreover, factors produced by HF and mainly by mCAF (represented by strain ZAM) can also positively influence the melanoma cells. It was demonstrated for factors such as IL-6 and IL-8 (Jobe et al. 2016), aggrecan (Iida et al. 2007) and CXCL-1 (Di Cesare et al. 2007). The same effect was also observed for BDNF (Marchetti and Nicolson 1997), TGF-B2 (Zhang et al. 2009), CXCL-16 (La Porta 2012), VEGF-C (Peppicelli et al. 2014), CTGF (Finger et al. 2014), PDGFRL (Sabbatino et al. 2014), IL-17D (Zelba et al. 2014), VEGF-A (Vartanian et al. 2011), and BMP-2 (Rothhammer et al. 2005) (Table 3).

In conclusion, UV-irradiation is not only an important factor in mutagenesis. UV light represents also an important factor for melanoma in vitro invasion. The role of UV irradiation on melanoma progression can be therefore expected. The described phenomenon seems to be important in the facilitation of either radial growth in superficial melanoma or in progression to more advanced stages of disease associated vertical growth and subsequent metastasis formation. In agreement with previously published data, IL-6, IL-8, and CXCL-1 can be an attractive target for intervention in the context of chronic UV light exposure. Further analysis needs to be done to shed light on those mechanisms and their consequence for cells. A proper understanding of these mechanisms may offer a new powerful target for skin cancer prevention and therapy. The hope is that increasing precaution will be taken by all population groups to avoid harmful exposure to repeated even small UV radiation even at early ages to prevent serious adverse health outcomes including melanoma later in life.

Acknowledgements This publication is a result of the project implementation: "The equipment for metabolomic and cell analyses", registration number CZ.1.05/2.1.00/19.0400, supported by Research and Development for Innovations Operational Programme (RDIOP) co-financed by European regional development fund and the state budget of the Czech Republic. This study was also supported by the Grant Agency of the Czech Republic (Project no. 16-05534S), AZV 16-29032A, the Charles University (project of Specific University Research, GAUK 165015 and PROGRESS 28 and UNCE 23014) and by the Ministry of Education, Youth and Sports of CR within the National Sustainability Program II (Project BIOCEV-FAR reg. no. LQ1604), and by the project BIOCEV (CZ.1.05/1.1.00/02.0109). The part of the study was performed by the equipment for metabolomics and cell analyses (Grant no. CZ.1.05/2.1.00/19.0400) supported by the Research and Development for Innovations Operational Program, co-financed by the European regional development fund and the state budget of the Czech Republic.

References

Adini I, Ghosh K, Adini A, Chi ZL, Yoshimura T, Benny O, Connor KM, Rogers MS, Bazinet L, Birsner AE, Bielenberg DR, D'Amato RJ (2014) Melanocyte-secreted fibromodulin promotes an angiogenic microenvironment. J Clin Investig 124:425–436

Adini I, Adini A, Bazinet L, Watnick RS, Bielenberg DR, D'Amato RJ (2015) Melanocyte pigmentation inversely correlates with MCP-1 production and angiogenesis-inducing potential. FASEB J 29:662–670

Barrientos S, Stojadinovic O, Golinko MS, Brem H, Tomic-Canic M (2008) Growth factors and cytokines in wound healing. Wound Repair Regen 16:585–601

Benke EM, Ji Y, Patel V, Wang H, Miyazaki H, Yeudall WA (2010) VEGF-C contributes to head and neck squamous cell carcinoma growth and motility. Oral Oncol 46:e19–e24

Brash DE (2015) UV signature mutations. Photochem Photobiol 91:15–26

Brennan M, Bhatti H, Nerusu KC, Bhagavathula N, Kang S, Fisher GJ, Varani J, Voorhees JJ (2003) Matrix metalloproteinase-1 is the major collagenolytic enzyme responsible for collagen damage in UV-irradiated human skin. Photochem Photobiol 78:43–48

Brenner M, Degitz K, Besch R, Berking C (2005) Differential expression of melanoma-associated growth factors in keratinocytes and fibroblasts by ultraviolet A and ultraviolet B radiation. Br J Dermatol 153:733–739

Catania A (2007) The melanocortin system in leukocyte biology. J Leukocyte Biol 81:383–392

Cheli Y, Giuliano S, Botton T, Rocchi S, Hofman V, Hofman P, Bahadoran P, Bertolotto C, Ballotti R (2011) Mitf is the key molecular switch between mouse or human melanoma initiating cells and their differentiated progeny. Oncogene 30:2307–2318

Childs BG, Durik M, Baker DJ, van Deursen JM (2015) Cellular senescence in aging and age-related disease: from mechanisms to therapy. Nat Med 21:1424–1435

Chou WC, Takeo M, Rabbani P, Hu H, Lee W, Chung YR, Carucci J, Overbeek P, Ito M (2013) Direct migration of follicular melanocyte stem cells to the epidermis after wounding or UVB irradiation is dependent on Mc1r signaling. Nat Med 19:924–929

D'Orazio J, Jarrett S, Amaro-Ortiz A, Scott T (2013) UV Radiation and the Skin. Int J Mol Sci 14:12222–12248

Di Cesare S, Marshall JC, Logan P, Antecka E, Faingold D, Maloney SC, Burnier MN Jr (2007) Expression and migratory analysis of 5 human uveal melanoma cell lines for CXCL12, CXCL8, CXCL1, and HGF. J Carcinogen 6:2

Dornelles S, Goldim J, Cestari T (2004) Determination of the minimal erythema dose and colorimetric measurements as indicators

of skin sensitivity to UV-B radiation. Photochem Photobiol 79:540–544
Drigeard Desgarnier MC, Fournier F, Droit A, Rochette PJ (2017) Influence of a pre-stimulation with chronic low-dose UVB on stress response mechanisms in human skin fibroblasts. PLoS One 12:e0173740
Dvořánková B, Szabo P, Lacina L, Kodet O, Matoušková E, Smetana K Jr (2012) Fibroblasts prepared from different types of malignant tumors stimulate expression of luminal marker keratin 8 in the EM-G3 breast cancer cell line. Histochem Cell Biol 137:679–685
Dvořánková B, Szabo P, Kodet O, Strnad H, Kolář M, Lacina L, Krejčí E, Naňka O, Šedo A, Smetana K Jr (2017) Intercellular crosstalk in human malignant melanoma. Protoplasma 254:1143–1150
Finger EC, Cheng CF, Williams TR, Rankin EB, Bedogni B, Tachiki L, Spong S, Giaccia AJ, Powell MB (2014) CTGF is a therapeutic target for metastatic melanoma. Oncogene 33:1093–1100
Fisher GJ, Datta SC, Talwar HS, Wang ZQ, Varani J, Kang S, Voorhees JJ (1996) Molecular basis of sun-induced premature skin ageing and retinoid antagonism. Nature 379:335–339
Fisher GJ, Datta S, Wang Z, Li XY, Quan T, Chung JH, Kang S, Voorhees JJ (2000) c-Jun-dependent inhibition of cutaneous procollagen transcription following ultraviolet irradiation is reversed by all-trans retinoic acid. J Clin Investig 106:663–670
Gentleman RC, Carey VJ, Bates DM, Bolstad B, Dettling M, Dudoit S, Ellis B, Gautier L, Ge Y, Gentry J, Hornik K, Hothorn T, Huber W, Iacus S, Irizarry R, Leisch F, Li C, Maechler M, Rossini AJ, Sawitzki G, Smith C, Smyth G, Tierney L, Yang JY, Zhang J (2004) Bioconductor: open software development for computational biology and bioinformatics. Genome Biol 5:R80
Ghosh K, Capell BC (2016) The senescence-associated secretory phenotype: critical effector in skin cancer and aging. J Investig Dermatol 136:2133–2139
Golan T, Messer AR, Amitai-Lange A, Melamed Z, Ohana R, Bell RE, Kapitansky O, Lerman G, Greenberger S, Khaled M, Amar N, Albrengues J, Gaggioli C, Gonen P, Tabach Y, Sprinzak D, Shalom-Feuerstein R, Levy C (2015) Interactions of melanoma cells with distal keratinocytes trigger metastasis via notch signaling inhibition of MITF. Mol Cell 59:664–676
Gyori BM, Venkatachalam G, Thiagarajan PS, Hsu D, Clement MV (2014) OpenComet: an automated tool for comet assay image analysis. Redox Biol 2:457–465
Hammer R, Harper DAT, Ryan PD (2001) Paleontological statistics software package for education and data analysis. Palaeontol Electron 4:1–9
Hochberg M, Gilead L, Markel G, Nemlich Y, Feiler Y, Enk CD, Denichenko P, Karni R, Ingber A (2013) Insulin-like growth factor-binding protein-7 (IGFBP7) transcript: A-to-I editing events in normal and cancerous human keratinocytes. Arch Dermatol Res 305:519–528
Iida J, Wilhelmson KL, Ng J, Lee P, Morrison C, Tam E, Overall CM, McCarthy JB (2007) Cell surface chondroitin sulfate glycosaminoglycan in melanoma: role in the activation of pro-MMP-2 (progelatinase A). Biochem J 403:553–563
Jackson SP, Bartek J (2009) The DNA-damage response in human biology and disease. Nature 461:1071–1078
Jobe NP, Rösel D, Dvořánková B, Kodet O, Lacina L, Mateu R, Smetana K, Brábek J (2016) Simultaneous blocking of IL-6 and IL-8 is sufficient to fully inhibit CAF-induced human melanoma cell invasiveness. Histochem Cell Biol 146:205–217
Johnson NR, Wang Y (2013) Controlled delivery of heparin-binding EGF-like growth factor yields fast and comprehensive wound healing. J Control Release 166:124–129
Kamp H, Geilen CC, Sommer C, Blume-Peytavi U (2003) Regulation of PDGF and PDGF receptor in cultured dermal papilla cells and follicular keratinocytes of the human hair follicle. Exp Dermatol 12:662–672
Kant V, Kumar D, Kumar D, Prasad R, Gopal A, Pathak NN, Kumar P, Tandan SK (2015) Topical application of substance P promotes wound healing in streptozotocin-induced diabetic rats. Cytokine 73:144–155
Kim EJ, Kim YK, Kim JE, Kim S, Kim M-K, Park C-H, Chung JH (2011) UV Modulation of subcutaneous fat metabolism. J Investig Dermatol 131:1720–1726
Kodet O, Dvořánková B, Krejčí E, Szabo P, Dvořák P, Štork J, Krajsová I, Dundr P, Smetana K Jr, Lacina L (2013) Cultivation-dependent plasticity of melanoma phenotype. Tumour Biol 34:3345–3355
Kodet O, Lacina L, Krejčí E, Dvořánková B, Grim M, Štork J, Kodetová D, Vlček Č, Šáchová J, Kolář M, Strnad H, Smetana K Jr (2015) Melanoma cells influence the differentiation pattern of human epidermal keratinocytes. Mol Cancer 14:1
Kolář M, Szabo P, Dvořánková B, Lacina L, Gabius H-J, Strnad H, Sáchová J, Vlček C, Plzák J, Chovanec M, Cada Z, Betka J, Fík Z, Pačes J, Kovářová H, Motlík J, Jarkovská K, Smetana K Jr (2012) Upregulation of IL-6, IL-8 and CXCL-1 production in dermal fibroblasts by normal/malignant epithelial cells in vitro, immunohistochemical and transcriptomic analyses. Biol Cell 104:738–751
Kondo T, Hearing VJ (2011) Update on the regulation of mammalian melanocyte function and skin pigmentation. Expert Rev Dermatol 6:97–108
Krejčí E, Kodet O, Szabo P, Borský J, Smetana K Jr, Grim M, Dvořánková B (2015) In vitro differences of neonatal and later postnatal keratinocytes and dermal fibroblasts. Physiol Res 64:561–569
Kučera J, Dvořánková B, Smetana K Jr, Szabo P, Kodet O (2015) Fibroblasts isolated from the malignant melanoma influence phenotype of normal human keratinocytes. J Appl Biomed 13:195–198
La Porta CA (2012) CXCR6: the role of environment in tumor progression. Challenges for therapy. Stem Cell Rev 8:1282–1285
Lacina L, Plzak J, Kodet O, Szabo P, Chovanec M, Dvorankova B, Smetana K Jr (2015) Cancer microenvironment: What can we learn from the stem cell niche. Int J Mol Sci 16:24094–24110
Lacina L, Kodet O, Dvořánková B, Szabo P, Smetana K Jr (2017) Ecology of melanoma cells. Histol Histopathol. https://doi.org/10.14670/HH-11-926
Lo JA, Fisher DE (2014) The melanoma revolution: from UV carcinogenesis to a new era in therapeutics. Science 346:945–949
Marchetti D, Nicolson GL (1997) Human melanoma cell invasion: selected neurotrophin enhancement of invasion and heparanase activity. J Investig Dermatol Symp Proc 2:99–105
Mateu R, Živicová V, Drobná Krejčí E, Grim M, Strnad H, Vlček Č, Kolář M, Lacina L, Gál P, Borský J, Smetana K Jr, Dvořánková B (2016) Functional differences between neonatal and adult fibroblasts and keratinocytes. Int J Mol Med 38:1063–1074
Merkel EA, Gerami P (2017) Malignant melanoma of sun-protected sites: a review of clinical, histological, and molecular features. Lab Investig 97:630–635
Ortiz-Montero P, Londoño-Vallejo A, Vernot JP (2017) Senescence-associated IL-6 and IL-8 cytokines induce a self- and cross-reinforced senescence/inflammatory milieu strengthening tumorigenic capabilities in the MCF-7 breast cancer cell line. Cell Commun Signal 15:17
Peppicelli S, Bianchini F, Calorini L (2014) Inflammatory cytokines induce vascular endothelial growth factor-C expression in melanoma-associated macrophages and stimulate melanoma lymph node metastasis. Oncol Lett 8:1133–1138
Quan T, Qin Z, Xia W, Shao Y, Voorhees JJ, Fisher GJ (2009) Matrix-degrading metalloproteinases in photoaging. J Investig Dermatol Symp Proc 14:20–24
Rastrelli M, Tropea S, Rossi CR, Alaibac M (2014) Melanoma: epidemiology, risk factors, pathogenesis, diagnosis and classification. In Vivo 28:1005–1011

Rothhammer T, Poser I, Soncin F, Bataille F, Moser M, Bosserhoff AK (2005) Bone morphogenic proteins are overexpressed in malignant melanoma and promote cell invasion and migration. Cancer Res 65:448–456

Rünger TM (2016) Mechanisms of melanoma promotion by ultraviolet radiation. J Investig Dermatol 136:1751–1752

Sabbatino F, Wang Y, Wang X, Flaherty KT, Yu L, Pepin D, Scognamiglio G, Pepe S, Kirkwood JM, Cooper ZA, Frederick DT, Wargo JA, Ferrone S, Ferrone CR (2014) PDGFRα up-regulation mediated by sonic hedgehog pathway activation leads to BRAF inhibitor resistance in melanoma cells with BRAF mutation. Oncotarget 5:1926–1941

Schneider CA, Rasband WS, Eliceiri KW (2012) NIH Image to ImageJ: 25 years of image analysis. Nat Methods 9:671–675

Shafritz TA, Rosenberg LC, Yannas IV (1994) Specific effects of glycosaminoglycans in an analog of extracellular matrix that delays wound contraction and induces regeneration. Wound Repair Regen 2:270–276

Smetana K Jr, Dvořánková B, Lacina L (2016a) Phylogeny, regeneration, ageing and cancer: role of microenvironment and possibility of its therapeutic manipulation. Folia Biol 59:207–216

Smetana K Jr, Lacina L, Szabo P, Dvořánková B, Brož P, Šedo A (2016b) Ageing as an important risk factor for cancer. Anticancer Res 36:5009–5017

Smyth GK (2006) Linear models and empirical Bayes methods for assessing differential expression in microarray experiments. Stat Appl Genet Mol Biol 3:3

Tice RR, Agurell E, Anderson D, Burlinson B, Hartmann A, Kobayashi H, Miyamae Y, Rojas E, Ryu JC, Sasaki YF (2000) Single cell gel/comet assay: guidelines for in vitro and in vivo genetic toxicology testing. Environ Mol Mutagen 35:206–221

Trylcova J, Busek P, Smetana K Jr, Balaziova E, Dvorankova B, Mifkova A, Sedo A (2015) Effect of cancer-associated fibroblasts on the migration of glioma cells in vitro. Tumour Biol 36:5873–5879

Vartanian A, Stepanova E, Grigorieva I, Solomko E, Baryshnikov A, Lichinitser M (2011) VEGFR1 and PKCα signaling control melanoma vasculogenic mimicry in a VEGFR2 kinase-independent manner. Melanoma Res 21:91–98

Volkmer B, Greinert R (2011) UV and Children's skin. Prog Biophys Mol Biol 107:386–388

Wang JX, Fukunaga-Kalabis M, Herlyn M (2016) Crosstalk in skin: melanocytes, keratinocytes, stem cells, and melanoma. J Cell Commun Signal 10:191–196

Wu XJ, Zhu JW, Jing J, Xue D, Liu H, Zheng M, Lu ZF (2014) VEGF165 modulates proliferation, adhesion, migration and differentiation of cultured human outer root sheath cells from central hair follicle epithelium through VEGFR-2 activation in vitro. J Dermatol Sci 73:152–160

Zelba H, Weide B, Martens A, Derhovanessian E, Bailur JK, Kyzirakos C, Pflugfelder A, Eigentler TK, Di Giacomo AM, Maio M, Aarntzen EH, de Vries J, Sucker A, Schadendorf D, Büttner P, Garbe C, Pawelec G (2014) Circulating CD4+ T cells that produce IL4 or IL17 when stimulated by melan-A but not by NY-ESO-1 have negative impacts on survival of patients with stage IV melanoma. Clin Cancer Res 20:4390–4399

Zhang C, Zhang F, Tsan R, Fidler IJ (2009) Transforming growth factor-beta2 is a molecular determinant for site-specific melanoma metastasis in the brain. Cancer Res 69:828–835